TRANSPORTATION RESEARCH RECORD 632

Design and Performance of Pavement Overlays

TRANSPORTATION RESEARCH BOARD

COMMISSION ON SOCIOTECHNICAL SYSTEMS
NATIONAL RESEARCH COUNCIL

NATIONAL ACADEMY OF SCIENCES
WASHINGTON, D.C. 1977

Transportation Research Record 632
Price $2.80
Edited for TRB by Susan L. Lang

subject areas
25 pavement design
26 pavement performance
40 general maintenance
62 foundations (soils)
63 mechanics (earth mass)

Transportation Research Board publications are available by ordering directly from the board. They may also be obtained on a regular basis through organizational or individual supporting membership in the board; members or library subscribers are eligible for substantial discounts. For further information, write to the Transportation Research Board, National Academy of Sciences, 2101 Constitution Avenue, N.W., Washington, D.C. 20418.

Library of Congress Cataloging in Publication Data
National Research Council. Transportation Research Board.
Design and performance of pavement overlays.

(Transportation research record; 632)
Includes bibliographical references.
1. Pavements—Addresses, essays, lectures.
I. Title. II. Series.
TE7.H5 no. 632 [TE250] 380.5'08s [625.8] 78-4679
ISBN 0-309-02658-X

Sponsorship of the Papers in This Transportation Research Record

GROUP 2—DESIGN AND CONSTRUCTION OF TRANSPORTATION FACILITIES
Eldon J. Yoder, Purdue University, chairman

Pavement Design Section
Carl L. Monismith, University of California, Berkeley, chairman

Committee on Rigid Pavement Design
Ronald L. Hutchinson, U.S. Army Engineer Waterways Experiment Station, chairman
Kenneth J. Boedecker, Jr., William E. Brewer, James I. Clark, Bert E. Colley, Roman L. Dankbar, Donald K. Emery, Jr., Wade L. Gramling, Yang H. Huang, Donald M. Jameson, T. J. Larsen, B. F. McCullough, L. Frank Pace, Robert G. Packard, Frazier Parker, Jr., Thomas J. Pasko, Jr., Karl H. Renner, Surendra K. Saxena, M. D. Shelby, Don L. Spellman, T. C. Paul Teng, William Van Breemen, William A. Yrjanson

Committee on Flexible Pavement Design
Roger V. LeClerc, Washington State Department of Highways, chairman
Ernest J. Barenberg, Robert A. Crawford, R. N. Doty, W. B. Drake, Fred N. Finn, Wade L. Gramling, R. G. Hicks, William S. Housel, Michael P. Jones, David J. Lambiotte, J. W. Lyon, Jr., Richard A. McComb, William M. Moore, Frank P. Nichols, Jr., Leon M. Noel, Dale E. Peterson, William A. Phang, Carl L. Schulten, Donald R. Schwartz, James F. Shook, Eugene L. Skok, Jr., Richard L. Stewart, Loren M. Womack

Committee on Design of Composite Pavements and Structural Overlays
Mathew W. Witczak, University of Maryland, chairman
Gordon W. Beecroft, Oregon Department of Transportation, secretary
Ernest J. Barenberg, Walter R. Barker, Richard D. Barksdale, W. G. Davison, William F. Edwards, H. K. Eggleston, Philp F. Frandina J. H. Havens, W. J. Head, R. E. Livingston, Richard A. McComb, Carl L. Monismith, August F. Muller, Leonard T. Norling, Frazier Parker, Jr., John L. Rice, Donald R. Schwartz, George B. Sherman, Lawrence L. Smith, Harvey J. Treybig, William Van Breemen, Loren M. Womack, Eldon J. Yoder

Lawrence F. Spaine, Transportation Research Board staff

Sponsorship is indicated by a footnote at the end of each report. The organizational units and officers and members are as of December 31, 1976.

Contents

Analysis of an Operational Rigid-Pavement System for Continuously Reinforced Concrete Pavements

R. F. Carmichael, Austin Research Engineers Inc., Texas
B. F. McCullough and W. R. Hudson, Center for Highway Research, University of Texas at Austin

A diagnostic study of four, in-service, continuously reinforced concrete pavements in Texas was prepared by using computerized performance models in the rigid-pavement design system. The performance models were developed by the American Association of State Highway Officials, and the rigid-pavement design system was developed by the Center for Highway Research of the University of Texas at Austin, the Texas Transportation Institute at Texas A&M University, and the Texas State Department of Highways and Public Transportation. The study shows that use of performance models in the rigid-pavement design system reliably predicts the change in serviceability for continuously reinforced concrete pavements. Data gathered and used for the diagnostic study show that the number of 8165-kg (18-kip) equivalent axle loads had a great influence on the condition of the pavements and the predictions made by the design program. The results indicate that not only does the design program reliably predict service life, but that the designs produced by the program, in light of the performance of the four pavement sections, are reasonable for these in-service sections. Information is also presented that begins to establish the correct level of confidence that should be used in the design of Interstate-type continuously reinforced concrete pavements. The conclusions include the belief that the capabilities of the program as a design tool should be further studied so that the ultimate goal of program implementation can be achieved. Future modifications of the system should include a simplification of program input by deleting those variables that are insensitive to the design. Thus, the program can be used as a design tool because of its economic capability that allows for ranking various designs based on the costs of construction, traffic delay, maintenance, and overlay strategies.

The working model for a rigid-pavement design system (RPS) can be used to analyze the variables associated with such a design. This study demonstrates the usefulness and accuracy of RPS service life and design thickness predictions by using input data obtained from four, continuously reinforced concrete pavements (CRCP) in Houston, Texas. By using RPS, the designer has the capability of choosing certain confidence levels for design, and the results of this diagnostic study can be used to establish a tentative level of confidence for use in designing urban freeway pavements. These analyses were undertaken during the development of RPS3, which is the current program version (1). That version contains the same performance models as the previous RPS2 version (2), and the results presented here can be verified by using either program version. The diagnostic study was made in cooperation with a study for the development of a design procedure for continuously reinforced concrete pavements (3). The reported findings partially validate the ability of RPS to correctly predict service life and support the further implementation of studies by using RPS. Detailed user's guides for RPS programs have been prepared (1, 4), and background information on the first methodology for conceptual systems and the first working model for RPS are found in two articles by Kher and others (5, 6).

The rigid-pavement system consists of performance, traffic, structural, and cost models that are solved to produce arrays of design strategies. The strategies are optimized because they are based on the total cost over the design life by considering design constraints to obtain the most economical designs. A summary flow chart for the working system is shown in Figure 1. The design process (5) is divided into the following major parts:

1. Reading, checking against invalid inputs, and printing input data;
2. Generating possible initial designs;
3. Selecting feasible initial designs;
4. Designing subbases, reinforcements, and joints;
5. Developing overlay strategies for feasible initial designs;
6. Analyzing cost of all strategies;
7. Storing, optimizing, and scanning; and
8. Printing output.

DATA GATHERING

A general performance survey was conducted to evaluate four concrete pavements in Houston, Texas (3), and a detailed study, using RPS2 (1), was made to determine why the observed sections performed as they did. Because there are many different combinations for designing concrete pavements, the four concrete pavements do not represent an experiment of adequate size. However, the pavements chosen are similar and allow for a study of RPS predictions for CRCP. The pavement sections are part of the Interstate system and are constructed with cement-stabilized base material that rests on mechanically stabilized clay subgrades. The four sections are characterized by current ratings of pavement conditions. These ratings are estimates based on (a) the current condition of each section made by highway and public transportation department engineers, (b) the present serviceability ratings (PSR) values estimated by National Cooperative Highway Research Program (NCHRP) personnel (3), and (c) the Mays meter readings, which are based on present serviceability index (PSI) values. Project study sections were chosen, and field measurements and material samples were taken. Laboratory tests were run on these samples, and the data were analyzed to ascertain, in particular, what caused the pavements to perform as they did. Table 1 gives the basic data gathered in February 1973 for each of the four test sections. The test sections were Memorial to Woodway (I-610W), Yale to Main (I-610W), San Felipe to Westheimer (I-610W), and Cavalcade to Patton (I-45N).

Each of the four 366-m (1200-ft) sections was closed to traffic by crews from the Texas State Department of Highways and Public Transportation while measurements were made of deflection, crack width, crack spacing, steel reinforcement depth, and rideability. A tabulation of the various distress manifestations present was also

Figure 1. Summary flow diagram of rigid pavement system.

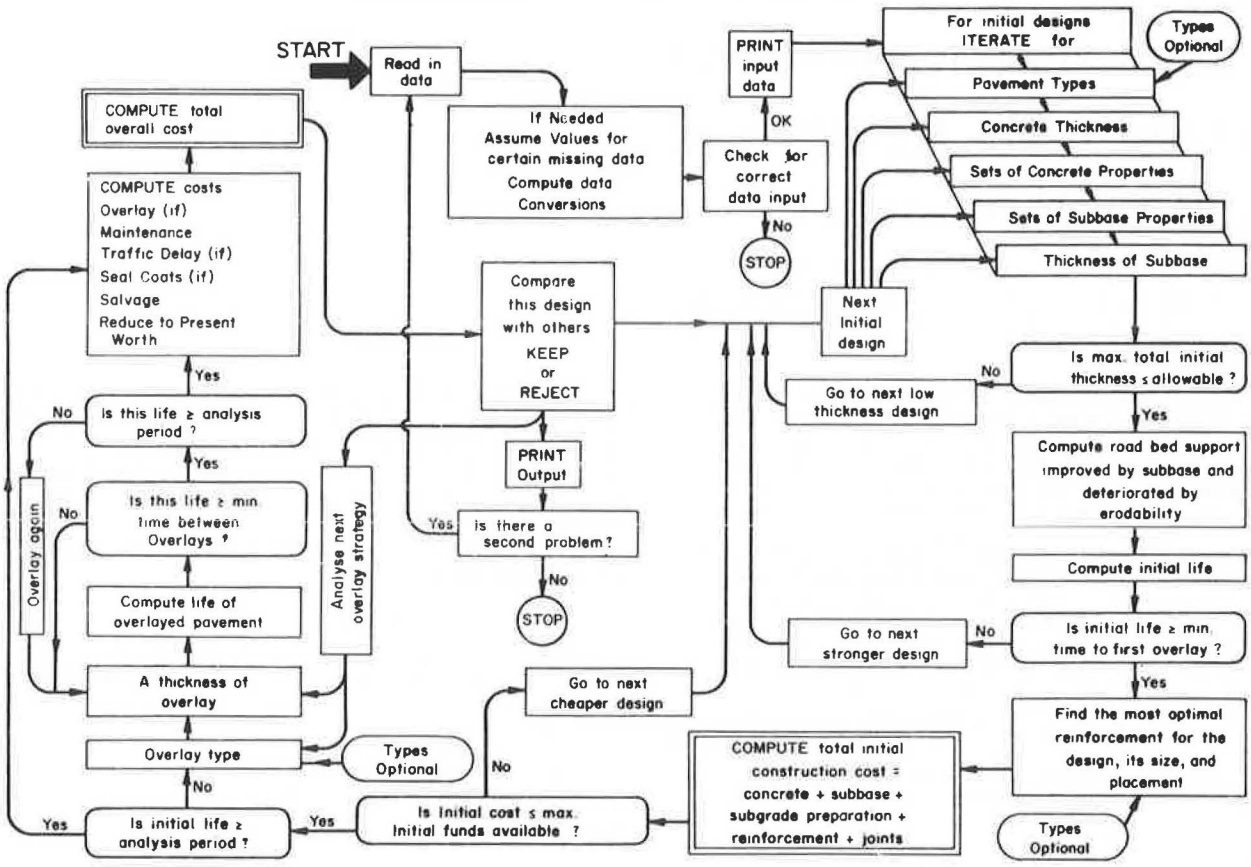

Table 1. Data for test sections.

Test Section	Subgrade[a]	Condition	Number	Age (years)	Thickness (cm)		PSR	PSI	Traffic[c] (thousands)		ESAWL (millions)
					Concrete	Subbase[b]			Avg	Com. Veh.	
Memorial to Woodway	Clay	Fair	271-17-8	7	20.3	15.2	3.2	3.15	80	5.3	9.2
Yale to Main	Clay	Poor	271-14-26	9	20.3	15.2	2.8	3.15	58	4.2	10.2
San Felipe to Westheimer	Clay	Poor	271-17-19	10	20.3	15.2	2.6	3.25	80	5.3	13.1
Cavalcade to Patton	Clay	Good	500-3-68	13	20.3	15.2	3.8	3.30	56	2.3	3.6

Note: 1 cm = 0.394 in and 1 kg/m^3 = 0.0624 lb/ft^3.
[a]Houston geological group average modulus of subgrade reaction = 1842 kg/m^3 (115 lb/ft^3).
[b]Cement-stabilized, sand-shell base.
[c]In one direction per day.

prepared for each individual section. Cores of the concrete, subbase, and subgrade in each section were taken at cracks and between cracks. Before tests were made, all cores were photographed and measurements of height, diameter, and mass were made to determine densities.

Indirect tensile tests were performed on the uncracked concrete and subbase samples to obtain Young's modulus of elasticity values and indirect tensile strengths. Table 2 gives the results of these tests to determine the mean indirect tensile strengths and elastic moduli for each section. Construction information was also obtained from the files of the Texas State Department of Highways and Public Transportation on each of the four sections.

RPS DIAGNOSTIC STUDY

Once data collection was complete, diagnostic studies were initiated. The objective of the diagnois was to explain the performance of each section with respect to its individual characteristics and design.

Comparison of Section Differences

A comparative study of section characteristics was performed to determine if there were any obvious differences in the sections that would explain their behavior. The bar graphs, shown in Figures 2 through 6, were plotted from the data given in Table 1 to ease assimilation. For the four sections chosen, age does not appear to be a critical factor. Although the Cavalcade to Patton section is the oldest section (Figure 2), its current condition is rated good (Table 1). It also has a PSR value of 3.8, which is the best value given by personnel from the Center for Highway Research to the four sections.

PSI values based on the Mays meter readings are shown in Figure 3. The Cavalcade to Patton section has the best average PSI value; however, from the Mays meter readings, which are based on measurements alone, all

the sections appear to be at approximately the same level of serviceability. The small difference in PSI values may have more significance than normally expected because the values represent the range of acceptability for Interstate-type pavements. This theory could be verified by checking the personnel ratings because those ratings seem to reflect the type of facility being rated in relation to the Interstate function. The current condition ratings, given in Table 1, are significant because personnel from the Texas State Department of Highway and Public Transportation are aware that each section requires maintenance and user response. The personnel rated the Memorial to Woodway section in fair condition, the San Felipe to Westheimer and Yale to Main sections were rated in poor condition, and the Calvalcade to Patton was rated in good condition. The PSR values of these sections, given by personnel from the Center for Highway Research, confirmed this appraisal.

The traffic variables considered are the average daily traffic (ADT), commercial vehicles, and number of 8165-kg (18-kip) equivalent single-axle loads (ESAWL) as shown in Figures 4 through 6 respectively. As indicated in these figures, the section that is in the best

Table 2. Results from indirect tensile tests on cores from test sections.

Test Section	Subbase		Pavement	
	Elastic Modulus[a] (GPa)	Tensile Strength[a] (MPa)	Elastic Modulus[b] (GPa)	Tensile Strength[b] (MPa)
Memorial to Woodway	11	1.4	39	3.4
Yale to Main	16	1.6	28	3.2
San Felipe to Westheimer	13	2.0	35	3.7
Cavalcade to Patton	12	1.5	37	3.9

Note: 1 Pa = 0.000145 lbf/in².
[a]Poisson's ratio of 0.25. [b]Poisson's ratio of 0.20.

Figure 2. Age of sections in years.

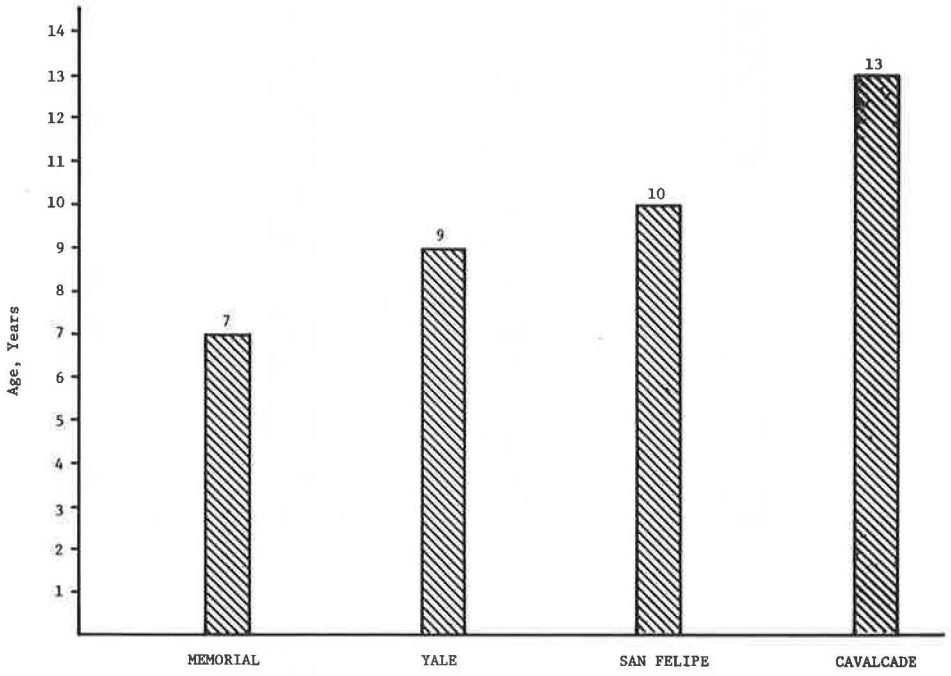

Figure 3. PSI values based on Mays meter readings.

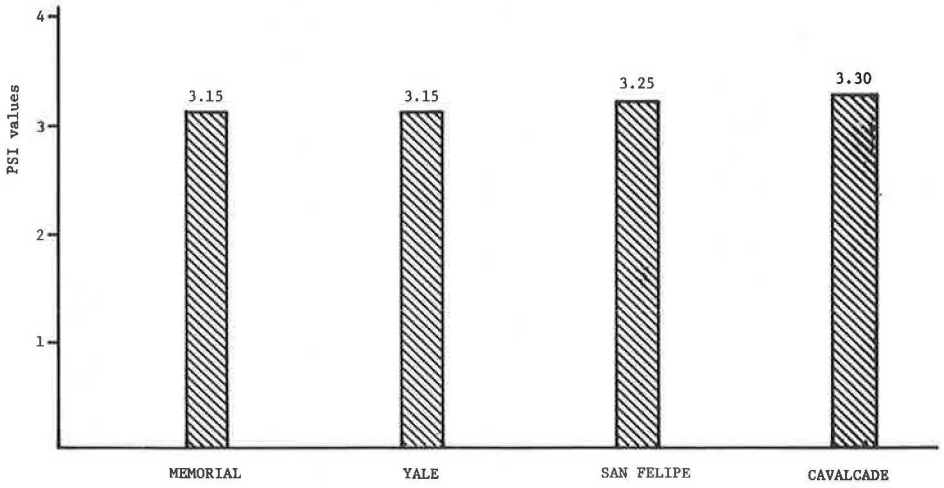

Figure 4. Average daily traffic in one direction.

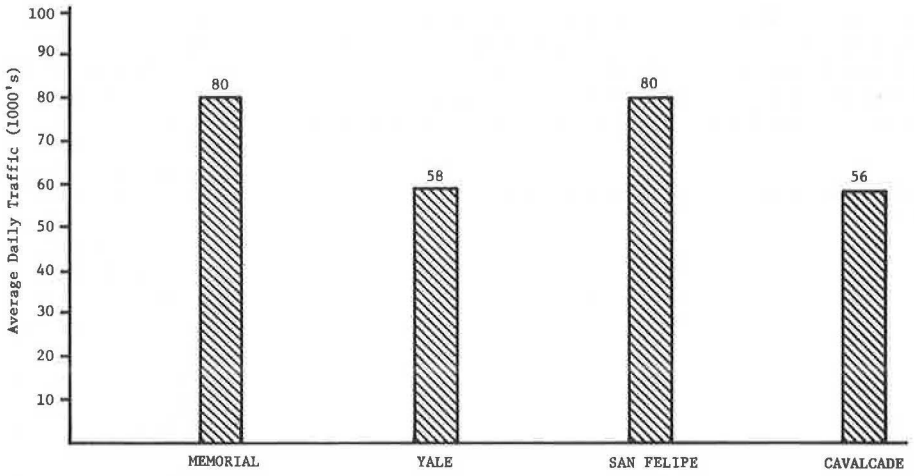

Figure 5. Commercial vehicles per day.

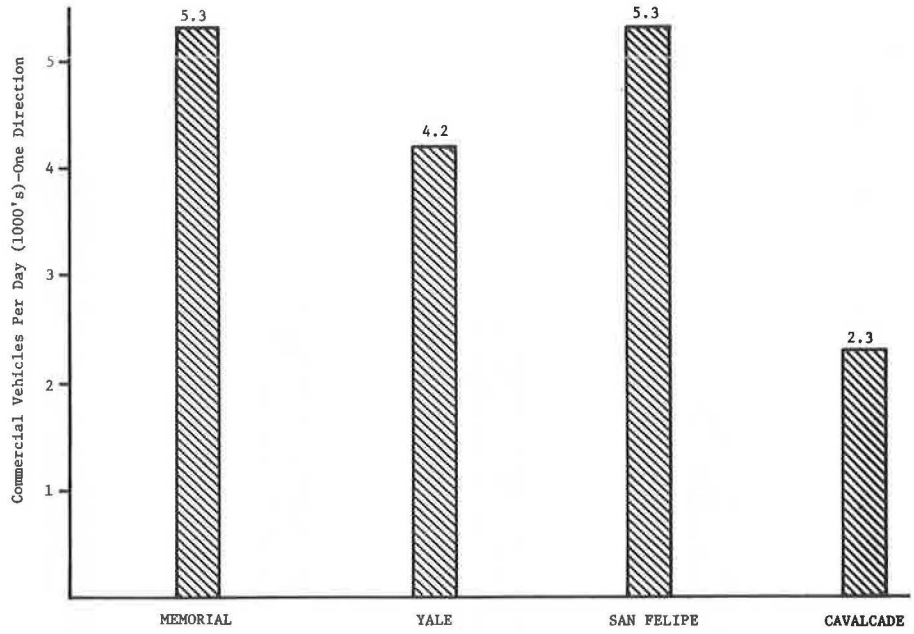

Figure 6. Total 8165-kg (18-kip) equivalent single axle wheel loadings to date.

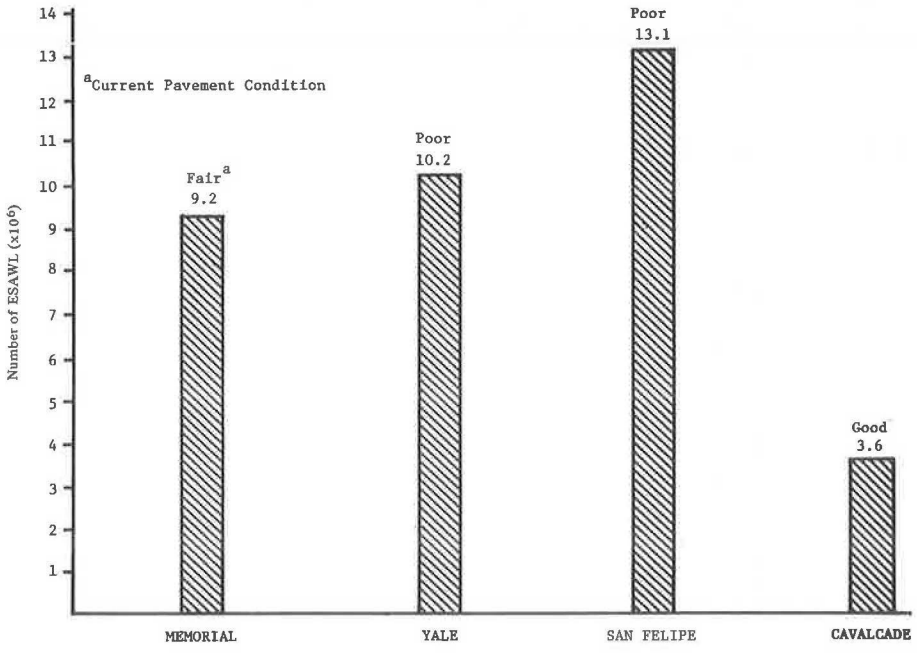

Table 3. Predicted age of test sections using RPS and AASHO performance models.

Test Section	Levels of Confidence (%)						Current Age[b] (year)
	50	80	95	99	99.9	99.99	
Memorial to Woodway	32	18	10	<7[a]	—	—	7
Yale to Main	44	20	<9	—	—	—	9
San Felipe to Westheimer	43	23	12	<10	—	—	10
Cavalcade to Patton	130	77	46	29	17	<13	13

[a]Predicted age less than actual age and overlays not allowed; therefore, there is no solution.
[b]The approximate age of the test sections as of April 1973.

Table 4. Thirty-year designs for test sections.

Test Section	Thickness[a] (cm)			Performance Periods[b]	
	Slab	Subbase	Overlay	Initial	Total
Memorial to Woodway	21.6	30.5	7.6	20	36
	22.9	15.2	7.6	20	35
	24.1	20.3	7.6	27	47
Yale to Main	27.9	15.2	7.6	21	36
	26.7	30.5	7.6	21	37
	29.2	20.3	7.6	27	46
San Felipe to Westheimer	24.1	20.3	7.6	21	37
	25.4	15.2	7.6	24	42
	26.7	20.3	0	32	0
Cavalcade to Patton	17.8	25.4	7.6	21	39
	19.1	15.2	7.6	23	40
	20.3	20.3	0	32	0

Note: 1 cm = 0.394 in.
[a]The design alternatives given by the RPS2 program.
[b]The initial performance periods are the times to the first overlay while the total performance periods are the amounts of time the pavements last with overlays.

condition has carried the least ADT, commercial vehicles, 8165-kg (18-kip) and ESAWL. In Figure 6, the 8165-kg (18-kip) ESAWL plot is especially significant because the current condition ratings and the PSR values both correlate exactly with the amount of 8165-kg (18-kip) ESAWL each section has carried. The current pavement condition is written on the graph for emphasis. Concrete cores from the Cavalcade to Patton section had the highest indirect tensile strength (Table 2), and this may also have contributed to its good performance. There are no specific material or structural differences because all four pavement cross sections consist of 20.3 cm (8 in) of continuously reinforced concrete in which quartz gravel and identical reinforcement were used, 15.2 cm (6 in) of cement-stabilized, sand-shell, subbase and clay subgrades.

Use of the Rigid Pavement System 2

The four CRCP sections provide a complete set of data that is used to evaluate the performance equations for concrete pavements developed by the American Association of State Highway Officials (AASHO) used in RPS. The study is separated into two distinct segments:

1. All the variables are fixed, and the program is used to predict pavement service life; and
2. The program is used to design pavements for a 30-year life with overlay at 20 years.

Initially, the RPS program is used as a tool to predict performance periods for the different sections. The actual pavement thicknesses, age, traffic, material properties, and serviceability at the time of the study are input into the program, and the thickness of the concrete and the subbase are held fixed. Thus, one design strategy results from the program. The output for every design strategy is a predicted performance period that is defined by the maximum and minimum serviceability levels, which are based on traffic, thickness, and material properties. The performance periods calculated by RPS were compared with the actual age of each pavement section to determine the capability of the program to predict performance periods correctly.

For each pavement section, this prediction was run at every confidence level, which began at 50 percent and increased until the program was stopped at some level. These results are given in Table 3. For example, the San Felipe to Westheimer section has a predicted performance life of 12 years at the 95 percent confidence level as compared with an actual performance life of 10 years. The reason the program was unable to design at a level higher than 95 percent is the program was not allowed to design an overlay. The analysis period input to the program is set at the actual performance life; therefore, at a confidence level of 99 percent for the San Felipe section to Westheimer, the predicted performance life is less than the 10-year actual performance life, and, with no overlay capability, the program stops. Analysis of the information in Table 3 indicates that the tentative level of confidence to be used in designing urban freeways may be 95 percent, since the Memorial to Woodway and San Felipe to Westheimer sections made good predictions at the 95 percent level.

The information from the diagnostic study was also used to check the design of each pavement. The procedure followed was to take the known traffic and increase it linearly to a 30-year total. This procedure was done by giving a range of values to the concrete and subbase thickness inputs while retaining the known material characteristics and allowing the program to overlay the facilities at 20 years. This information was supplemented with additional design information, and the RPS program was allowed to design each section.

Table 4 gives the three most economical designs that were computed by the program for each section. The program designs thicker sections for San Felipe to Westheimer, Memorial to Woodway, and Yale to Main sections than the actual 20.3-cm (8-in) CRCP and 15.2-cm (6-in) cement-stabilized subbase originally constructed. The program gives the Cavalcade to Patton section some designs that have thinner concrete than the current 20.3 cm (8 in); however, these designs have thicker subbases. The Yale to Main section, which is in poor condition, is designed by the program to have a minimum concrete thickness of 26.7 cm (10.5 in). These designs are made by using current traffic counts and extrapolating the values to 30-year totals. The accuracy obtained by using past traffic data on these sections enhances the chances of the RPS program to provide adequate design thicknesses.

CONCLUSIONS

These studies, conducted with RPS2, indicate that RPS program predictions that are made by using the modified AASHO performance equations (2) are reasonable. The designs generated by the program for the sections studied are valid and are what might have been built if the current traffic had been anticipated. The pavement-performance lives predicted by RPS agree closely with the actual performance lives of the pavements, thereby providing one verification of the program with data from CRCP freeway sections. The study also indicates that a 95 percent level of confidence is reasonable to use for the design of urban Interstate freeways. In practice, the quality control and high-quality materials, used in Interstate construction, assure high levels of confidence in the design and associated construction. The major conclusions from this study are as follows:

1. Confidence levels of 95 and 99 percent are reasonable for use in designing Interstate CRCP pavements with RPS;
2. Modified AASHO performance equations used in RPS give reasonable results;
3. In lieu of traffic rates, RPS thickness designs for a 30-year analysis period are valid; and
4. This study provides partial verification of RPS, CRCP design capability.

The potential for use of RPS as a tool to design overlays on existing concrete pavements is another important aspect of RPS that should be stressed as well as the capabilities of the program to make economic comparisons of the designs. Results of this study provide one verification of RPS capabilities; however, other studies should be made to validate other areas of RPS design. The current RPS program version, RPS3, is well-documented for implementation (1) and should be used in other studies such as this one to validate and implement the program.

ACKNOWLEDGMENTS

This paper was developed as part of project sponsored by the Texas Department of Highways and Public Transportation. The work was carried out at the Center for Highway Research of the University of Texas at Austin. The opinions, findings, and conclusions expressed in this paper are ours and are not necessarily those of the sponsoring agency.

REFERENCES

1. R. F. Carmichael and B. F. McCullough. Modification and Implementation of the Rigid Pavement Design System. Texas Highway Department, Texas Transportation Institute, Texas A&M University; and Center for Highway Research, Univ. of Texas at Austin, Res. Rept. 123-36, Jan. 1975.
2. R. K. Kher, W. R. Hudson, and B. F. McCullough. A Systems Analysis of Rigid Pavement Design. Texas Highway Department; Texas Transportation Institute, Texas A&M University; and Center for Highway Research, Univ. of Texas at Austin, Res. Rept. 123-25, Nov. 1970.
3. B. F. McCullough, A. Abou-Ayyash, W. R. Hudson, and J. P. Randall. Design of Continuously Reinforced Concrete Pavements of Highways. Center for Highway Research, Univ. of Texas at Austin, Res. Rept. NCHRP 1-15, Aug. 1974.
4. R. F. Carmichael and B. F. McCullough. Rigid Pavement Design System Input Guide for Computer Program RPS2. Texas Highway Department; Texas Transportation Institute, Texas A&M University; and Center for Highway Research, Univ. of Texas at Austin, Res. Rept. 123-21, Feb. 1974.
5. R. K. Kher, W. R. Hudson, and B. F. McCullough. Comprehensive Systems Analysis for Rigid Pavements. HRB, Highway Research Record 362, 1971, pp. 9-20.
6. R. K. Kher, W. R. Hudson, and B. F. McCullough. A Working System Model for Rigid Pavement Design. HRB, Highway Research Record 407, 1972, pp. 130-145.
7. W. R. Hudson, B. F. McCullough, J. Brown, G. Peck, and R. Lytton. Overview of Pavement Management Systems Developments in the State Department of Highways and Public Transportation. Texas State Department of Highways and Public Transportation; Texas Transportation Institute, Texas A&M University; and Center for Highway Research, Univ. of Texas at Austin, Jan. 1976.

Publication of this paper sponsored by Committee on Rigid Pavement Design.

Report on an Experiment for Continuously Reinforced Concrete Pavement in Walker County, Texas

B. F. McCullough, Center for Highway Research, University of Texas at Austin

This report summarizes the findings that resulted from a 16-year study on the performance of a continuously reinforced concrete pavement placed on I-45 in Walker County, Texas. An examination of data provides numerous guidelines for design requirements and construction specifications of future projects in which this type of pavement will be used. Specifically, there were more failures for the pavement in which a lower percentage of reinforcing steel and higher curing temperatures were used. The data indicate that type 3 cement withstands higher steel stresses and that special attention should be given to concrete vibration at all times. The 7-year performance of a short section of an asphalt-concrete overlay with varying thicknesses indicates that the rate of failure and the deflection can be substantially reduced by increasing overlay thickness.

An experiment was conducted to evaluate the relative performance of 0.5 and 0.6 percent, longitudinal steel sections that were used to continuously reinforce a concrete pavement. The continuously reinforced concrete pavement (CRCP) used for this experiment was constructed during 1960 on I-45 in Walker County, Texas [Project I-45-2(3) 102; Control 675-7-4; Walker-Montgomery county line to Huntsville loop]. Since construction of the pavement, there have been numerous studies done by the Texas State Department of Highways and Public Transportation (SHPDT) and other agencies. Some of these studies have been reported in professional journals

(1, 2), other reports (4, 5, 6, 11), and SHPDT reports (3, 7, 8, 9, 10) that discuss steel stress, crack spacing, and failure studies conducted during the first 4 years of the project; failure repairs made after an age of approximately 10 years; use of asphalt overlays on the CRCP; construction and maintenance of the pavement; and various other studies conducted during the project.

Studies concerning the original surface were terminated when an asphalt-concrete overlay was placed over the entire length of the Walker County Project. However, before the overlay was placed, final surveys were conducted so that conclusions could be derived from data gathered during the 16 years of service. The objectives of this report are as follows:

1. Evaluate the relative performance of the steel percentages used to continuously reinforce the concrete pavement during the 16-year period, and
2. Consolidate the findings from all studies into one report so that the appropriate conclusions and recommendations can be formulated.

PROJECT BACKGROUND

The project begins at the Walker-Montgomery County line and proceeds northward to a point 3.21 km (2 miles) south of Huntsville. Figure 1 shows the location and general layout of the divided highway, which has two lanes of traffic in each direction. The pavement, 20.32 cm (8 in) thick and 7.32 m (24 ft) wide, was placed monolithically during the latter half of 1960 and during the spring of 1961. The subbase layer consists of open-graded sandstone, and the top layer of natural clay-sand soil 15.24 cm (6 in) thick was treated with 3 percent lime (by weight) to provide an additional layer.

Because the highway serves as a main connecting route between the Houston and Dallas metropolitan areas there is a high percentage of trucks traveling on it. Traffic counts indicate that the roadway had seven hundred and sixty, 8165-kg (18-kip) equivalent axle load (EAL) applications per day in 1960, had 4 300 000 cumulative EAL applications by 1974, and will have an estimated 5 600 000 EAL applications by 1981.

EXPERIMENTAL NATURE OF PROJECT

The 0.5 percent steel design was achieved by using number 5 bars at a center-to-center spacing of 19.05 cm (7.5 in) and the 0.6 percent steel design was achieved by using number 5 bars at a center-to-center spacing of 16.51 cm (6.5 in). In each direction, the roadway [18.19 km (11.3 miles) long] was equally divided between the two steel percentages. In addition to the steel performance study, another experimental consideration was the use of a minimum center factor of 22.308 kg/m^3 (4 sacks per yd^3), minimum and maximum flexural strengths of 3.8 kPa (550 lbf/in^2) and 4.7 kPa (675 lbf/in^2) respectively, and a specified air-entrained content of 2 to 5 percent.

As part of the development of design criteria for CRCP in Texas, the hypothesis was that a minimum concrete strength should be used to provide sufficient resistance to wheel loads and that a maximum concrete strength should be used to prevent overstressing of the steel because of the development of wide crack patterns. Thus, for several projects in the state during the 1959 to 1963 period, minimum and maximum flexural-strength specifications of 3.8 kPa to 4.7 kPa (550 to 675 lbf/in^2) respectively were used for 7 days. The specified air-entrained content was used to control strength. The two experimental steel percentages were inserted at the request of the Bureau of Public Roads (now Federal Highway Administration) to ascertain the performance variation.

During the designated period, SDHPT performed numerous studies to evaluate the performance of the pavement. Various study sections, test sections, and overlay test sections were selected from the project. The effect of flexural strength and curing temperature on average crack spacing was evaluated by studying the sections that were 122 to 183 m (400 to 600 ft) long over the duration of the project. That study gave a range for the two parameters. Two test sections were also selected for making longitudinal stress studies and a crack pattern development study for each steel percentage. The steel stress study was discontinued in 1961 and an internal summary report was prepared (1). The effect of various parameters on average crack spacing and rates of pavement failure can be found in internal and formal reports (1, 2, 3, 4, 5). The overlay test sections represented an experiment with various thicknesses of asphalt-concrete overlay to reduce the deflection incident of failure and improve riding quality. A report of these studies is given by McCullough and Monismith (5).

STEEL STRESS STUDIES

The conclusions for the study on the detailed analysis of steel stress may be found in a report (1). It was found that steel stress and concrete movement are greater at the crack than in the area between the cracks. The study indicated that the longitudinal steel stress and the concrete movement at the crack are a direct function of the slab temperature decrease and the average crack spacing and are an inverse function of the longitudinal steel percentage. These factors, which were measured by the Wagner turbindimeter test method (Tex-310D), have a significant influence on the steel stress and the concrete movement and thus should be included in any rational design procedure. In addition, it was found that the type of portland cement used had a profound influence on the steel stress at the crack. Inadvertently, during the construction, type 3 cement met the specification requirements of type 1 cement; therefore, the contractor experimented by using the type 3 cement to meet the strength specifications with that minimum cement factor.

During the early periods of concrete curing, it was found that type 3 cement produced three to four times more longitudinal steel stress than type 1 cement. The cracking in concrete with type 3 was found to be explosive in nature. The stresses and crack patterns of both pavements tended to approach each other in time, but the early differentials are of such magnitude that the use of type 3 was banned from use in CRCP in Texas. A maximum specific surface area of 2000 cm^2/gm (140907.68 in^2/lb) was included in the concrete pavement specifications to prohibit the use of type 3 cement (10). The CRCP-1 computer program developed in connection with the National Cooperative Highway Research Program (NCHRP) included these variables (11).

CRACK PATTERN OBSERVATIONS

Crack pattern observations were made at periodic intervals from the time of construction to the end of the survey. These data provided a historical development of the crack pattern over the 16-year period. Crack surveys were recorded on two test sections and eight study sections. The test sections represented the amount of pavement placed for an entire day [approximately 609.6 m (2000 ft)] for each steel percentage. These data were studied to evaluate the crack development at various points along the placement and the effect of steel percentage. The study sections, 122 to 183 m (400 to 600 ft) long, were

Figure 1. Location and layout of Walker County Project.

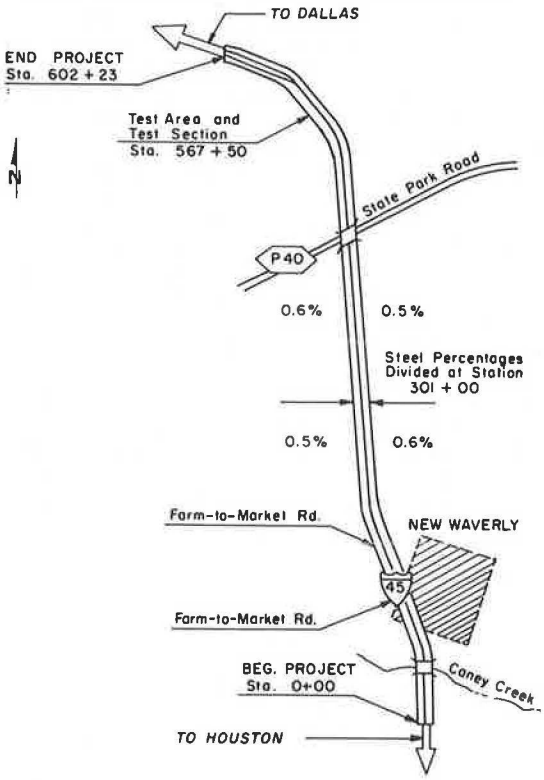

selected to provide information about variations in concrete strength, curing temperature, roadway direction, and steel percentage. During the final survey, seven additional sections were used to provide a large data base.

Test Sections

The effect of longitudinal steel percentage on the average crack spacing for each of the two test sections that were about 1417 m (4650 ft) long was evaluated by periodic surveys that were made since the project began. Figure 2 shows the age-crack spacing relations for these two test sections from construction to 1974. Cracking patterns had developed quickly during the first 5 months on the project. Initially, a large rapid decrease occurred in both sections as a result of curing. From about 150 days onward, only a slight decrease in the average crack spacing is seen for the next 10 to 12 years, which is mainly attributable to environmental and seasonal effects. Between 1963 and 1974, a small continued decrease was experienced in both sections because of increased traffic loading and increased rates of failures.

Study Sections

The crack patterns on the study sections follow the same trend as those on the test section; however, several significant differences were found in the 1974 data. Table 1 gives the crack-spacing data taken at different locations throughout the project in 1974. These sections were randomly selected to provide the experiment with data for ascertaining the effect of traffic direction, steel per-

Figure 2. Relation between age and average crack spacing on test sections.

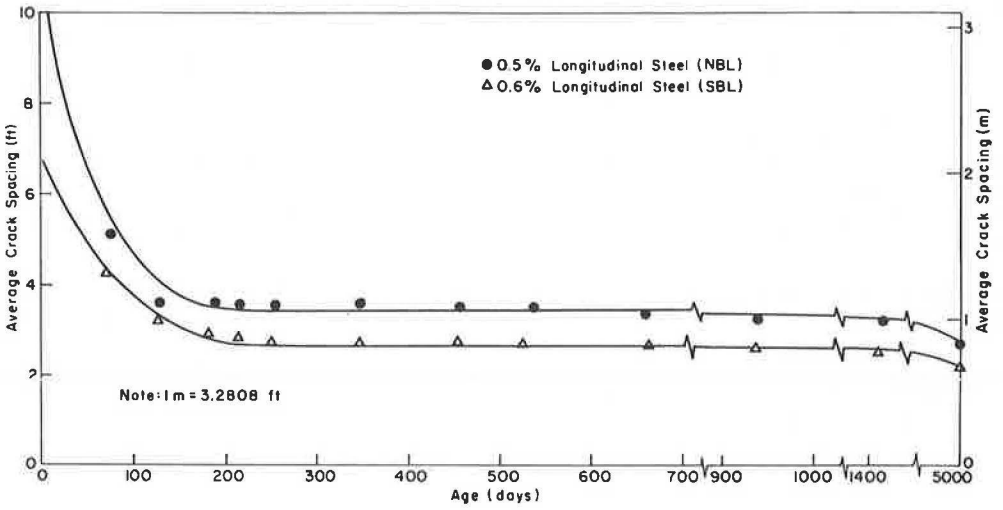

Table 1. Analysis of variance results for crack spacing data taken at various locations on the project in 1974.

Station	Section[a]	Steel Percentage	Length (m)	Number of Cracks	Crack Spacing (m)
SBL					
99 + 00 - 105 + 00	Study 6	0.5	183	242	0.76
105 + 00 - 109 + 00	—	0.5	122	160	0.76
109 + 00 - 119 + 00	—	0.5	305	306	0.99
119 + 00 - 129 + 00	—	0.5	305	288	1.06
129 + 00 - 132 + 75	—	0.5	114	97	1.18
298 + 00 - 303 + 00	Study 4	0.5, 0.6	152	236	0.65
334 + 00 - 339 + 00	Study 3	0.6	152	270	0.56
565 + 00 - 589 + 00	Test	0.6	427	825	0.63
NBL					
70 + 00 - 75 + 27	Study 7	0.6	161	195	0.82
109 + 00 - 114 + 00	—	0.6	152	139	0.88
114 + 00 - 124 + 00	—	0.6	305	396	0.77
124 + 00 - 134 + 00	—	0.6	305	405	0.75
530 + 00 - 535 + 00	Study 3	0.5	152	231	0.66
553 + 00 - 565 + 00	Test	0.5	366	504	0.72

Note: 1 m = 3.28 ft.

[a] Column indicates if the section encompasses one of the regular sections shown in Figure 3.

centage, and relative location of section on the project. The results of an analysis of variance for Table 1 are as follows (1 m = 3.28 ft):

Variable	Avg Crack Spacing (m)
Traffic	
NBL	0.75
SBL	0.76
Steel	
0.5 percent	0.82
0.6 percent	0.70
Placement	
0.5 percent steel	
North end, NBL	0.70
South end, SBL	0.89
0.6 percent steel	
North end, NBL	0.79
South end, SBL	0.61

For the above variables, only those for traffic direction were not significantly different. The average crack spacing ($\overline{X}$) did not differ appreciably between directions, i.e., northbound lanes (NBL) [0.75 m (2.47 ft)] and southbound lanes (SBL) [0.76 m (2.51 ft)]. The differences in average crack spacings between steel percentages were and have always been small but separable: 0.82 m (2.70 ft) for 0.5 percent steel and 0.70 m (2.30 ft) for 0.6 percent steel. The $\overline{X}$'s for each steel percentage in each roadway also varied as much as the percentage of steel: $\overline{X}$ = 2.91 for 0.5 percent steel on SBL and $\overline{X}$ = 2.58 for 0.6 percent steel on NBL. For both steel percentages, the crack spacing at the north end of the project was smaller than that at the south end of the project. This difference indicates that the cooler curing temperatures used for the pavement at the south end of this roadway were a controlling feature. (In general, the temperatures during concrete placement were cooler at the

Table 2. Average crack spacing for all sections.

Survey	Date	Test Section 1	Test Section 2	Study Section 0	Study Section 1	Study Section 2	Study Section 3	Study Section 4	Study Section 5	Study Section 6	Study Section 7
1	8/26/60	3.10	2.01	4.69	—	—	—	—	—	—	—
2	10/26/60	1.53	1.29	1.85	—	—	—	—	—	—	—
3	12/21/60	1.08	0.96	1.25	—	—	—	—	—	—	—
4	2/17/61	1.05	0.89	1.08	—	—	—	—	—	—	—
5	3/17/61	1.05	0.85	0.96	1.00	0.85	1.07	1.23	2.73	2.54	2.92
6	4/27/61	1.04	0.83	—	—	—	—	—	—	—	—
7	7/27/61	1.04	0.83	0.94	0.96	0.83	0.96	1.22	2.69	2.41	2.28
8	12/16/61	1.04	0.83	—	—	—	—	—	—	—	—
9	3/15/62	1.04	0.82	—	—	—	—	—	—	—	—
10	7/7/62	1.01	0.80	—	—	—	—	—	—	—	—
11	5/12/63	0.98	0.78	0.88	0.89	0.8	0.86	1.03	1.62	1.45	1.26
12	9/16/74	0.72	0.59	0.77	0.65	—[a]	0.56	0.65	—	0.99	0.94

Note: 1 m = 3.28 ft.
[a] Located in overlay test section.

Figure 3. Average crack spacing versus approximate curing temperature for study sections.

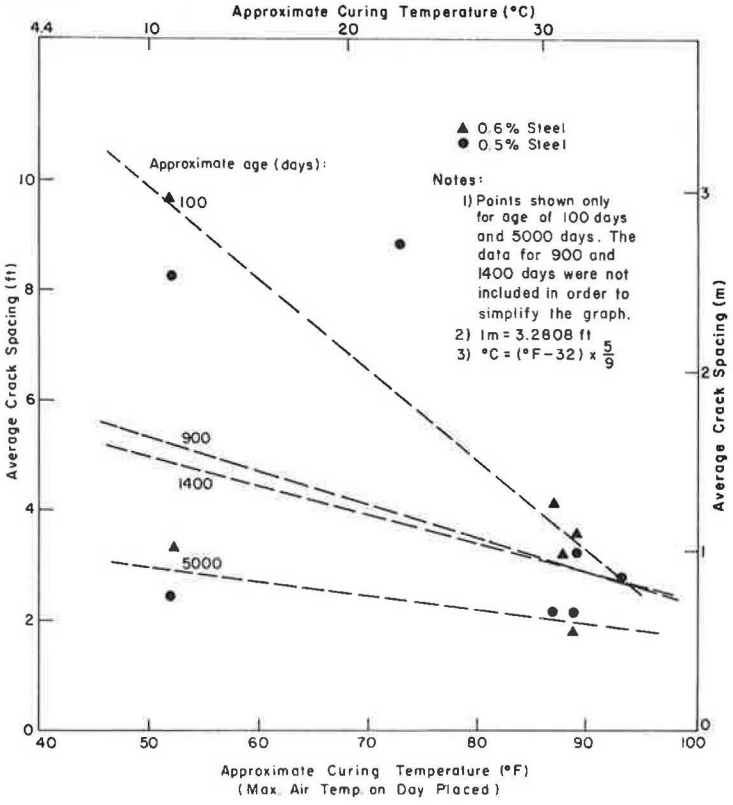

south end than at the north end.)

Table 2 gives the crack-spacing data for the various test sections that were observed during the life of the facility. The study sections had been selected earlier to provide a range in design factors such as steel percentage, flexural strength, and curing temperature.

Earlier studies had indicated that several factors such as relative position within a slab from a construction joint, steel percentage, average 7-d flexural strength, and air entrainment percentage affected the average crack spacing. Initially, a strong interrelation existed, but all the relations have been progressively nullified with time to the point that by 1974, no positive relation existed between average crack spacing and any of the above investigated factors, except for curing temperature (Figures 3 and 4).

Figure 4. Average crack spacing versus steel percentage.

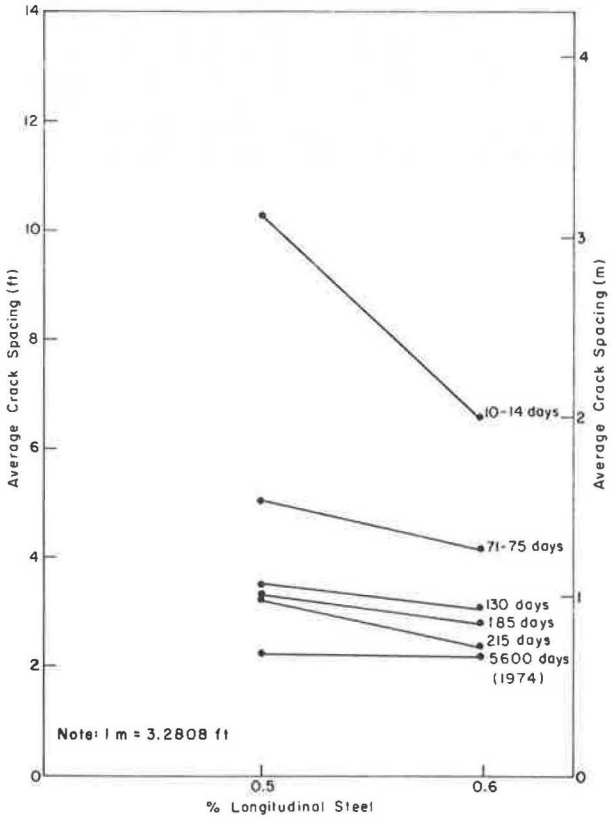

These data show that slabs with the same steel percentage will have the same crack spacings over a long period of time even though the curing temperature, flexural strength, and location for the amount of pavement placed for an entire day may vary. Since attempts were made to control the maximum and minimum flexural strengths, the effect of flexural-strength variation cannot be fully evaluated on this project because the range was small. Generally, crack patterns develop at different rates during the first years; therefore, these observations should not be construed to mean that curing temperature is not an important factor for consideration in design. Thus, as previously indicated, the steel stresses and consequently the performance will vary significantly.

DEFLECTION STUDIES

Deflection studies were made on this project for three different purposes: the first two were concerned with the behavior of CRCP, and the third was concerned with the experimental overlay. In 1962, the first study investigated the surface irregularities found on the project. The second study attempted to determine the effect that steel percentage had on deflection. Shortly after the project was opened to traffic, surface irregularities were noticed in the vicinity of the construction joints at numerous locations over the length of the project. It was found that on the down placement side of the construction joint excessive deflection was occurring. According to the American Association of State Highway Officials (AASHO) deflection data, the pavement in these troubled areas was acting similar to that of a 14-cm (5.5-in) road test pavement; whereas, the satisfactory sections were deflecting similar to that of a 24.1-cm (9.5-in) road test pavement. The results of a subsurface investigation

Figure 5. Failed construction joints in NBL versus year.

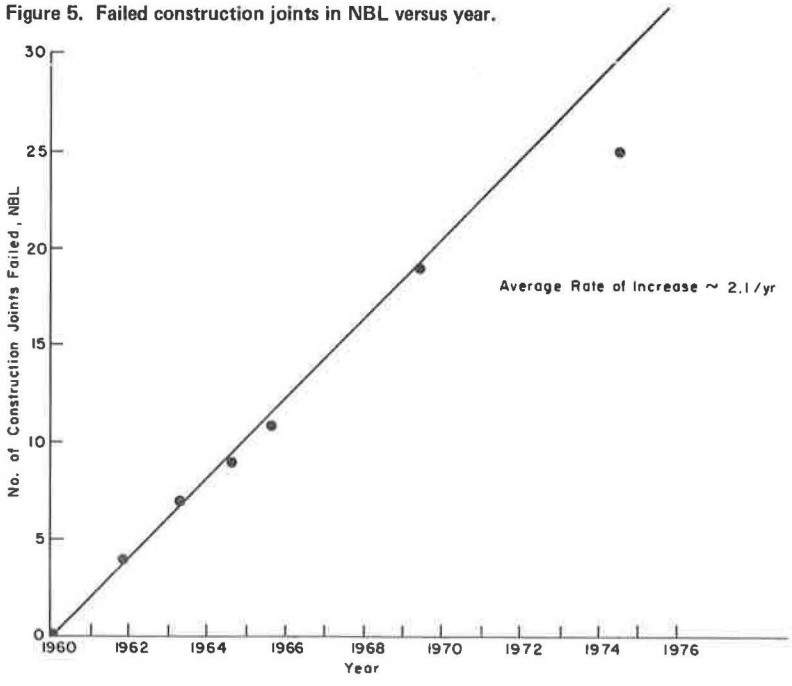

showed that the down side of the construction joint received inadequate vibration in the lower part of the slab, which caused the bottom 7.6 to 10.2 cm (3 to 4 in) of the slab to become honeycombed. As a result, the effective thickness of the slab ranged from 10.2 to 12.7 cm (4 to 5 in), and thus the data agreed with the results of the deflection study. As a result of that study, it is suggested that, for all future jobs, extra precautions should be taken in vibrating the concerte on the down side of a construction joint. Additional requirements were added to the design standards and specifications.

Studies on the effect that steel percentage had on deflection were inconclusive. Generally, there seemed to be no apparent trend that indicated that the sections with a higher percentage of steel exhibited less deflection. Thus, it was tentatively concluded that, if there was enough steel in the slab to retain the aggregate interlock, the slab would act as a continuous unit. Although followup studies were not conducted in 1974, a limited study during the life of the facility indicated no apparent change in these observations.

PERFORMANCE STUDIES

Overall, the riding qualities of the roadway on the Walker County Project were very good, especially when compared to those of the jointed concrete pavement project that is to the north and south of the Walker Project. However, as early as 1962, a large number of failures occurred in the pavement. In 35.4 km (22.6 miles) of roadway, 35 failures occurred by 1964, 109 by 1969, and over 350 by 1974. These failures occurred both at and between construction joints. The term failure is used to describe a serious disintegration of the pavement structure that includes patches, repairs, punchouts, and severe spalling. Over the years, these failures have been correlated with numerous factors related to pavement construction such as mix design, flexural strength, and curing temperature.

Construction Joint Failures

Shortly after the project opened, serious failures were found to have developed quickly at several construction joints. The repairs made on these areas verified what the deflection studies had shown in that the lower 7.6 to 10.2 cm (3 to 4 in) of pavement thickness could not be counted on to act as pavement because the concrete beneath the reinforcement mat was seriously honeycombed. The effective depth of the pavement in these areas was from 10.2 to 12.7 cm (4 to 5 in). Since hand vibrators were not required at construction joints, sufficient vibration of the bottom 7.6 to 10.2 cm (3 to 4 in) did not occur in the range of 6.1 m (20 ft) from a construction joint. In 1965, a nuclear road density logger was used to determine how widespread the honeycombing problem was in the pavement. Moderate success was achieved by using this method. It was predicted that 70 percent of the construction joints would fail because of honeycombing; however, this estimate was thought to be unrealistic at the time.

A history of construction joint failures on the project was compiled over the years. At the time of the overlay, approximately 75 percent of the construction joints in NBL had experienced failures. This percentage is similar to the percentage predicted by using the nuclear road logger. Although there was some question as to the magnitude of the amount of failures during 1965, the 1974 data indicate that the prediction is reliable. Hence, the feasibility of using such equipment to identify the problem area is reinforced. Figure 5 shows the rate of increase in failures per year and age as a linear relation on this project. However, this rate of increase must be correlated with the traffic build-up on the project. The average increase per year in construction joints from 1960 through 1974 was 2.1, i.e., every year 2.1 additional construction joints in this pavement fail because of excessively close crack spacing, punchouts, and spalling. Of the construction joints that have less than 2 d separation between placement, 82 percent (23 of 28) experienced some type of failure. Of the construction joints that have 2 d or more between placement, 57 percent (8 of 14) experienced failures. This difference is significant; however, it may be because of general construction practices rather than the steel strength properties of the concrete.

Intermediate Failures

By 1963, there was a rise in the number of failures between constructions. These failures have frequently been mentioned and studied by previous investigators. The primary reason for the failures was believed to be flash sets of the concrete during paving operations in hot weather. In 1964, a significant early trend was detected between the percentage of failures in a pavement slab versus the curing temperature of that slab (2). This same type of information was analyzed for the years 1969 and 1974 for the same sections. No definitive correlation exists for these years.

It is felt that, over the years, the differing weathering, soil support, traffic, and pavement properties had a more significant effect on failure than did that of the initial curing temperatures. However, part of the problem in analyzing the data is evidenced by the survey methods themselves and by the manner in which the surveys were made. The survey methods used were visual and photographic. Photographs cannot capture all the failures, and an experienced technician cannot perfectly describe the extent and seriousness of a certain failure. Also, a visual survey was made the first year, a photographic survey was made the second year, and no survey was made the third year. Thus, the limitations of these methods significantly affect the data analysis. Although each survey can pinpoint trends in one pavement, it cannot be viably related to the magnitude of trends found by the other survey method; therefore, a source for experimental error was introduced into this analysis.

The following is the number of failures in terms of steel percentages and roadway direction for 1964 and 1974.

Traffic Direction	Number of Failures	
	1964	1969
0.5 percent steel		
NBL	13	186
SBL	4	96
0.6 percent steel		
NBL	4	97
SBL	14	59

It appears from the 1969 data that substantially more failures were observed in the 0.5 percent steel sections than the 0.6 percent steel sections. Furthermore, there are substantially more failures in NBL than in SBL. Approximately 43 percent of the failures occur in the NBL and 0.5 percent combination, which is a low-steel percentage and a high-curing temperature condition, whereas, the low-temperature curing and high-steel percentage combination had only 13 percent of the failures.

Table 3 gives the percentage of the roadway experiencing failure in NBL and SBL for a range of maximum air temperatures during concrete placement. By using both the 1969 and 1974 data from the road repair survey,

it is seen that substantially more failures occurred when the concrete placement temperature was in the range of 32 to 37°C (90 to 99°F). The same trend is evident in the SBL, although the percentages are not as high.

Experimental Overlay

An experimental asphalt-concrete overlay that had varying thicknesses was placed over CRCP with both steel percentages in 1969. The section overlaid was 1417.32 m (4650 ft) in both NBL and SBL. A profile of the thickness variation is shown in Figure 6, and thicknesses were 5.1, 10.2, and 15.3 cm (2, 4, and 6 in). Dynaflect readings were taken on sections both before and after overlay to determine the effect of the overlay on the load-carrying capability of the pavement (Table 4).

A significant decrease occurred in the dynaflect readings after the overlay. The dynaflect readings, if averaged for NBL and SBL and plotted against the thickness of overlay, show a strong interrelation (Figure 7). As expected, the readings significantly decrease with an increase in thickness. The same data are plotted as percentage reduction of dynaflect readings versus the thickness of overlay (Figure 8). The graph shows approximately 5 percent deflection reduction for each 25.4 mm (1 in) of asphalt-concrete pavement.

When the overlay was placed, the average crack spacing of CRCP was estimated to be 0.67 m (2.2 ft) in NBL. Since the overlay was placed, cracks developed in all thicknesses of asphalt overlay. This cracking is termed reflection cracking, i.e., cracking that is in the overlay, which forms at or near the crack in CRCP. The percentage of reflection cracking is defined as the ratio of crack spacing in CRCP in 1969 to the crack spacing in the overlay in 1974, which is then multiplied by 100. A plot of the percentage of reflection cracking versus overlay thickness (Figure 9) shows a very strong decrease in the reflection-cracking percentages, as expected. Note that for the 15.2-cm (6-in) overlay, zero reflection cracking was experienced. A design study indicated at least 6.4 cm (2.5 in) of asphalt-concrete pavement was needed to prevent reflection cracking.

Table 3. Percentage of roadway experiencing failure during 1969 and 1974 for NBL and SBL.

Curing Temperature (°C)	1969		1974		
	NBL[a]	SBL[a]	NBL[a]	NBL[b]	SBL[b]
4.4 to 9.4	3.45	1.31	3.26	2.74	2.81
10.0 to 15.0	1.56	4.39	2.53	5.10	1.40
15.5 to 20.5	2.94	1.33	3.70	4.39	1.20
21.1 to 26.1	4.83	9.30	7.04	2.93	3.28
26.7 to 31.7	2.72	7.15	8.72	2.79	2.64
32.2 to 37.2	7.49	5.40	19.03	8.80	5.92

Note: 1°C = (°F - 32) x 5/9.
[a] From actual road repairs. [b] From photographic survey.

Figure 6. Experimental asphalt-concrete overlay in 1969.

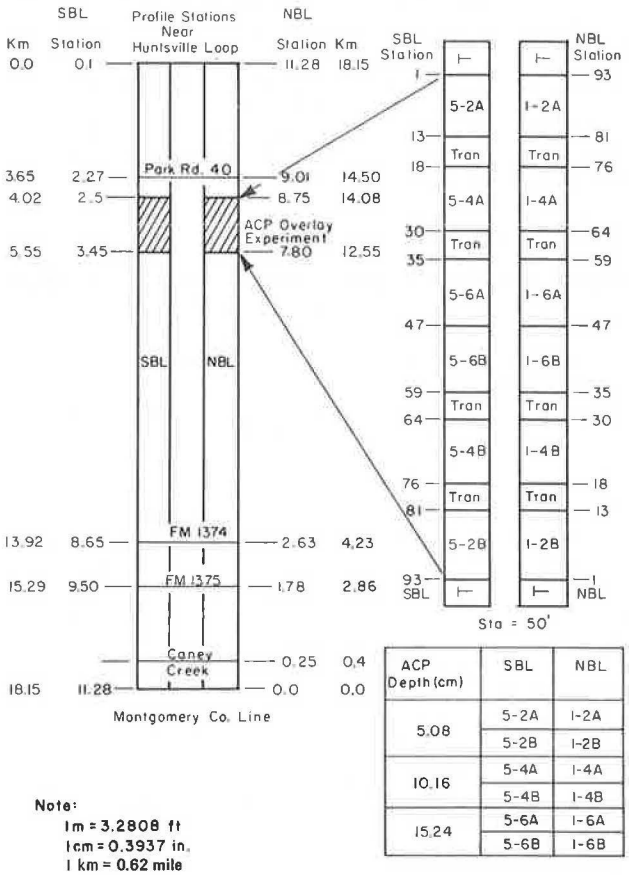

ACP Depth (cm)	SBL	NBL
5.08	5-2A	1-2A
	5-2B	1-2B
10.16	5-4A	1-4A
	5-4B	1-4B
15.24	5-6A	1-6A
	5-6B	1-6B

Table 4. Dynaflect deflection readings before and after overlay.

Date	Section 2B Avg	2B Std.	4B Avg	4B Std.	6B Avg	6B Std.	2A Avg	2A Std.	4A Avg	4A Std.	6A Avg	6A Std.
NBL												
Before												
6/67	0.024 485	0.000 172	0.019 355	0.000 139	0.020 980	0.000 176	0.919 685	0.000 143	0.009 626	0.000 137	0.021 209	0.000 218
9/67	0.027 407	0.000 226	0.019 482	0.000 144	0.021 742	0.000 327	0.021 209	0.000 133	0.022 834	0.000 112	0.022 225	0.000 215
11/67	0.024 587	0.000 171	0.019 202	0.000 119	0.021 412	0.000 230	0.023 749	0.000 313	0.027 889	0.000 166	0.027 991	0.000 376
1/68	0.028 118	0.000 247	0.020 244	0.000 145	0.023 261	0.000 402	0.023 393	0.000 184	0.030 353	0.000 212	0.029 235	0.000 372
After												
2/68	0.023 520	0.000 369	0.015 062	0.000 089	0.014 300	0.000 148	0.019 964	0.000 102	0.021 158	0.000 132	0.017 653	0.000 150
8/68	0.023 470	0.000 407	0.014 402	0.000 093	0.013 157	0.000 156	0.016 256	0.000 124	0.017 475	0.000 106	0.014 757	0.000 124
1/69	0.025 730	0.000 435	0.014 859	0.000 090	0.014 122	0.000 152	—[a]	—[a]	—[a]	—[a]	—[a]	—[a]
SBL												
Before												
9/67	0.020 828	0.000 076	0.017 424	0.000 099	0.016 967	0.000 160	0.016 713	0.000 066	0.022 250	0.000 134	0.021 209	0.000 089
11/67	0.025 476	0.000 103	0.021 895	0.000 115	0.020 777	0.000 178	0.021 209	0.000 089	0.029 413	0.000 246	0.023 266	0.000 226
1/68	0.019 380	0.000 074	0.015 951	0.000 075	0.018 720	0.000 138	0.020 675	0.000 089	0.027 991	0.000 215	0.020 244	0.000 180
After												
2/68	0.022 123	0.000 115	0.017 043	0.000 187	0.013 513	0.000 121	0.018 644	0.000 068	0.019 126	0.000 090	0.016 815	0.000 142
8/68	0.017 272	0.000 092	0.014 122	0.000 161	0.012 243	0.000 123	0.015 215	0.000 046	0.016 510	0.000 056	0.013 767	0.000 114
1/69	0.023 546	0.000 158	0.015 799	0.000 126	0.013 030	0.000 112	0.018 745	0.000 056	0.019 914	0.000 095	0.016 713	0.000 157

Note: All average and standard dynaflect readings are in millimeters (1 mm = 0.03937 in).
[a] Indicates no reading taken.

Figure 7. Dynaflect deflection readings after overlay sections versus overlay thickness.

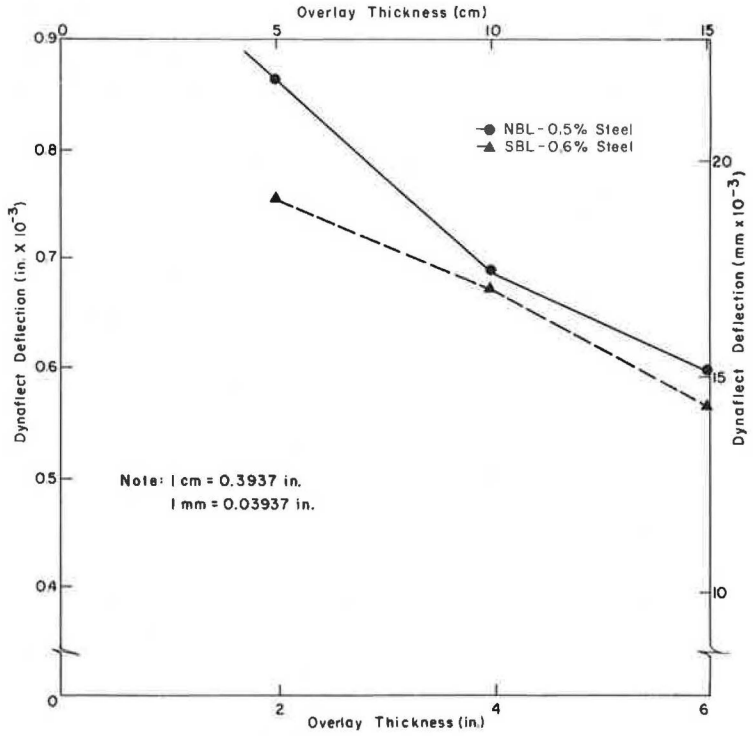

Figure 8. Decrease in deflection readings versus overlay thickness.

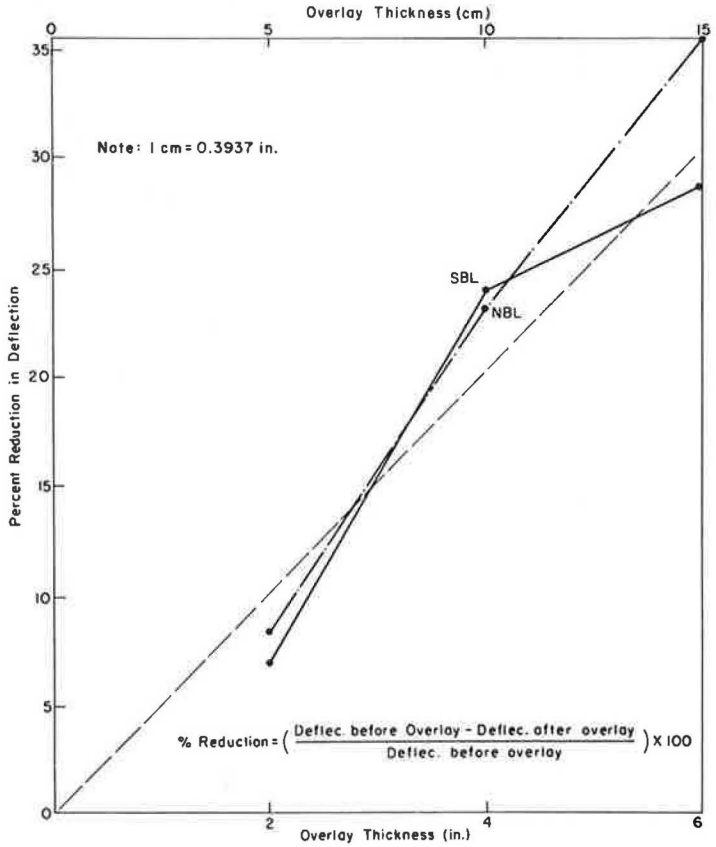

Figure 9. Reflection cracking versus overlay thickness in NBL for 1974.

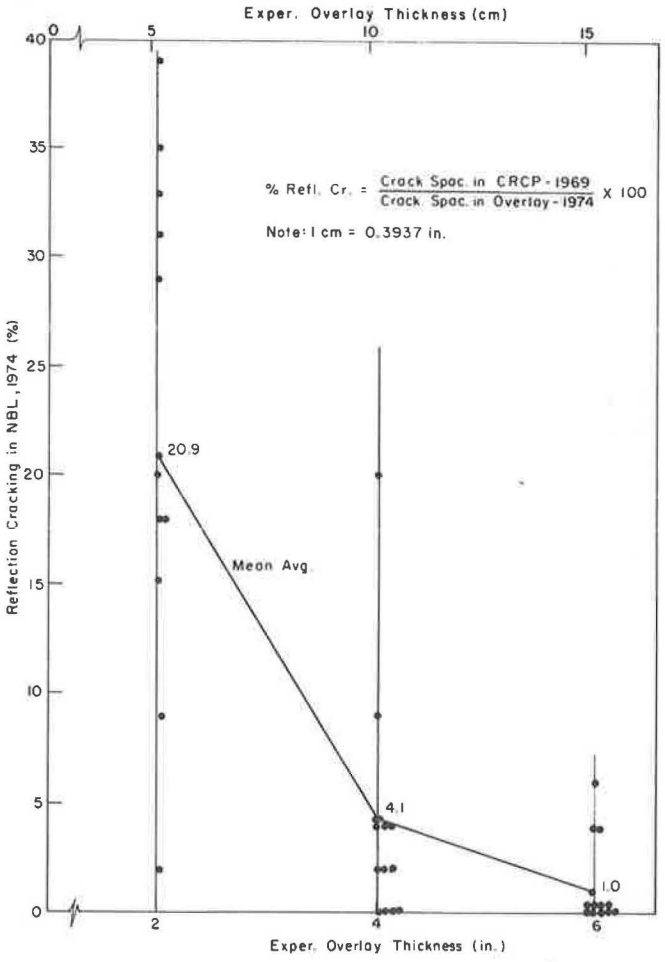

Thus, this procedure should be modified in light of these data.

1974 Overlay

The Walker County CRCP experiment ended in 1974 when the length of the roadway, both NBL and SBL, was overlayed with asphalt concrete. Currently, its behavior is being studied as a flexible pavement over a CRCP. CRCP was placed in as good a condition as possible before overlay, i.e., all patches were repaired or replaced with concrete and most of the failures were remedied.

DISCUSSION OF RESULTS

The 16-year performance history of the Walker County experimental project provides an excellent insight into the construction and maintenance guidelines for CRCP. Even though numerous failures were present, the riding quality of the pavement always remained high. Thus, the importance of the visible distress manifestations in the pavement was emphasized in that they can be used by an engineer to rate the performance of a pavement. At the time of overlay, the average present serviceability index (PSI) was 3.0, which is above the generally accepted value of 2.5. Failures are visibly apparent, i.e., they can be seen as one rides over the pavement. Thus, even though the PSI is high, the visibility of the failures has an effect on the pavement-rating performance.

During the preparation of the plans and specifications for the project, a critical oversight was made by not requiring concrete vibration. The specifications for concrete pavement were adopted without including a vibration requirement; hence, the contractor was not required to adequately vibrate the concrete. This lack of vibration resulted in numerous problems that showed up during the 16 years of pavement performance before the asphalt overlay.

The first area experiencing problems was the concrete on the down placement side of a transverse construction joint (morning placement). In this area, the equipment used for concrete placement did not adequately vibrate the concrete; therefore, the area immediately below the steel became honeycombed, and this resulted in failures. The use of fine-grind cement resulted in high stresses, thus, the effect of the steel percentage showed up clearly during the performance period. There were substantially more failures in the 0.5 percent sections than in the 0.6 percent sections.

Another problem evident on the project was that concrete placed on days with high atmospheric temperatures experienced more failures. Substantially more failures were found on slabs placed when the temperature was 32.2°C (90°F) or above than at lower temperatures.

In examining the performance of the project from an overall viewpoint, it is apparent that steel stress, average crack spacing, and pavement performance were affected by the percentage of longitudinal steel, the cement type, the change in temperature from the curing temperature, and the construction techniques on the project. Thus, any design procedures for CRCP should reflect these factors. The computer program recently developed in connection with the NCHRP accounts for many of these factors in the prediction of stresses, crack width, and crack spacing for a project (11). In the past, one standard design has been used regardless of the location in the state, type of subbase used, or time of placement. It is evident from the findings of this study and the NCHRP study, that all of the abovementioned factors should be taken into account when designing a project. Hence, the slabs should be designed for a range of conditions, and, then, use a specific condition on a project basis, rather than using one pavement standard, as has been done in the past.

CONCLUSIONS

1. The use of a type 3 cement with CRCP results in cracking of an explosive nature that produces a high initial stress level in the steel, possibly even overstressing the steel.
2. Results at the end of 16 years indicated that the percentage of longitudinal steel was the only factor that influenced crack spacing. However, it should be kept in mind that steel stresses during the entire period were influenced by the other factors and thus they are important in design.
3. A study of the failures on the project indicated more failures were experienced with 0.5 percent longitudinal steel than with 0.6 percent longitudinal steel, and more failures were experienced with high-curing temperatures than with low-curing temperatures. The maximum failures were observed in areas where 0.5 percent longitudinal steel and high-curing temperatures were used.
4. Good vibration during construction is necessary for satisfactory pavement performance.
5. Deflection measurements before and after an asphalt-concrete overlay indicated that the deflection reduction was approximately 5 percent for each 25.4 mm (1 in) of overlay.

RECOMMENDATIONS

1. The maximum specific surface area requirement currently used in the specifications for CRCP should be retained. The performance over a 16-year period indicates the necessity for prohibiting fine-grind cement on a large-scale basis.
2. Consideration should be given to revising the specifications to provide closer control of concrete during hot weather placement.
3. Measuring techniques for deflection and the use of a nuclear road logger should be considered on future projects to help locate problem areas, especially for those in which there is concrete honeycombing or low density.
4. The CRCP for a given project should be designed specifically by taking into account the variables enumerated in the conclusions. The CRCP-1 computer program currently available to SDHPT can be used to design the steel and concrete for a specific project by taking into account the factors that are known to influence the pavement performance.

ACKNOWLEDGMENTS

This investigation was conducted at the Center for Highway research, the University of Texas at Austin. I wish to thank the sponsors, the Texas State Department of Highways and Public Transportation and the Federal Highway Administration of the U.S. Department of Transportation.

REFERENCES

1. M. D. Shelby and B. F. McCullough. Determining and Evaluating Stresses of an In-Service Continuously Reinforced Concrete Pavement. HRB, Highway Research Record 5, 1963, pp. 1-49.
2. W. B. Ledbetter, A. H. Meyer, H. J. Treybig. A Field Investigation of Concrete Pavement in Texas. HRB, Special Rept. 116, 1960, pp. 167-173.
3. Survey of Structural Failures in a Continuously Reinforced Concrete Pavement. Texas Highway Department, Rept. SS1.1, Oct. 1969.
4. B. F. McCullough and P. Strauss. A Performance Survey of Continuously Reinforced Concrete Pavements in Texas. Center for Highway Research, Univ. of Texas at Austin, Res. Rept. 21-1F, Nov. 1974.
5. B. F. McCullough and C. L. Monismith. Application of a Pavement Design Overlay System. Center for Highway Research, Univ. of Texas at Austin, Special Rept. 1, Oct. 1969.
6. Experimental Project for a Continuously Reinforced Concrete Pavement: Post Construction Report. Bureau of Public Roads, U.S. Department of Commerce, Repts. 1-3, Dec. 1961.
7. F. Shenkir. Cracking Patterns on IH-45 Continuously Reinforced Concrete Pavement. Texas Highway Department, May 1961.
8. J. Nemec. Paving Operation: Continuously Reinforced Concrete Pavement—Walker County Experimental Project. Texas Highway Department, Rept., Sept. 1961.
9. H. J. Treybig. Repair of Continuously Reinforced Concrete Pavement. Texas Highway Department, Res. Rept. SS7.0, Aug. 1969.
10. B. F. McCullough and T. F. Sewell. An Evaluation of Terminal Anchorage Installations on Rigid Pavement. Texas Highway Department, Res. Rept. 39-F, Sept. 1966.
11. B. F. McCullough, A. Abou-Ayyash, W. R. Hudson, and J. P. Randall. Design of Continuously Reinforced Concrete Pavements for Highways. Center for Highway Research, Univ. of Texas at Austin, Res. Rept. NCHRP 1-15, Aug. 1974.

Publication of this paper sponsored by Committee on Rigid Pavement Design.

Effectiveness of Pressure-Relief Joints in Reinforced Concrete Pavements

K. H. McGhee, Virginia Highway and Transportation Research Council

This paper discusses the effectiveness of a 100-mm (4-in) wide compressible material that was installed at 305-m (1000-ft) intervals in a jointed, reinforced concrete pavement to reduce pavement blowups. The studies were made on an Interstate highway that carries some 30 000 vehicles/d, which includes approximately 7000 trucks and buses. This paper compares the behavior of the pavement both before and after the installation of the pressure-relief joints. Brief discussions of the factors that indicate the need for such joints, the problems associated with their use, and the potential for their use under overlays are included.

The performance of jointed concrete pavements in some areas of Virginia has been seriously impaired by the infiltration of incompressible materials into the joints, which results in blowups. This infiltration can come from below the pavement because of the slab-pumping action related to water trapped below the pavement structure, or it can come from above the pavement because of poorly sealed transverse joints. Water is entrapped when the densely graded subbase materials prohibit drainage through the shoulder (1). Transverse joints are poorly sealed when the long slabs and narrow joints, which have seasonal hydrothermal movements, are in excess of the capabilities of the sealing materials (2). The causes and mechanism of blowups in the state have been discussed in a report by Tyson and McGhee (3).

Corrective action to overcome pumping and blowup problems in Virginia has not been totally successful. Pavement-edge drains are effective in removing en-

trapped water, but they are costly and time-consuming to install after the fact and are used only in the worst pumping cases. Maintenance contracts to replace or patch damaged joints and to furnish preformed seals have been successful in most cases, but, in several instances, the patches have failed early and at a rapid rate.

One case of early patch failure took place on a maintenance contract executed in 1973 on I-95 in Spotsylvania County. As a result of a study in that area, it was suggested that residual pressures in the pavement were among several factors that caused the premature patch failure. However, joint movement studies were also made in that same area over a period of several years, and these studies showed that the occurrence of a blowup tends to relieve pavement pressures for some 150 m (500 ft) on either side of the blowup. Consequently, it was concluded that, if special stress-relieving joints were provided, pavement pressures might be reduced, and, thus, subsequent failures would also be reduced.

Therefore, in October 1973, a pilot experiment was conducted in which three pressure-relief joints were installed on a segment of I-95 where maintenance operations were under way. The joints were installed approximately 305 m (1000 ft) apart, and they extended the full width of the 7.3-m (24-ft) pavement. Because of the difficulty in sawing dowels and the danger of unstable subbase conditions near the old joints, the relief joints were installed at midlength on the 18.7-m (61.5-ft) long slabs. Two parallel saw cuts that were spaced 100 mm (4 in) apart were made through the full depth of the slabs. After the concrete was removed, two of the joint openings were filled with a patented sponge rubber product, and the third was filled with a styrofoam rubber.

Movement was measured as soon as the pressure-relief joints were installed. During the spring of 1974, which was about 8 months after the joints were in place, the measurements showed that the closures were from 28 to 80 mm (1.1 to 3.2 in). These large movements showed that pavement pressures were significantly relieved by provision of the special joints. In addition, field personnel were pleased with the performance of the relief joints and reported that no blowups occurred in their vicinities and that no difficulties with the performance of the joints themselves were noted. Finally, it was noted that the relief joints themselves are good indicators of pavement pressures. For example, a field engineer might decide that when a relief joint 100 mm (4 in) wide has closed to less than 25 mm (1 in) pavement pressures have reached the point where additional relief joints or restoration of the original 100-mm (4-in) wide joint is justified.

On the basis of the above information, a contract for pavement repair and resealing was let on I-95 in September 1974. As part of this contract, pressure-relief joints were installed in pavements where early distress of previous repairs had been noted. The relief joints were installed at approximately 305-m (1000-ft) intervals in both directions on a 24-km (15-mile) segment of I-95.

The increasing use of the pressure-relief joints in various parts of the state has indicated a need for quantitative data concerning their effectiveness. The development of these data was the objective of the study reported here.

PURPOSE AND SCOPE

As indicated above, the purpose of the study was to evaluate the effectiveness of pressure-relief joints in protecting jointed concrete pavements from the self-destructive effects of joint infiltration and seasonal hydrothermal movements. The study included approximately 24 km (15 miles) of I-95, which is divided into four lanes. Data were collected on the performance of the 230-mm (9-in) reinforced concrete pavement for periods of 8 months before and 8 months after installation of the pressure-relief joints. Information was also developed as a basis for brief discussions of the factors that led to the need for and use of relief joints under overlays.

RELIEF JOINT DESIGN

Pressure-relief joints are 100 mm (4 in) wide and are installed full depth [230 mm (9 in)] and full width [7.3 m (24 ft)] of the pavement. The pavement has contraction joints that are nominally 10 to 13 mm (⅜ to ½ in) wide and that are spaced on 18.7-m (61.5-ft) centers.

For cases in which major joint repairs, including full-depth joint replacement, were required, the relief joints were installed as shown in Figure 1. Pressure-relief joints installed in conjunction with such full-depth repairs are type A. For reasons given earlier, when no full-depth pavement repairs were necessary, the relief joints were installed at midlength of the 18.7-m (61.5-ft) long slabs. These installations are type B. A total of 142 relief joints were installed in the 24-km (15-mile) long segment of roadway. The relief-joint filler material is preformed, cellular-plastic, pressure-relief joint filler that meets the requirements of American Society of Testing and Materials specification D 3204.

The pressure-relief joints were installed in projects 1, 2, and 3, according to construction completion dates of May 27, 1964; October 22, 1963; and May 3, 1965 respectively.

PROCEDURES

Evaluation procedures included pavement-condition surveys and a study of the pavement movements as reflected in the closure of selected pressure-relief joints. Four condition surveys were conducted as follows:

1. Winter 1973-1974—The first survey was conducted in February 1974 as a part of other studies on the three projects.
2. Fall 1974—The second survey was conducted immediately before repairs were begun on the three study pavements and was completed in September 1974. The results from this survey, during the spring and summer of 1974, were compared with those from the first survey to determine pavement damage that might be related to pavement pressures.
3. Winter 1974-1975—The third survey was conducted after the repairs were completed and the pressure-relief joints were installed. The contractor began work on October 15, 1974, and the survey was completed in April 1975.
4. Fall 1975—The final survey was conducted during the spring and summer of 1975 and completed in October 1975. This survey was made to obtain data for determining the damage subsequent to the repairs.

Each survey included a detailed summary of pavement conditions at the time the survey was made. Every pavement joint was noted on a sketch in which the defects from the other surveys were superimposed on one another. In the survey made immediately after repairs were completed, each pressure-relief joint was noted. Defects that were directly related to pavement pressures such as blowups were especially identified.

Information concerning pavement movements that were influenced by pressure relief was provided by measuring the width of each relief joint shortly after installation and

at the time of the last survey. In addition, several sites were chosen for the installation of instrumentation at intermediate joints. This instrumentation, gage points imbedded in the pavement on either side of selected joints, made it possible to study the effect of the relief joints on adjacent joints. The final field work was completed in December 1975, and it involved choosing one section of pavement between the pressure-relief joints for a detailed study of the joint movement associated with the release of pavement pressure. The joint cleaning and resealing work that was done about the same time the relief joints were installed resulted in saw cuts in the bituminous shoulders so that the location of each joint before the pressure was relieved could be established. Each of the above aspects of the overall study is discussed below.

Figure 1. Cross section view of type A pressure-relief material in a full-depth pavement repair.

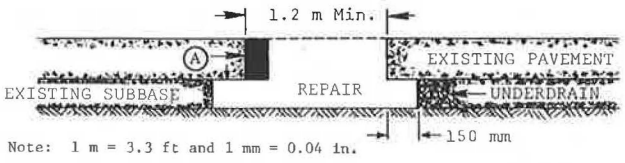

Note: 1 m = 3.3 ft and 1 mm = 0.04 in.

Table 1. Blowup occurrence with and without pressure-relief joints.

		Blowups		
		Without Joints		With Joints
Project	Lane	To February 1974	Summer 1974	Summer 1975
1	NB	25	8	0
1	SB	29	5	0
2	NB	18	0	0
2	SB	18	4	0
3	NB	3	5	0
3	SB	2	2	0
Total		95	24	0

Table 2. Total number of distressed joints.

		Total Relief Joints	Distressed Joints			
Project	Lane	Surveyed	1/74	9/74	4/75	10/75
1	NB	418	249	267	287	293
1	SB	412	217	248	255	259
2	NB	395	302	309	316	319
2	SB	402	258	276	285	294
3	NB	488	96	111	114	120
3	SB	493	47	62	67	70

Table 3. Average widths of pressure-relief joints.

		Relief Joints In Each	Joint Width (mm)			Total Closure
Project	Lane	Lane	Installed[a]	5/75	10/75	(mm)
1	NB	23	104	—	70	35
1	SB	20	109	89	82	27
2	NB	20	105	—	67	38
2	SB	21	108	81	71	37
3	NB	30	105	—	55	50
3	SB	26	103	55	38	65
Average			106	73	62	43

Note: 1 mm = 0.0393 in.
[a]From 10/74 to 3/75.

EFFECT OF PRESSURE-RELIEF JOINTS

The effectiveness of the pressure-relief joints in halting the occurrence of blowups is given in Table 1. Before installation of the relief joints there were 24 blowups in the 24-km (15-mile) segment during the summer of 1974, whereas after the relief joints were in place, there were no blowups in the summer of 1975. Therefore, it may be concluded that the relief joints were totally effective during their first summer in service. The observations, which are discussed later, made on the current widths of the relief joints suggest that they should be effective for several more years.

The differences in pavement performance indicated by the number of blowups for the three projects before February 1974 are of interest. There is evidence that the differences in performance are related to at least two factors:

1. The lower-strength concrete found in projects 1 and 2 (evidenced by signs of poor consolidation or high water content), and
2. The presence of better draining subbase and shoulder material under project 3.

The relation between blowup frequency and pavement strength is evidenced by the fact that lower-strength concrete will fail at a pressure lower than that for higher-strength concrete. The relation between blowup frequency and subbase type for these projects has been discussed in an earlier report (3). It was pointed out that the pavement pumping associated with poor subbase material may result in the migration of fine, incompressible material into the joints from their outer edges and bottom portions (3). It was also shown in that study that the modified subbase used on project 3 reduced pumping by approximately 75 percent.

The abovementioned factors, along with the metal joint-forming insert used in project 2, contributed to the differences in total joint distress that were experienced by the three projects. Total distress, in terms of the number of joints affected, is given in Table 2. Although there is a greater blowup frequency for the joints in project 1, the total number of distressed joints in project 2 is greater than that in project 1. This difference is due to the presence of the metal joint-forming insert that results in numerous semicircular joint spalls located in the wheel paths. This phenomenon was also discussed in the earlier report (3).

An examination of the new occurrences of joint distress in the summers of 1974 and 1975 suggested that the pressure-relief joints were at least partially effective in reducing the rate of development of distress other than blowups. The northbound lane (NBL) of project 1 had 18 new occurrences of joint distress in the summer of 1974, but only 6 occurrences during the summer of 1975 after the relief joints were installed. Similarly, the southbound lane (SBL) of project 3 had 15 and 3 occurrences for the summers of 1974 and 1975 respectively.

Pavement Movement

The effectiveness of pressure-relief joints in reducing pavement distress, particularly blowups, was discussed above; however, there are some characteristics of the relief joints themselves that affect pavement movement. These characteristics are (a) the behavior of the relief joints, and (b) the effect of the relief joints on the movement of other joints in the vicinity of and between the relief joints.

Joint Closure

In sections of the roadway where there is appreciable pressure, the relief joints begin to close almost as soon as they are installed. Pavement pressures of some significance are indicated by the difficulty in making the saw cut because of blade pinching and by the difficulty in removing the sawed segment.

Tests in the Research Council laboratories have shown that a pressure of approximately 165 kPa (24 lbf/in^2) is required to compress the 100-mm (4-in) wide, pressure-relief material to 50 percent of its original width. This pressure is negligible even on very weak concrete, but it is sufficient to hold the relief material tightly in place.

The widths of all pressure-relief joints in the three study projects were measured soon after they were installed (October 1974 and March 1975) and at the end of the study period (October 1975). In addition, those in the SBL were measured at an intermediate stage (May 1975). These measurements are given in Table 3.

Several significant observations can be made from the data given in Table 3. First, the average relief-joint closure of 43 mm (1.71 in) during the first year suggests that there were very significant stresses remaining in the pavement, even though numerous blowups had already relieved these stresses in many areas. Second, a careful study of the data shows that about 75 percent of the total closure occurred before the summer months when stresses, if unrelieved, would be the highest. This finding clearly indicates that pavement stresses, even in the winter, were too high to be relieved by the natural tendency of the pavement to shrink in cold weather. Third, project 3, which had the lowest blowup frequency, showed significantly more closure of the relief joints during the summer of 1975 than did the other two projects. Thus, project 3 was observed closely to determine if there was a need for additional relief joints. As indicated earlier, the higher-strength concrete in this project sustained more pressure without failure. However, the relative increase in blowups for this project shortly before the installation of the relief joints, along with the behavior of these joints, indicates that the project would become subject to blowups when the benefits of the relief joints are completely exhausted. The SBL of this project sustained only 4 blowups in its 10-year life, but after only one summer, the relief joints closed an average of 65 mm (2.57 in) or about 65 percent. Such behavior reinforces the previously mentioned possibility that pressure-relief joints can be used to indicate pavement pressures so that corrective action can be taken before pavement damage results.

The relative behaviors of types A and B relief joints are of some interest. The following is the annual relief-joint closure for each project and each type of joint (1 mm = 0.393 in).

	Annual Average Closure (mm)			Annual Average Closure (mm)	
Project	Type A	Type B	Project	Type A	Type B
1	27	35	3	48	65
2	37	38			

It should be recalled that type A joints were installed in conjunction with full-depth pavement repairs while type B were installed at midslab length in sound pavement sections. In many cases, the full-depth repairs were made on blowup sections where pavement stresses had been partially relieved because of the blowups. Therefore, it is not surprising to find that the type B joints were somewhat more effective because no natural stress relief had been provided before installation of the joints. This finding suggests that, in future installations, it may be advisable to omit type A joints in lieu of providing more type B joints at strategic locations.

Movement of Intermediate Joints

The movement of intermediate joints within a typical section that has pressure-relief joints at each end is shown in Figure 2. The section is comprised of 17 slabs, and each slab is 18.8 m (61.5 ft) long. Individual joint movements were measured from the saw marks in the asphalt-concrete shoulder, as previously mentioned. As expected, the movement was maximum at the pressure-relief joints, gradually decreased toward the center of the section, and was negligible at the center. In all cases, joint movement was toward pressure-relief joints with the node point at midsection, which indicated a balance of pavement pressures and movements. The dramatic pavement behavior at a relief joint in service for 1 year is shown in Figure 3.

It is clear from the above data that relief joints were effective for at least the 300 m (1000 ft) contained in the typical section. Careful study of Figure 2 also suggests that the relief joints might have been capable of providing some stress relief for sections longer than 300 m (1000 ft). Theoretically, the joints are effective until there is more than one stationary joint at midsection. The determination of the maximum effectiveness of a section length is not a straightforward procedure. A paradox develops when one considers that the more internal stresses a pavement has, the longer the effectiveness of a section length will be. Conversely, when there are few internal stresses, the relief joints may be immediately effective only over a short distance. In the latter case, the relief joints are probably not needed, but, if used, they will serve for a long period of time. Several examples of this behavior occurred in projects 1 and 2 in which the pressure-relief joints were installed close to the blowups. Because pavement pressures had already been relieved, these relief joints closed less than 13 mm (½ in) during their first year in service.

One type of undesirable behavior of joints between relief joints is shown in Figure 4. An intermediate joint opened so widely that the preformed compression seal was no longer in contact with the walls of the joint. This behavior gives rise to the possibility of initiating a vicious circle in which the provision for too much freedom of joint movement can create conditions in which joint infiltration is aggravated, and, in turn, can require the provision for more pressure relief. Such behavior only occurs at the joints that are located near the relief joints or previous blowups. Since it is not possible to predict when an excessively wide opening might occur, it appears that pavements with preformed seals should be observed for some time after the relief joints are installed. This possibility of an excessively wide, intermediate joint opening is one consideration that should not be overlooked when deciding to use relief joints. There may be instances in which it is advisable to install several relief joints for purposes of observation, possibly 1 year before full-pressure relief is contemplated. Thus, a final determination of the need for the joints could be made.

It is interesting to compare the movement of joints in a pavement that has no stress relief with that of a pavement that has relief joints located at 300-m (1000-ft) intervals. This comparison is shown in Figure 5 for the period of April through September 1975. Although the seasonal movement for the control section was approximately 0.20 mm (0.008 in), the joint located 18.7 m (61.5 ft) from a pressure-relief joint opened a total of 4.5 mm (0.18 in). Similar but less severe movements were recorded for joints located 56.3 m (184.5 ft)

Figure 2. Joint shift between pressure-relief joints.

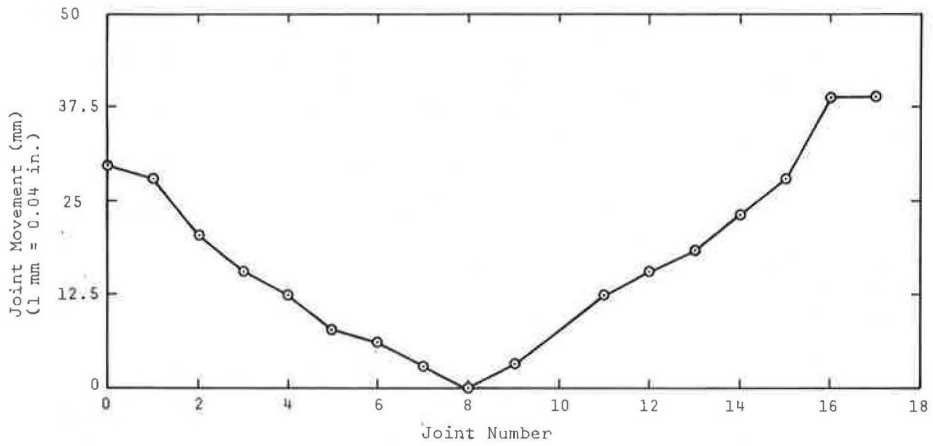

Figure 3. Closure of pressure-relief joint after 1 year in service.

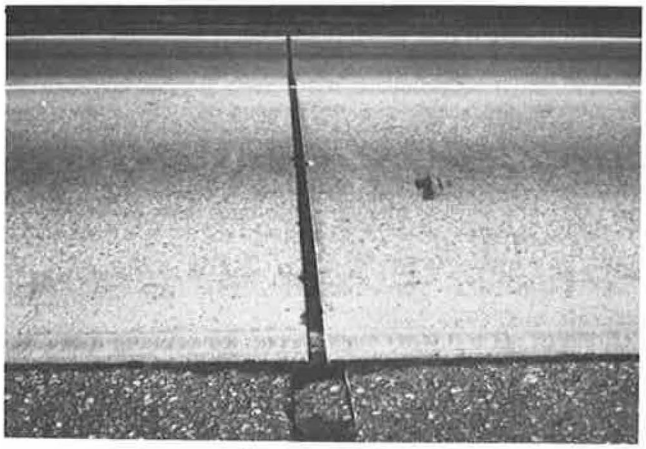

Figure 4. Excessive opening of joint near pressure-relief joint.

and 93.8 m (307.5 ft) from the pressure-relief joints. The pavements contrasted in this figure are also discussed in an earlier report (3) in which the behaviors of pavements that are prone to blowups were compared with those pavements of the control section that had no history of blowups.

Figure 5. Comparison of pavements with and without pressure-relief joints.

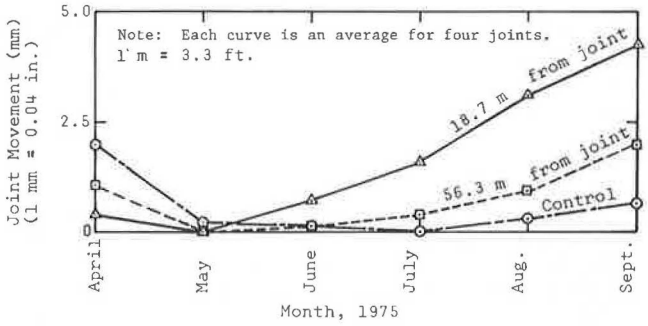

Figure 6. Failure caused by redistribution of stresses between lanes, repairs in near lane, and new blowup in far lane.

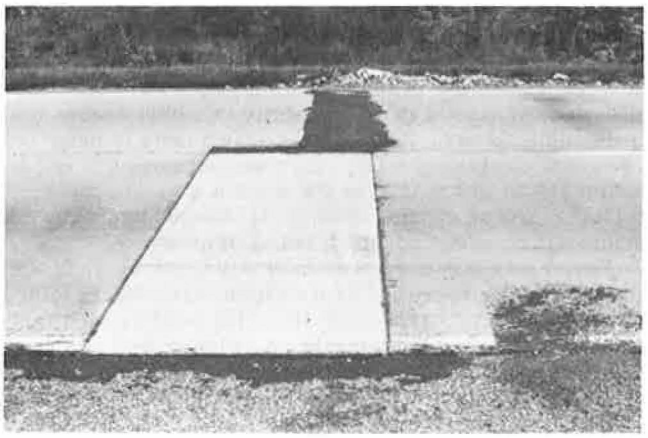

PROBLEMS WITH PRESSURE-RELIEF JOINTS

The use of pressure-relief joints in several locations, including the one discussed earlier, has shown that certain precautions are necessary to achieve their most effective use. Some of these precautions and the related problems are discussed below. Virginia specifications that have been developed for installation of the pressure-relief material have recently covered several of these precautions.

Multilane Pavements

The pressure-relief material will almost always be used on pavements that have more than one traffic lane; therefore, it is usually impossible to install the material for the full width of the pavement in 1 d. However, the relief of pressure in one lane can substantially increase the pressures in other lanes so that the unrelieved lanes become subject to blowups. Therefore, it is necessary to install relief joints in all adjoining lanes as soon as possible. Figure 6 shows a pavement on which repairs and pressure relief were provided for the near lane, while the sound far lane was left until later. Unfortunately, several weeks of warm weather passed and a blowup occurred in the far lane before the work crew returned to install the pressure relief joint in that lane.

For cases in which the adjoining lane is made of good quality concrete, restraint between the lanes has prevented the pressure-relief joint from functioning, thus, the material is not held tightly in position and can float out during a heavy rain.

Both of these potential problems should be prevented by the new specifications that require installation of the pressure-relief material in adjacent lanes within 24 h. This specification also places restrictions on the width of the material and requires the use of a lubricant-adhesive to install the material, which provides further insurance against floating.

Hot Weather

The high pressures encountered in the pavement during hot weather make the summer a poor time for installing pressure-relief joints, even though the need might be greatest in this season. Saw-pinching problems and the problem of unequal pressures between lanes are both aggravated during warm weather. Therefore, the new specifications mentioned above provide for the installation of pressure-relief material in a temperature range of from 4 to 20°C (40 to 70°F).

Too Frequent Installation

In a few instances, pressure-relief joints have been ineffective because of their proximity to other stress-relieving features. Although there is a need to judge the pavement condition, relief joints are not normally needed within 150 to 180 m (500 to 600 ft) of a standard XJ-1 bridge approach expansion joint (4), because such a joint inherently provides adequate relief of pressure.

Pavements that have sustained full-width blowups may not need pressure-relief joints within about 150 m (500 ft) of the blowups, especially if the blowup has been temporarily repaired with bituminous concrete and has remained in that condition for some period of time. This natural relief of pavement pressures will be indicated by unusually wide joints in the vicinity of the blowup.

PROVISION OF PRESSURE-RELIEF JOINTS

Because the provision of pressure-relief joints is a rather expensive and time-consuming operation, the following discussion is offered. Pavements that have no history of blowups should not have pressure-relief joints installed until the history and condition of the pavement have been carefully considered. Extensive studies of pavements that are prone to blowups in Virginia have shown that blowups will occur or are impending when some or all of the following factors exist.

1. The pavement is more than 5 or 6 years old,
2. The transverse joints are poorly sealed,
3. The pavement is subject to joint or edge pumping because of a poor quality subbase,
4. The pavement is constructed of concrete that contains a siliceous coarse aggregate,
5. Sand or other traction-improving aids are used liberally on the pavement,
6. The pavement is constructed of slabs more than 6 to 9 m (20 to 30 ft) long,
7. The pavement is constructed of poor quality concrete,
8. Dowel bars are misaligned during pavement construction, and
9. Truck traffic volume is high.

Not all of the above factors will be present in every pavement that is prone to blowups, and not all of the factors are given equal weight. For example, when other conditions are equal, pavements with 18.8-m (61.5-ft) long slabs appear to be subject to more blowups than those with shorter slabs. On the other hand, pavements with short slabs have been observed to blowup, but only after many years of service and under adverse conditions. Similarly, pavements can become subject to blowups because of surface infiltration, infiltration from the subbase, or a combination of the two.

Because the relative contributions of each factor noted above are poorly defined, it is necessary to make field inspections so that the probability of blowups can be determined. In general, at least two or three of the following types of visual evidence will be present when blowups are impending.

1. Some transverse joints are tightly closed while others are wide and badly infiltrated.
2. The presence of fines on the shoulder or a depression of the shoulder at the pavement edge show evidence of joint pumping.
3. Joint faulting is evident.
4. Misalignment of the transverse joints is evident, especially at lane additions or drops.
5. Transverse joints show evidence of crushing.

PROVISION UNDER OVERLAYS

Observations have shown that pavements subject to blowups while in service as a wearing course will often be subject to blowups after they have been overlaid with a bituminous-concrete surface. For this reason, the decision was made to provide pressure-relief joints on I-495 in Northern Virginia when it was widened. The 7.2-m (24-ft) wide existing pavement had suffered a number of blowups in its approximately 10-year life. The primary factors contributing to these blowups were heavy traffic, poor subbase, difficult-to-maintain joints, and long slabs. Since these conditions could not be effectively corrected as a part of reconstruction, the provision of pressure-relief joints was an acceptable effort to reduce future maintenance. Relief joints were also called for in the base so that the old pavement and the 7.2 m (24 ft) of widening base concrete would function together. While the project was still under construction, most of the pavement and widening had been overlaid, and this did not cause any apparent adverse effects other than a slight depression in the overlay at some relief joints. Many of the relief joints closed up to 50 mm (2 in), which is an indication that they were serving their intended purpose.

Based on this experience, it would appear reasonable to continue the use of pressure-relief joints under overlays if an old pavement has a history of blowups or if the causative factors that contribute to blowups are in evidence.

CONCLUSIONS

1. Pressure-relief joints can contribute substantially to the reduction of blowups and general distress of portland-cement concrete pavements.
2. Pavement containing pressure-relief joints can experience an excessively wide opening of intermediate joints such that the effectiveness of preformed seals is impaired.
3. Rapid, pressure-relief joint closure may be an indication that additional relief is needed.
4. Pressure-relief joints installed at midslab are somewhat more effective than those installed in conjunction with full-depth pavement repairs.
5. Pressure-relief joints are not useful when they are in close proximity to a bridge that has protection expansion joints or when they are near blowups where a full-depth or full-width portion of a pavement has been replaced with bituminous concrete.
6. When making the decision to provide pressure-relief joints, careful consideration should be given to the pavement design and performance history.
7. Pressure-relief joints can be used effectively under bituminous-concrete overlays on portland-cement concrete pavements.

ACKNOWLEDGMENTS

I gratefully acknowledge the cooperation and interest of R. W. Gunn for the collection and analysis of data. The efforts of J. P. Bassett and R. P. Wingfield are sincerely appreciated for reviewing a draft of this report.

This work was conducted under the general direction of J. H. Dillard of the Virginia Highway and Transportation Research Council and was financed from state research funds.

The opinions, findings, and conclusions expressed in this paper are mine and are not necessarily those of the sponsoring agencies.

REFERENCES

1. H. R. Cedergren and A. G. Kneeland, Jr. Water: Key Cause of Pavement Failure. Civil Engineering, Sept. 1974.
2. K. H. McGhee and B. R. McElroy. Study of Sealing Practices for Rigid Pavement Joints. Virginia Highway and Transportation Research Council, June 1971.
3. S. S. Tyson and K. H. McGhee. Deterioration of Jointed Portland Cement Concrete Pavements. Virginia Highway and Transportation Research Council, Nov. 1975.
4. Road Designs and Standards. Virginia Department of Highways and Transportation, 1975.

Publication of this paper sponsored by Committee on Rigid Pavement Design.

Performance Evaluation for Bituminous-Concrete Pavements at the Pennsylvania State Test Track

M. C. Wang and T. D. Larson, Pennsylvania State University

The Pennsylvania State Test Track, which was completed in August 1972, will be used to develop engineering data and criteria for the design and construction of new pavements and for the improvement and maintenance of existing pavements. The test track is composed of sections with various base-course materials and different layer thicknesses. This paper presents the results of performance analyses for sections containing bituminous-concrete base. The analysis was made by using an elastic-layer computer program; only the spring weather condition was considered. Critical responses analyzed were maximum vertical compressive strain at the top of the subgrade, maximum radial tensile strain at the bottom of the base course, and maximum deflection on the pavement surface. Performance data collected included present serviceability index, rut depth, and cracking. Correlations between critical response and pavement performance were established. These correlations permit prediction of pavement performance from pavement response determined in the spring season. A maximum compressive strain of 450 μm/m (0.000 450 in/in) at the top of the subgrade, a maximum tensile strain of 120 μm/m (0.000 120 in/in) at the bottom of the base course, and a maximum deflection of 0.51 mm (0.020 in) on the pavement surface were established as the limiting criteria for flexible pavements with bituminous bases to withstand 1 000 000 applications of an 8165-kg (18-kip) axle load without significant fatigue cracking. Based on these limiting criteria, structural coefficients of the bituminous-concrete base and the crushed-limestone subbase were developed. The structural coefficients vary significantly with layer thickness.

Recognizing the need for an integrated program for pavement research, The Pennsylvania Transportation Institute in cooperation with the Pennsylvania Department of Transportation constructed a one-lane 1.6-km (1-mile) long highway. This facility was completed in August 1972 and is located 9.7 km (6 miles) northeast of State College and 1.1 km (0.7 miles) northeast of University Park Airport in an agricultural area owned by the Pennsylvania State University.

The goal of pavement research at the facility is to develop engineering data and criteria that can be used in the design and construction of new pavements and in the improvement and maintenance of existing pavements. To achieve this goal, two long-range objectives were developed to guide research at the facility. The first is to validate, refine, or, if necessary, regenerate the flexible-pavement design procedure in Pennsylvania. The second is to evaluate the ability of existing pavement-damage models to predict pavement performance.

This paper presents the results of the performance evaluation based on pavement response for the sections that have a bituminous-concrete base course. From field performance data together with pavement response, limiting strain and limiting deflection criteria were de-

veloped. Based on these criteria, structural coefficients of the bituminous-concrete base and limestone subbase were determined.

PENNSYLVANIA STATE TEST TRACK

In the first cycle of study, the test track was composed of 17 sections of various lengths. Each section contained either different base-course materials with the same layer thickness or one type of base material with different layer thicknesses. After the first cycle of study was completed, one section was resurfaced with a 6.3-cm (2.5-in) overlay and four sections were replaced by eight shorter sections. Figure 1 shows the plan view and the longitudinal profile of the test track.

The subgrade soil had classifications ranging from A-4 to A-7, and the predominant classification was A-7. The average in situ dry density, moisture content, and soaked California bearing ratio were about 1690 kg/m^3 (105.5 lb/ft^3), 18.9 percent, and 11 respectively. The subbase material was a crushed limestone, natural to central Pennsylvania. The four different base-course materials used were bituminous concrete, aggregate-lime-pozzolan, aggregate-cement, and aggregate-bituminous. Only the bituminous-concrete sections are analyzed in this paper.

The wearing surface was constructed with one type of material for the entire test track. Seven sections were surfaced with a 3.8-cm (1.5-in) wearing course. Other sections had a 2.5-cm (1.0-in) wearing course underlaid by a 3.8-cm (1.5-in) ID-2A binder course. The characteristics of the wearing, binder, base, subbase, and subgrade materials are given elsewhere (1).

Since the testing facility was designed for an accelerated life, the test track was subjected to traffic for 18 h/d, 7 d/week for the first 11 months and then for 10.5 h/d, 5 d/week for an additional 9 months. The first cycle of study was completed in December 1974, and, by that time, all sections had been subjected to about 1 100 000 applications of an 8165-kg (18-kip) equivalent axle load (EAL). For the second cycle of study, traffic operation began in December 1975. Because of bridge construction, traffic operation was discontinued in May 1976. By that time, a total of about 1 500 000 EAL applications had been applied to the old pavements. The traffic was a conventional truck tractor that pulled a semitrailer and a full trailer. Complete information on design, construction, material properties, and traffic operation is documented elsewhere (1, 2).

FIELD MEASUREMENTS

Field testing of pavement response and measurement of test track performance were conducted periodically. Surface deflections were determined biweekly by using the Benkelman beam and the road rater. Rut depth was measured weekly every 6.1 m (20 ft) on both wheel paths by using an A-frame that was attached to a 2.1-m (7-ft) long base channel. Surface cracking was surveyed and mapped weekly; the total length of class 1 crack and the total area of class 2 and class 3 cracks were determined. Surface roughness was measured biweekly by using a MacBeth profilograph on both wheel paths. The roughness factors obtained from the profilograph data were converted into present serviceability index (PSI) of the pavement by using the following equations:

$$PSI = 11.16 - 4.06 (\log RF) \quad (1)$$

$$RF = 63.27 + 1.083 (R) \quad (2)$$

where

R = profilograph readings and
RF = roughness factor.

Equation 1 was developed by the Bureau of Materials Testing and Research of the Pennsylvania Department of Transportation, and it is based on the correlation of profilograph data with the PSI value that was obtained by using a surface dynamic profilometer.

In addition to the above testing and measurements, pavement temperature profile and subgrade moisture distribution were measured by using thermocouples and moisture cells. These cells were embedded at various depths in various sections. Also, two frost-depth indicators were installed in the pavement to measure the depth of frost penetration. Various meterological gauges were installed at the track to collect weather data that included wind velocity, precipitation, and temperature.

PERFORMANCE DATA

Figure 2 shows the variation of PSI with an 8165-kg (18-kip) EAL application. Each value represents the average of both wheel paths. Section 8, which was overlaid at the end of the first cycle of study, reached a PSI value of 2.1. Also, the initial PSI values are generally low and vary considerably. For this reason, the analysis presented later considers only the difference in PSI that occurred after the initial measurements in August 1972.

The number of 8165-kg (18-kip) EAL applications when significant fatigue cracking was observed, the total length of class 1 cracks, and the total area of class 2 and class 3 cracks are given in Table 1. These crack data form major bases for determination of limiting criteria used in the analyses.

MATERIAL CHARACTERIZATION

The material properties needed to analyze the pavement response were determined by using various testing methods. Both a static-plate load test and laboratory-repeated load tests on laboratory-compacted specimens were used to determine the elastic modulus of each constituent layer. The laboratory-repeated load tests were conducted under various deviating and confining pressures. Results obtained from these two test methods agreed reasonably well, although the plate load test generally gave relatively higher moduli values. Final selection of appropriate elastic moduli from these two sets of results was made by using an elastic-layer computer program in conjunction with the surface deflection data determined from the Benkelman beam tests. Figure 3 shows the elastic moduli of surface and base materials for various temperatures. The subgrade modulus decreases significantly with increasing moisture content and is approximately 55.2 MPa (8000 lbf/in^2) at a moisture content of 23 percent. The subbase modulus equals about 330.9 MPa (48 000 lbf/in^2).

Fatigue tests on beam specimens of surface and bituminous-concrete base materials were conducted by the Asphalt Institute (3). These tests were performed at three temperatures: 13, 21, and 29° C (55, 70, and 85° F) on high-density specimens and only a limited number of tests on low-density specimens. The values of the constants in the following fatigue equation were evaluated and are given in Table 2.

$$N = K_1 (1/\epsilon)^{K_2} \quad (3)$$

where

N = number of load repetition to failure,

Figure 1. Plan view and longitudinal profile of test track.

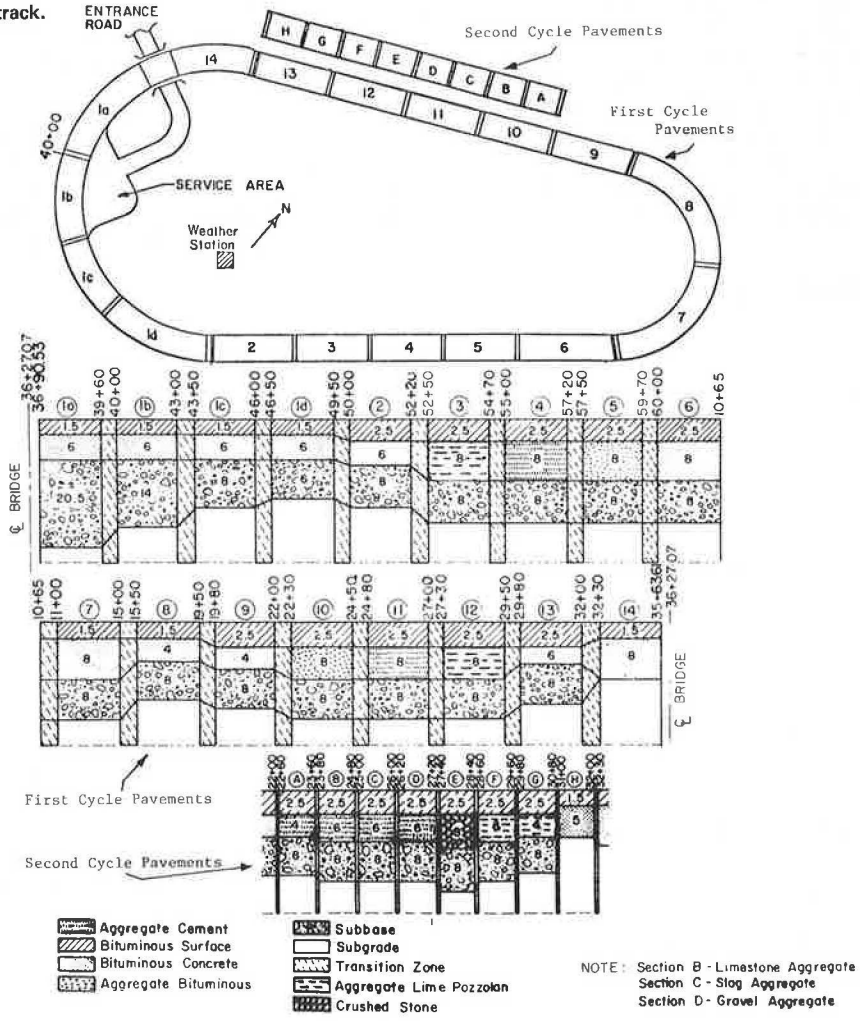

Figure 2. Variation of present serviceability index versus test sections with 8165-kg equivalent axle loads.

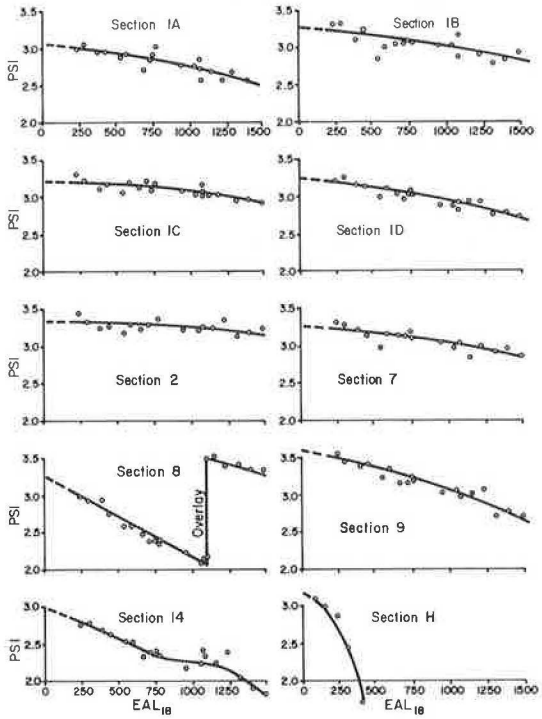

ϵ = tensile strain, and
K_1 and K_2 = constants.

These results were developed from laboratory-compacted beam specimens tested under a frequency of 20 cycle/min and a duration of 0.1 s.

ANALYSIS OF PAVEMENT RESPONSE

The response of the test pavements to traffic loading was analyzed by using an elastic-layer computer program together with the material properties obtained above. The computer program adopted was the Bitumen Structures Analysis in Roads (BISAR) program that was developed at Koninklijke Shell Laboratorium in Amsterdam. Only the spring weather condition was considered in the analysis because of the spring thaw effect. The pavement temperature and moisture data indicate an average surface temperature of about 21° C (70° F) and subgrade moisture of 23 percent in the spring season. Also, the temperature in the base layer was about -15.6° C (4° F) below the surface temperature. These temperature and moisture data were used to select appropriate moduli values for surface, base, and subgrade materials.

The trend of decreasing temperature with increasing depth was accommodated by dividing all base courses that were thicker than 15.2 cm (6 in) into two equal layers. The temperature of the lower sublayer was then taken at -15.6° C (4° F) below that of the upper sub-

layer. Therefore, these sections were treated as a system of four elastic layers overlying an elastic half space. Poisson's ratios were assumed to be 0.40, 0.35, 0.40, and 0.45 for the surface material, base material, subbase material, and subgrade soil respectively.

The traffic loading used was an 8165-kg (18-kip) EAL on dual wheels that had a tire pressure of 552 kPa (80 lbf/in^2). Critical responses analyzed were maximum radial tensile strain in the surface and the base layers, maximum vertical compressive strain in the subgrade, and maximum deflection on the pavement surface. These critical responses were considered because the maximum tensile strain and the maximum surface deflection are associated with fatigue cracking, whereas the maximum vertical compressive strain is related with rutting. It was found, for the conditions analyzed, that in most cases the maximum tensile strain occurred at the bottom of the base course below the center of a loading wheel and the maximum compressive strain occurred at the top of the subgrade mostly under the middle of the dual tires.

Table 1. Results of crack survey.

Section	Number of EALs at First Appearance of Significant Cracking	Amount of Cracking[a]	
		Class 1 (m/km^2)	Class 2 & 3 (m^2/km^2)
1A	—	None	None
1B	—	None	None
1C	1 367 000	None	10 000
1D	1 367 000	None	14 000
2	—	None	None
6	—	None	None
7	—	None	None
8	386 000	—	85 500[c]
9	1 137 000	322 000	122 000
13	—	None[b]	None[b]
14	906 000	49 000	95 500
H	359 000	—	330 000

Notes: 1 m = 3.28 ft, 1 m^2 = 10.8 ft^2, and 1 km^2 = 0.386 mile^2.
[a] As of 7/19/76 EAL = 1 441 000.
[b] At the end of first cycle of study.
[c] Before overlay.

Figure 3. Elastic moduli of surface and base materials.

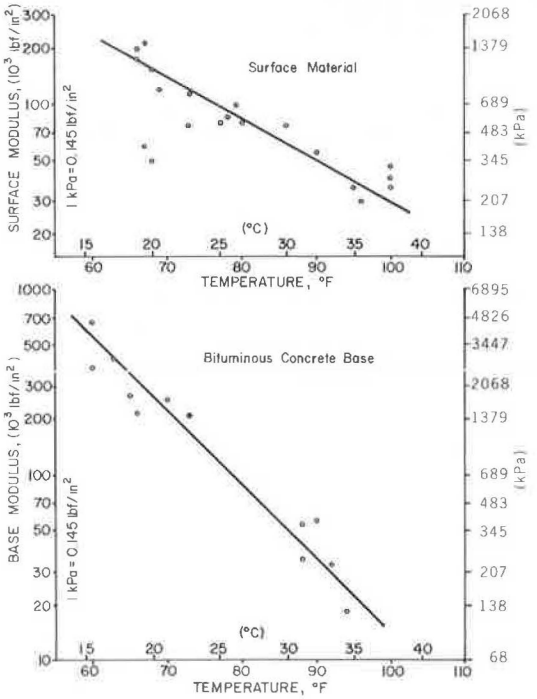

Table 2. Values of constants for fatigue equation.

Material	Temperature (°C)	K_1	K_2	R^2
ID-2A	12.8	6.2840×10^{-9}	3.9192	0.94
Surface	21.1	4.6624×10^{-7}	3.6128	0.95
	29.4	2.9312×10^{-6}	3.5145	0.99
Bituminous	12.8	5.1922×10^{-10}	3.9530	0.95
Concrete	21.1	1.0577×10^{-6}	3.1368	0.97
Base	29.4	2.6097×10^{-3}	2.1675	0.97

Figure 4. Correlation between rut depth and maximum compressive strain at top of subgrade.

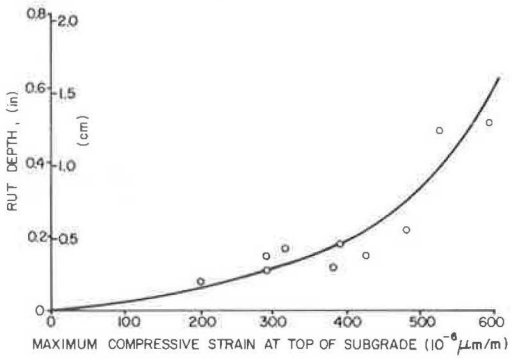

Figure 5. Maximum compressive strain at top of subgrade with 8165-kg equivalent axle load to produce 0.64-cm rutting.

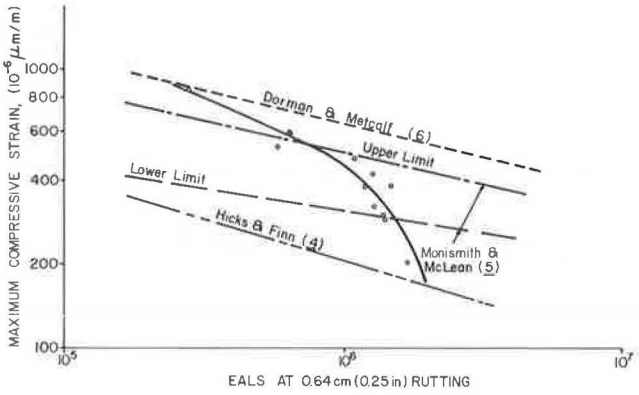

Figure 6. Correlation between ΔPSI and maximum tensile strain at bottom of base course.

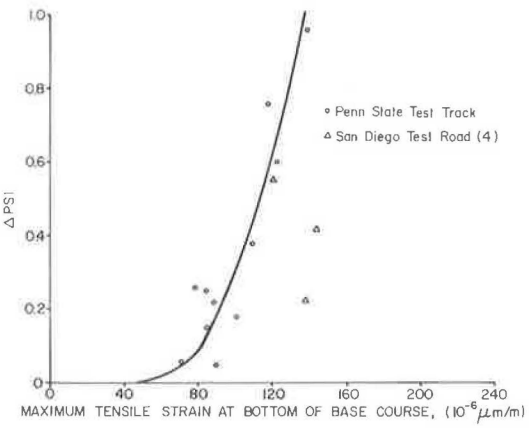

PAVEMENT RESPONSE AND PERFORMANCE

Pavement response was related to performance by using a base of 1 000 000 repetitions of an 8165-kg (18-kip) EAL. This EAL application was adopted because it is widely associated with 20-year pavement life. A relation between rut depth and maximum compressive strain at the top of the subgrade is established in Figure 4. As expected, rut depth increases with increasing maximum compressive strain; the rate of increase becomes greater at higher compressive strains.

Since a rut depth of 6.3 mm (0.25 in) has been widely used for developing the limiting strain criteria (4, 5, 6), the 8165-kg (18-kip) EAL required to produce 6.3-mm (0.25-in) rutting for each section concerned is related with the maximum compressive strain at the top of the subgrade shown in Figure 5. Also shown are the results of the San Diego test road (4) and the criteria developed by Monismith and McLean (5) and Dorman and Metcalf (6). The test results are bracketed between the results of the San Diego test road (4) and Dorman and Metcalf (6) and fit with the criterion developed by Monismith and McLean (5). The figure shows that the relation between maximum compressive strain and EAL is curved rather than linear, which is often used by most researchers. Both Figures 4 and 5 indicate that the limiting compressive strain at 1 000 000 EAL equals 450 μm/m (0.000 450 in/in). This strain criterion is used to determine the structural coefficient.

The change in PSI value up to 1 000 000 EALs is highly correlated with the maximum tensile strain at the bottom of the base course, as shown in Figure 6. The greater the maximum tensile strain is, the larger the PSI change will be. This relation implies that an increase in tensile strain will increase fatigue cracking; increasing fatigue cracking increases pavement roughness and consequently decreases the pavement serviceability. Also shown is a comparison with the results of the San Diego test road. One of three data points available from the San Diego test road falls on the curve. This relation permits prediction of PSI change from the calculated tensile strain.

The number of EALs at first appearance of significant cracking increases with decreasing maximum tensile strain at the bottom of the base course following the trend of the laboratory fatigue curve, as shown in Figure 7. However, the laboratory test results overpredict the number of EALs required for fatigue failure in the field. Similar overprediction was also encountered at the San Diego test road (4). The laboratory tests were performed on laboratory-compacted specimens for both cases. Possible causes for this overprediction could be attributed to test specimen, field loading conditions, and others.

The laboratory-compacted specimens generally possess the same density and composition as those of the field material. Because of the difference in aging and curing environment, however, the laboratory specimens can hardly duplicate the weathering effect associated with field specimens. Weathering might cause chemical degradation and physical disintegration and consequently results in a change in fatigue property. For this reason, field cores were also tested to determine fatigue property at the San Diego test road. The field specimens yielded better results but still overpredicted, implying other possible causes that have yet to be clarified. Unfortunately, no field specimens from the test track are available for verifying the findings of the San Diego test road.

Another possible cause in connection with the test specimen could be the effect of the nonhomogeneous nature of pavement materials from the subgrade soil to the surface material. This nonhomogeneous nature does not guarantee the absence of relatively weak spots in the pavement. These weak spots will no doubt undergo failure earlier than the predicted time.

The effect of field-loading conditions on overprediction of fatigue life is concerned primarily with the effect of vehicle inertia force due to downward and upward accelerations. This effect would be particularly manifested for traffic on an uneven road. The occurrence of this additional downward loading could accelerate fatigue failure of the pavement. Other possible traffic loadings that have often been overlooked in studies of pavement failure are the force created by braking and eccentric force at curves. These forces may result in raveling and cracking on the pavement surface and lead to inaccurate prediction of fatigue life.

In summary, the primary cause for overprediction of fatigue life of the test track has yet to be clarified. Figure 7 indicates that the limiting tensile strain at 1 000 000 EALs equals 120 μm/m (0.000 120 in/in). This limiting strain is compatible with the work of Monismith and others (7) and is bracketed between the results of San Diego test road (4) and Kingham (8).

Based on the number of axle loadings at first appearance of significant surface cracking, the pavement maximum-surface deflection is related with EAL in Figure 8. The test results fall between the findings of Kingham (8) and the San Diego test road (4) and coincide closely with the results of Zube and Forsyth (9) for pavements with a 7.6-cm (3-in) asphalt-concrete surface. The figure indicates a limiting maximum surface deflection of 0.51 mm (0.020 in) for flexible pavements with a life of 1 000 000 EALs for the range of thicknesses studied.

STRUCTURAL COEFFICIENTS

As previously mentioned, one objective of the test track research was to validate and refine, if necessary, the current flexible-pavement design procedure in Pennsylvania that is an adaptation from VanTil and others (11). This objective is fulfilled by evaluating the structural coefficients for materials currently being used in Pennsylvania. Accordingly, the structural coefficients of the bituminous-concrete base and crushed-limestone subbase are evaluated in the following by using the limiting criteria developed previously.

By using the BISAR computer program, pavement sections having various combinations of layer thickness and satisfying the limiting maximum tensile strain at bottom of base course, maximum vertical compressive strain at top of subgrade, and maximum surface deflection were determined. Results of the calculation for three thicknesses of surface course are summarized in Table 3. The required base thicknesses among the three limiting criteria are compared to give in the last column of the table a base thickness required to satisfy all three criteria simultaneously. The layer thicknesses in columns 1, 2, and 6 form the pavement sections for determining the structural coefficients below.

Because the structural-coefficient concept was originated from the AASHO Road Test, the following basic equation relating EAL with structural number is used as the basis for computation.

$$\rho = 0.64\,(SN + 1)^{9.36} \qquad (4)$$

where

ρ = EAL at failure and
SN = structural number.

Figure 7. Correlation between maximum tensile strain at bottom of base course and number of 8165-kg equivalent axle-load applications.

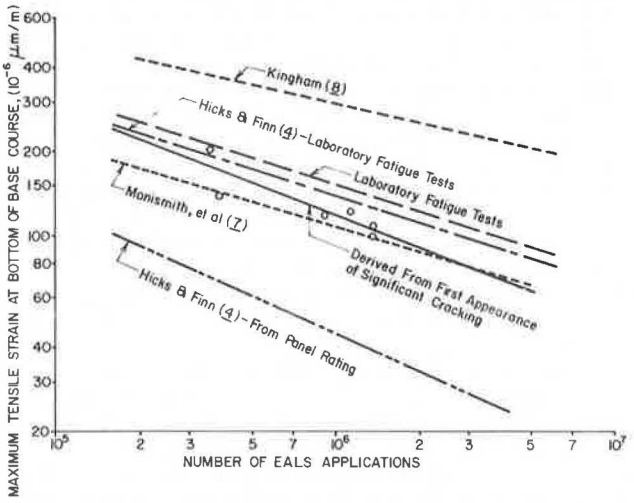

Figure 8. Correlation between surface deflection and number of 8165-kg equivalent axle-load applications.

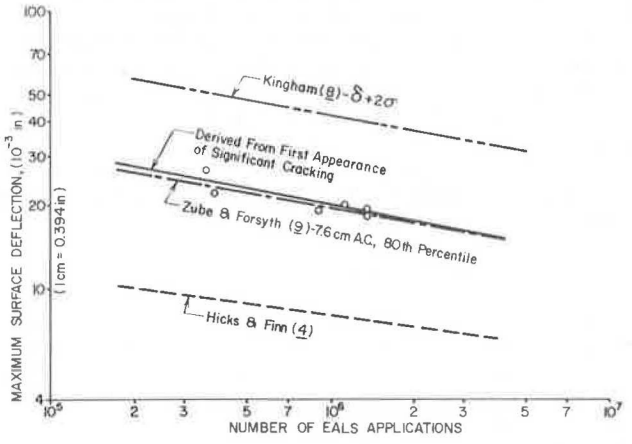

SN is defined as follows:

$$SN = a_1H_1 + a_2H_2 + a_3H_3 \quad (5)$$

where

a_1 = structural coefficient of surface material,
H_1 = layer thickness of surface course,
a_2 = structural coefficient of base material,
H_2 = layer thickness of base course,
a_3 = structural coefficient of subbase material, and
H_3 = layer thickness of subbase course.

For this analysis, the structural coefficient of the asphalt-concrete surface material is 0.44, which is the value originally developed from the AASHO Road Test. Since the surface layer thickness used in Pennsylvania generally ranges from 3.8 to 8.9 cm (1.5 to 3.5 in), it is assumed that the structural coefficient of the surface material does not vary significantly with the layer thickness. It is also assumed that the structural coefficient of the subbase material does not change appreciably within a thickness of 5.1 cm (2 in).

Three curves result from plotting the base thickness against the subbase thickness for each section listed in columns 1, 2, and 6 of Table 3. For each curve, i.e., for each surface thickness, the base thickness required for each 5.1-cm (2-in) difference in subbase thickness was obtained. The layer thicknesses determined were substituted into Equation 5, resulting in a family of linear equations that relate the structural coefficient of the base material with that of the subbase material. The structural coefficients were then solved from equations for two consecutive subdivisions of 5.1-cm (2-in) subbase layer.

Table 3. Layer thicknesses of pavements satisfying limiting criteria.

Subbase (cm)	Surface (cm)	Base (cm) by Limiting Criteria: Deflection	Tensile Strain	Compressive Strain	Combined
0	3.8	19.3	20.3	18.8	20.3
	6.4	17.8	18.3	16.8	18.3
	8.9	15.5	16.8	15.5	16.8
15.2	3.8	14.5	13.7	16.5	16.5
	6.4	13.2	12.2	15.2	15.2
	8.9	10.9	10.2	13.2	13.2
20.3	3.8	12.7	12.4	15.0	15.0
	6.4	11.2	10.9	13.7	13.7
	8.9	8.9	8.9	11.7	11.7
35.6	3.8	6.9	10.2	7.1	10.2
	6.4	4.6	8.4	5.1	8.4
	8.9	—	6.4	2.8	6.4
52.1	3.8	1.0	9.7	—	9.7
	6.4	—	7.9	—	7.9
	8.9	—	5.6	—	5.6

Note: 1 cm = 0.394 in.

Figure 9. Effect of layer thickness on structural coefficient.

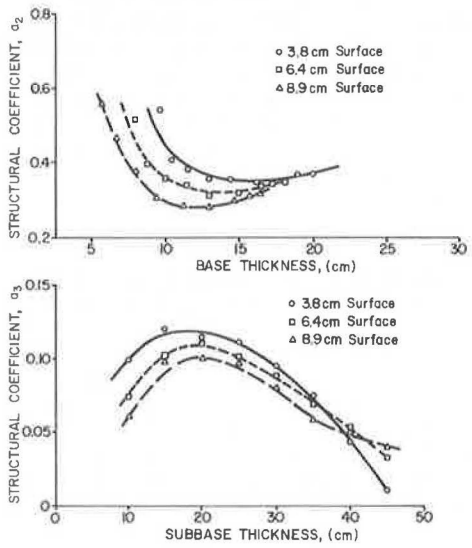

The structural coefficients computed above are shown in Figure 9. The effect of layer thickness on structural coefficient is immediately seen. As the structural coefficient of the base layer decreases with increasing base thickness, the structural coefficient of the subbase layer increases with increasing subbase thickness and vice versa. This is as expected because the sum of the products of the structural coefficient and the layer thickness for the two layers remains constant, as previously mentioned. The trend of variation of structural coefficient with layer thickness seems to depend on which limiting criterion controls the pavement behavior. Table 3 and Figure 9 seem to suggest that, when the criterion of maximum compressive strain dominates, the structural coefficient of the base layer will increase with an increase in the base-layer thickness and that,

when the maximum tensile strain criterion prevails, the structural coefficient of the base layer will decrease with an increase in the layer thickness.

Figure 9 also shows that the structural coefficient of any layer (base or subbase) depends not only on its own layer thickness but also on the thickness of the surface layer. In general, when the subbase layer is thinner than 35.6 cm (14 in), the thicker the surface layer is, the smaller the structural coefficient will be. These structural coefficients are based on the spring weather condition only. As weather conditions vary, the structural coefficient will also vary because of the change in limiting criteria. This effect has also been pointed out by Coffman and others (10) and VanTil and others (11).

The structural coefficient of the bituminous-concrete base fluctuates around 0.40 and that of the subbase layer around 0.10. These two values are close to those that were originally proposed by AASHO (11). Practical applications of these two sets of curves require a simple trial-and-error procedure, similar to that required in the AASHO guide (11), to select a proper combination of layer thicknesses. It is possible that different layer combinations may equally satisfy the structural number requirements. When this condition develops, the most economical combination should be adopted.

SUMMARY AND CONCLUSIONS

The flexible-pavement design procedure used in Pennsylvania was validated or refined by using the Pennsylvania State test track, which was completed in August 1972. The test track is composed of sections that have various base-course materials and different layer thicknesses. This paper presents the results of performance analyses for sections containing a bituminous-concrete base.

The BISAR computer program together with spring temperature and moisture condition was used to analyze the maximum-vertical compressive strain at the top of the subgrade, maximum-radial tensile strain at the bottom of the base course, and maximum deflection on the pavement surface. Correlations between critical response and pavement performance were established. These correlations permit prediction of pavement performance from the pavement response determined in the spring season.

A maximum compressive strain of 450 μm/m (0.000 450 in/in), a maximum tensile strain of 120 μm/m (0.000 120 in/in), and a maximum surface deflection of 0.51 mm (0.020 in) were established as the limiting criteria for flexible pavements with bituminous bases to withstand 1 000 000 applications of an 8165-kg (18-kip) EAL without significant fatigue cracking. Based on the criteria developed, the structural coefficients of the bituminous-concrete base and the crushed-limestone subbase were determined.

ACKNOWLEDGMENTS

The study presented here is a part of the research project entitled An Evaluation of Pennsylvania's Flexible Pavement Design Methodology and A Study of Flexible Pavement Base Courses and Overlay Design sponsored by the Pennsylvania Department of Transportation in cooperation with the Federal Highway Administration of the U.S. Department of Transportation. Their support is gratefully acknowledged. We wish to express our gratitude to the National Crushed Stone Association for lending us its repeated-load test apparatus for laboratory testing and to the Asphalt Institute for its cooperation in conducting the fatigue testing. B. A. Anani, P. J. Kersavage, W. P. Kilareski, and S. A. Kutz assisted in collecting and reducing field data. We are especially grateful to W. P. Kilareski for his participation in the preparation of this paper. Becky Nelson typed the manuscript.

REFERENCES

1. E. S. Lindow, W. P. Kilareski, G. Q. Bass, and T. D. Larson. Construction, Instrumentation, and Operation. Pennsylvania Transportation Institute, Vol. 2, Interim Rept. on An Evaluation of Pennsylvania's Flexible Pavement Design Methodology, Rept. PTI 7504, Feb. 1973.
2. W. P. Kilareski, S. A. Kutz, and G. Cumberledge. Modification Construction and Instrumentation of an Experimental Highway. Pennsylvania Transportation Institute, Interim Rept. on A Study of Flexible Pavement Base Course and Overlay Designs, Rept. PTI 7607, April 1976.
3. R. E. Root. Results of Laboratory Tests on Materials From the Pennsylvania State University Pavement Durability Test Track Facility. Asphalt Institute, College Park, Md., Dec. 1973.
4. R. G. Hicks and F. N. Finn. Prediction of Pavement Performance From Calculated Stresses and Strains at the San Diego Test Road. Proc., Association of Asphalt Paving Technologists, Vol. 43, 1974, pp. 1-40.
5. C. L. Monismith and D. B. McLean. Structural Design Considerations. Proc., Association of Asphalt Paving Technologists, Vol. 41, 1972, pp. 258-305.
6. G. M. Dorman and T. Metcalf. Design Curves for Flexible Pavements Based on Layered System Theory. HRB, Highway Research Record 71, 1965, pp. 69-84.
7. C. L. Monismith, J. A. Epps, D. A. Kasianchuk, and D. B. McLean. Asphalt Mixture Behavior in Repeated Flexure. Institute of Transportation and Traffic Engineering, Univ. of California, Berkeley, Rept. TE70-5, 1970.
8. R. I. Kingham. Fatigue Criteria Developed From AASHO Road Test Data. Proc., 3rd International Conference on the Structural Design of Asphalt Pavements, 1972, pp. 656-669.
9. E. Zube and R. Forsyth. Flexible Pavement Maintenance Requirements as Determined by Deflection Measurements. HRB, Highway Research Record 129, 1966, pp. 60-75.
10. B. S. Coffman, G. Ilves, and W. Edwards. Theoretical Asphaltic Concrete Equivalencies. HRB, Highway Research Record 239, 1968, pp. 95-119.
11. C. J. VanTil, B. F. McCullough, B. A. Vallerga, and R. G. Hicks. Evaluation of AASHO Interim Guides for Design of Pavement Structures. NCHRP, Rept. 128, 1972.

Publication of this paper sponsored by Committee on Flexible Pavement Design.

Design and Performance of Flexible Pavements in the Tropics

P. C. Todor, Lyon Associates, Inc., Rio de Janeiro, Brazil
W. J. Morin, Lyon Associates, Inc., McLean, Virginia

A procedure is presented for flexible pavement design in the tropics along with deflection criteria for flexible pavements. The deflection data were obtained during a research program that included pavement evaluation of over 200 sections in Africa and South America. Maximum permissible deflections were established for various ranges of traffic and are given in terms of average deflections plus two standard deviations. For the selection of a design deflection, emphasis is placed on the degree of uniformity in construction that is generally obtained by local construction practices. The flexible pavement design procedure is based on two relations: The first is between deflection and performance, and the second is between deflection and pavement strength. The structural evaluations were conducted on 170 test sections where deflections had been measured. Index properties and California bearing ratio density-moisture relations were determined for each soil layer within the excavated depth of 90 cm (36 in). The thickness and density of each structural course was measured. Structural coefficients were developed for various depths beneath the pavement surface rather than by layer description because of the multiple-layer systems encountered. A minimum thickness of cover for various California bearing ratio values was established to provide adequate support. A minimum thickness was also established to prevent excessive pavement cracking. Structural design curves were developed that provide a relation between design traffic and pavement structural index for 3 degrees of pavement uniformity. Design curves were also developed that provide a measure of the subgrade support and show minimum thickness of surface, base, and subbase that is required.

The pavement design procedures used in most tropical countries have been adopted from those developed in temperate climates. Because such procedures take into account the characteristics of the climate and the materials that prevail in the location where the design was developed, they do not really apply to the tropics. The design procedure described in this paper was developed from the analysis of pavement sections in South America (1) and Africa (2). The procedure was primarily derived from the establishment of relations between performance and deflection and between deflection and the structural strength of each component layer within the pavement structure.

The design procedure has been termed tropical design procedure for flexible pavements because it was developed principally for red, tropical, residual soils that form the basic layers of most pavement structures in the tropics. It is also considered applicable to all other tropical or subtropical soils that are residual or transported.

PAVEMENT PERFORMANCE EVALUATION

Pavement deflection measurements have been used to evaluate the performance of flexible pavements for over 20 years. Recently, several investigators have established relations between pavement strength and deflection (3, 4, 5, 6). A relation between deflection and the combined effect of California bearing ratio (CBR) and thickness was used to establish the relative strength coefficients of flexible pavement components in a study of pavements in Africa (2).

Deflection measurements also allow an evaluation of the structural uniformity of pavement sections. In this study, a coefficient of variation of 35 percent was selected to define the maximum tolerable variation when generally accepted quality control is exercised during construction.

Deflection tests were conducted on more than 200 test sections throughout Brazil. Deflections were measured at six stations, 30 m (98 ft) apart, within each 150-m (492-ft) test section. Measurements were obtained in both inside and outside wheel paths (IWP and OWP) and at various distances from the point of loading. The latter values provided data to define the deflection basin. The rebound deflection was obtained at each of the six stations within the test section. The slope of the deflection basin was determined by using Kung's description (3) in which the slope is defined by the maximum tan value. Both rebound deflection and the slope of the deflection basin were evaluated to establish the maximum value of each that allows satisfactory pavement performance. Vehicles with two axles were used and were loaded to provide an 8165-kg (18-kip) rear-axle loading. Tire pressures were maintained between 583 and 617 kPa (85 and 90 lbf/in^2). All deflection measurements were corrected to a standard temperature of 21°C (66°F).

Traffic Analysis and Present Serviceability Rating

The traffic data available included traffic counts by Departamento Nacional de Estradas de Rodagem (DNER) and various Departamento de Estradas de Rodagem (DER). The total number of vehicles that traversed the test sections since construction, or last overlay, was determined from these data and classified according to vehicle type. A loadometer survey, conducted in the state of Minas Gerais, was analyzed to establish the loading patterns of commercial vehicles, which was needed to determine the traffic equivalence factors (TEF) for each truck-unit classification.

TEFs were calculated in accordance with the interim guide (8) by the American Association of State and Highway Officials (AASHO) for each truck classification. TEFs for triple axles were extrapolated from the relation of single- and tandem-axle equivalencies. Unit equivalencies for the various truck classifications were based on the percentage of loaded and unloaded trucks and the loaded and curb weight of each unit. Unit equivalents for vehicles not included in the loadometer survey were estimated from information obtained from manufacturers and commercial agencies. For convenience, the 8165-kg (18-kip) single-axle loading is referred to as the standard load.

The traffic analysis and the loadmeter survey were used to determine the accumulated equivalent standard axle-load applications experienced by each test section. The average daily percentage of each group was multiplied by the applicable equivalent factor and summed according to the following:

$$AE18KSAL = 365(N)(ADT)\Sigma(n)(UE18KSAL) \quad (1)$$

where

AE18KSAL = the accumulated equivalent standard single-axle load,
N = the age of the pavement in years,

ADT = the mean daily traffic,
(n) = the percentage of ADT for each group, and
UE18KSAL = the unit equivalent standard axle load.

Pavements were evaluated by means of a subjective rating of the riding quality while a standard vehicle traversed the test section at a constant speed of 80 km/h (48 mph). A mean value was selected from a minimum of two independent ratings but usually from three or more ratings. This rating, called the present serviceability index (PSI), ranged from 1 (excessive deterioration) to 9 (excellent). Pavements with ratings above 5 were considered as performing satisfactorily, regardless of intended life, while those with ratings of 5 or less were considered as terminated or in need of major repair. Variations in assigned ratings were usually not large, seldom varying from the mean by more than one rating point.

Discussion of Results

Deflection and Performance

The relation between performance and deflection was established for the OWP because this path, being the weakest zone of the pavement structure, usually controls the performance of the pavement.

Pavement performance is usually correlated with representative deflection, or the mean deflection plus two standard deviations. This correlation defines a deflection level that is exceeded by 2 percent of the length of the test section (9). The weaker sections, although limited in area, control the performance of the pavement. The relation between the representative deflection and performance is shown in Figure 1 in which data from Africa (2) were added. The recommended criterion represents a confidence level of about 95 percent; therefore, only 5 percent of the pavements meeting the deflection criterion were rated unsatisfactory.

The deflection testing in Brazil was conducted during the rainy season, but, since seasonal variations in moisture content beneath pavements are usually slight, seasonal variations in deflection are far less than those in temperate regions.

Permissible Deflection and Design Deflection

The design deflection is governed by the degree of uniformity obtained in the final pavement structure that is dependent on variations in the subgrade, borrow materials, construction practices, and the effectiveness of quality control. Variations in the test sections were examined and the mean coefficient of variation was found to be 25 percent. The maximum coefficient of variation was as high as 83 percent. A coefficient of variation of 35 percent is believed to indicate adequate quality control during construction. Accordingly, a maximum variation of 35 percent was selected in determining the recommended deflection criterion.

The relation between the coefficient of variation and design deflections is shown by the design curves in Figure 2. These curves demonstrate the importance of uniformity with relation to performance. For example, if two pavements had a mean deflection after construction of 0.864 mm (0.034 in) but different standard deviations (0.2 and 0.4), the performance of the two pavements would be different. The pavement with the lower standard deviation (0.2) would have an expected life of 350 000 standard, axle-load applications while the other pavement would have an expected life of only 100 000 standard axle-load applications and would require an overlay to extend its life.

DEFLECTION AND PAVEMENT STRENGTH

A relation between deflection and pavement strength provides the basic requirement for a structural design procedure for flexible pavements. The measurement of the thickness of individual structural layers and the evaluation of the strength of each component layer are required to establish such a relation. The measurement of the individual structural layers is straightforward. The evaluation of the strength of the individual layers is accomplished by one of several methods (CBR, R-value, triaxial compression, or others). The strength parameter is an index of the ability of the layer to transfer the vehicle load to the underlying layer at a lower stress level. The lateral distribution of the vertical load (load-spreading characteristic) of each soil layer depends on the magnitude and concentration of the applied stress, the shear resistance of the material, and the position of the layers within the pavement structure.

The most common method for determining the relative strength of soils in pavement design is CBR. This method is used more than any other combined methods in tropical countries. Pavement evaluations in Brazil were based on CBR tests on unbound soil layers within the pavement structures. Bound or chemically stabilized soil layers were excluded.

Structural Evaluation of the Test Sections

A total of 170 test pits, selected through analysis of the deflection results, were excavated at the stations where the deflections most nearly approached the mean value for the entire section. The test pits were excavated to the full width of one traffic lane and were 90 cm (36 in) deep. Excavation to this depth allows examination of the structural layers that are affected by vehicle loadings. The distributed vehicle load at a depth of 90 cm (36 in) is less than 1 percent of the applied vehicle load. The thickness of each structural course was measured at both the IWP and OWP. In some sections, as many as six layers were encountered; the thickness of each was measured. Density determinations were conducted in both wheel paths for each structural layer. When layer thicknesses exceeded 20 cm (8 in), a density determination was made in the top half of the layer and again in the bottom half of the layer.

Samples for laboratory testing were obtained from each of the soil layers. A CBR moisture-density relation was established for each soil layer component of the pavement structure. CBR was determined from three samples compacted at the field moisture content and at three compactive efforts: AASHTO standard T99-70, AASHTO modified T180-70, and the Brazilian standard that is about midway in compactive effort between the other two. For each layer, CBR was selected to correspond to the in situ density determined in the field test.

Structural Coefficients

A simple CBR-coefficient relation could not be used because the performance of a given layer depends not only on the material properties (shear resistance) but also on the magnitude of stress imposed. A material with CBR of 70, for example, will not be subjected to the same stress level when used as subbase as when it is used as

a base course nor will it have the same load-spreading characteristics. The structural coefficients were developed to relate both CBR load-spreading characteristics and position of the layers within the pavement structure.

Structural coefficients were initially estimated from those developed in Africa (1, 2). These coefficients were later modified for various depths beneath the pavement surface, as given in Table 1. The basic structural equation in which the coefficients are used follows.

Figure 1. Relation between deflection and performance.

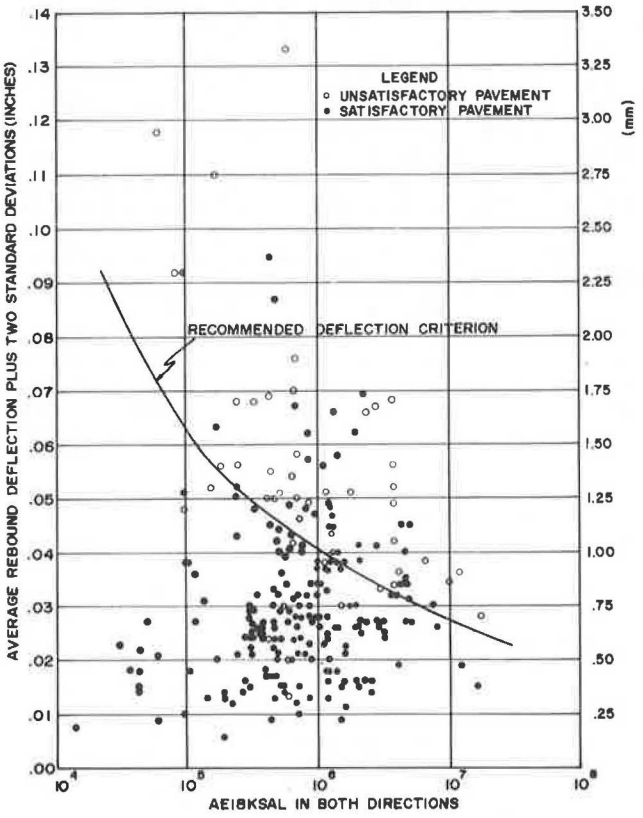

Figure 2. Relation between design deflection and traffic for practical range of coefficients of variation.

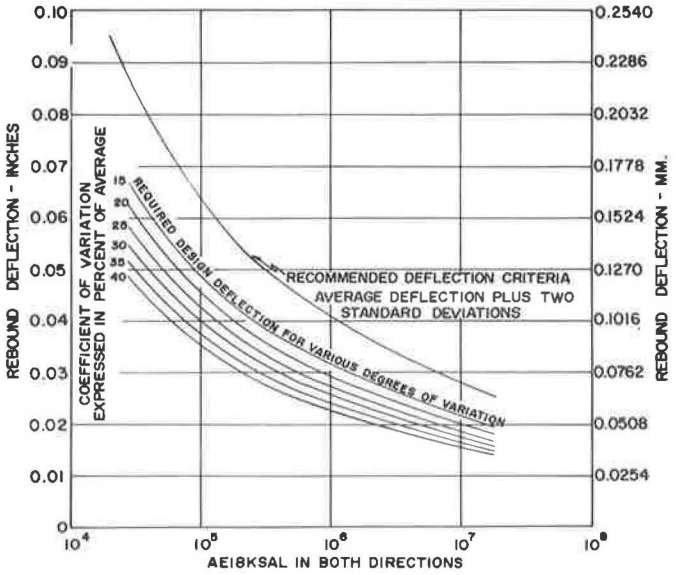

Pavement structural index (SI) = $a_1t_1 + a_2t_2 + \ldots a_nt_n$ (2)

where

$a_1, a_2, \ldots a_n$ = the structural coefficients in dimensionless units per cm; and

$t_1, t_2, \ldots t_n$ = the thicknesses of the component layers in cm.

The surface course is referred to by a_1t_1, the base course is referred to by a_2t_2, and so on. SI is computed to a depth of 90 cm (36 in).

SI is related to the pavement deflection by the following equations:

$$SI = (0.039\ RD)^{-1} \quad (3)$$

where RD = the measured Benkelman beam deflection in mm. For the corresponding U.S. customary unit in inches, the following equation is used.

$$SI = (RD)^{-1} \quad (4)$$

Maximum and Minimum Structural Coefficients

The maximum and minimum structural coefficients given in Table 1 represent the two extremes in stress distribution beneath flexible pavements. The maximum structural coefficient represents the maximum angle of lateral distribution beyond which there is no vertical stress

Table 1. Pavement coefficients for flexible pavement design.

Pavement Component	Strength Coefficient
Base course	
Crushed stone (Macadam hydraulic)	
Open graded	1.037
Graded	1.394
Cement treated (compressive strength 7 d)	
4500 MPa or more	2.400[b]
2750 MPa to 4500 MPa	2.100[b]
2750 MPa or less	1.600[b]
Lime treated	1.4 to 1.6[b]
Concretionary gravels	
CBR (design)	
+100	1.394
90	1.232
85	1.167
80	1.102
75	1.037
70	0.940
60	0.552
50 (min)[a]	0.383
Subbase course	
CBR (design)	
+40	0.576
35	0.290
30	0.205
25 (min)	0.075
Subgrade layer	
CBR (design)	
+20	0.481
15	0.357
10	0.212
9	0.183
8	0.133
7	0.084
6	0.053
5	0.033
4	0.020
3	0.015
2 (min)	0.010

Notes: 1 Pa = 0.000 145 lbf/in^2.
Design coefficient limits: Base course refers to materials to a depth of 25 cm, subbase course refers to material layers between 25 to 50 cm, and subgrade layer refers to material layer between 50 to 90 cm.

[a] Material with a CBR of 40 can be used between the depth intervals of 10 and 25 cm and assigned the same coefficient.

[b] Values estimated from structural coefficient relations given in the 1972 AASHO Interim Guide for Design of Pavement Structures.

while the minimum coefficient represents the case in which the increased load exceeds the shearing resistance of the soil that results in a concentration of the vertical stress in the central cone, i.e., perimeter shear (10). The maximum and minimum coefficients in Table 1 were initially estimated and then modified by trial and error computations, using the sections that displayed the lower extremes of CBR values.

The results of the analyses of test sections with CBR values below the minimum value are shown in Figure 3. Deflections of these sections were calculated by using Equations 2 and 3 or 4, but without assigning structural coefficients to the layers with low CBR values. The solid points represent the sections where the calculated values of deflection were equal to or near the measured deflection. The open circles represent the sections where the calculated values of deflection were much less than the measured deflections. Thus, the solid points represent those layers that had poor load-distribution qualities but did not cause excessive elastic deflection in the pavement system. On the other hand, the open circles represent those layers that had poor load-

Figure 3. Critical CBR values with depth below pavement surface based on field analysis.

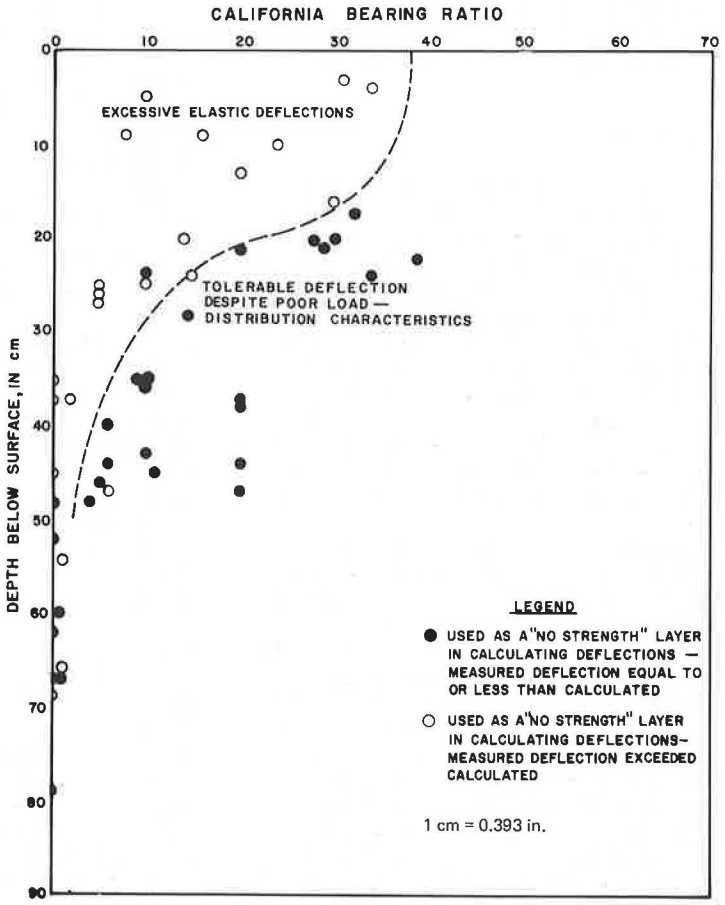

Figure 4. Effect of asphalt on pavement strength for various thicknesses of asphalt and unbound soil layer strengths.

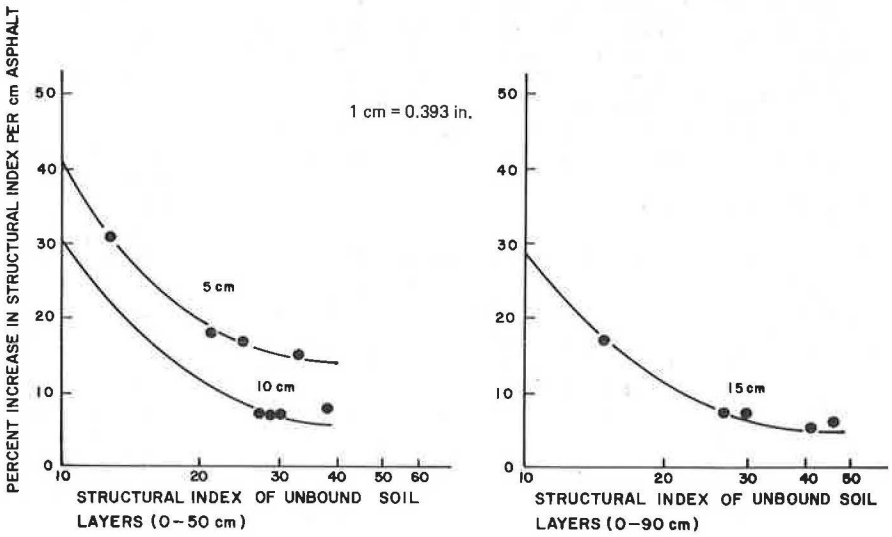

spreading qualities and allowed excessive elastic deflection. The minimum thicknesses of cover for various CBR values were based on this analysis.

Calculated Deflections and Benkelman Beam Deflections

Surface Treatment Pavements

The measured deflections of single and double bituminous-surface treatments (SBST and DBST) pavements were compared with calculated deflections from Equations 2 and 3 or 4. After sections with low CBR or density values were eliminated, there were 55 test sections available that displayed good correlation when the precision of the field measurements was taken into account. The structural error of estimate was ±0.0739 mm (0.00291 in).

Asphalt-Concrete Pavements

An asphalt layer provides two benefits to the pavement system: It increases the strength and load-spreading characteristics of the layer itself, and it increases the load-spreading characteristics of the underlying unbound layers. This second benefit was substantiated by comparing the strengths of the unbound underlying soil layers, computed from Equation 2, with the composite strength determined from measured deflections and Equations 3 or 4. In the first analysis, the difference in these strengths was attributed to the asphalt layer and was considered residual strength. However, when the difference in strength was converted to structural coefficients, the results were unsatisfactory for use in the design procedure.

In the second analysis, it was assumed that the load-spreading characteristics of the soil layers beneath the asphalt layer increase with depth. This assumption was verified by separating the test sections into groups with mean asphalt thicknesses of 5, 10, and 15 cm (2, 4, and 6 in). The curves that are shown in Figure 4 display a relation between the strength increases of the unbound materials down to a depth of about 50 cm (20 in) for the 5-cm (2-in) asphalt group and also for the 15-cm (6-in) asphalt group. The latter group is based on a depth of 90 cm (36 in). The curve for the 10-cm (4-in) asphalt group was extrapolated to parallel the 5-cm (2-in) curve. It appears reasonable that the residual strength is partially attributable to the asphalt layer and partially attributable to the increase in the load-spreading characteristics of the underlying soil layer.

The strength increase factors were used to calculate the deflection in 65 out of 87 test sections with asphalt surfacing. Twelve sections were eliminated because of surface deterioration, low CBR or density values, and other obvious discrepancies. The remaining data displayed good correlation with measured deflection when the precision of the field measurements was considered.

Natural Cementing or Slab Action

There were 20 test sections that exhibited deflections significantly lower than the deflections calculated by Equations 2 and 3 or 4. The values for CBR were no higher than those encountered in the other sections; therefore, the test did not measure the actual strength these layers exhibited in the field.

The majority of these sections were located in northeastern Brazil. This area is subject to long, dry periods that allow for a natural hardening of certain types of red tropical soils. During excavation of the test sections, one or more of the layers were naturally cemented. These layers were a part of an older pavement structure or were part of a newer pavement that had been unsurfaced for a period of time. Data from these sections could not be included in the design analysis; therefore, further study is required for effective utilization of these soils.

Slope of the Deflection Basin and Structural Strength

A pavement design procedure should include minimum thickness requirements for asphalt that will reduce pavement cracking to tolerable limits for a given design period. It was felt that these requirements should be based on a relation between the thickness of the asphalt layer and the slope of the deflection basin (slope index). However, it was found that a suitable relation could not be established without indicating CBR of the base material. Figure 5 shows the minimum slope indexes for given thicknesses of asphalt after base CBR values have been grouped into appropriate ranges. These curves were used to establish minimum thicknesses of asphalt to prevent excessive cracking.

STRUCTURAL DESIGN CURVES AND DESIGN PROCESS

The structural design curves were developed from the relations between design deflection and traffic that were established for selected coefficients of variation, and from the relation between deflection and SI. The relation between calculated deflection and measured deflection is shown in Figure 6 in which the standard error of estimate is ±0.081 mm (0.003 in). Because that portion of the error attributable to the structural coefficient affects the development of the design curves, the design deflection data were adjusted during the translation of deflection to SI to account for the errors. The adjusted values provide a more conservative relation for design purposes.

The structural design curves are shown in Figure 7. These curves illustrate the relation between design traffic, given in terms of standard axle applications in both directions, and SI. The coefficient of variation is a reflection of local construction practices and should be determined for each general design area by analyzing deflections in existing roads. SI obtained from Figure 8 represents the minimum required strength for a standard 90-cm (36-in) pavement section. This SI forms the basis for a flexible pavement design.

The objective of the structural design process is to use SI to determine the thickness of each pavement layer, i.e., the surface (t_1), the base (t_2), and so on. Design traffic, CBR of each structural layer, and applicable coefficient of variation are required to use this procedure. Thus, SI is determined by assuming SIs for each layer in a standard 90-cm (36-in) pavement section by using Equation 2. In that equation, a_1 is the structural coefficient of the surface material, a_2 is the coefficient of the base material, and so on. Also, $t_1 + t_2 + \ldots t_n$ is 90 cm (36 in).

Structural coefficients for various soils are given in Table 1 that also provides structural coefficients for crushed stone, and cement- and lime-treated soils. The coefficient for crushed stone was determined from test sections that have macadam base courses. The structural coefficient of open-graded crushed stone is less than the higher quality concretionary gravels because of cohesion in the concretionary material. The structural coefficients for cement- and lime-treated soils are estimated from relations given in the interim guide by AASHO (8).

The strength of the subgrade, or the subgrade CBR, is a key element in the design of the overlying structural layers and is shown in Figure 8, which was partially replotted from Figure 3. The minimum thickness of cover varies inversely with the value of the subgrade CBR. Figure 8 also shows the relation between subgrade CBR and SI. Because SI of the subgrade influences the design thickness of the structural layers, it is referred to as the subgrade support. Higher strength subgrades furnish greater support and permit the use of thinner structural layers. The combined SI for the structural layers (surface, base, and subbase) is equivalent to the required SI (from Figure 7) less the subgrade support.

Flexible Pavement Design

More than one trial may be required to design a flexible pavement. The first trial begins with the selection of a surface type and concludes with the determination of the base and subbase thickness. The surface type and thickness are determined from Table 2 and is based on the base-course CBR value and the design traffic.

The minimum design thickness of the unbound structural layers (base and subbase) in a surface treatment (ST) pavement design is equal to the minimum thickness of cover as derived from Figure 8. The thickness of ST is not considered because it does not contribute signifi-

Figure 5. Relation between slope index and thickness of asphalt concrete for the practical range of base-course CBR values.

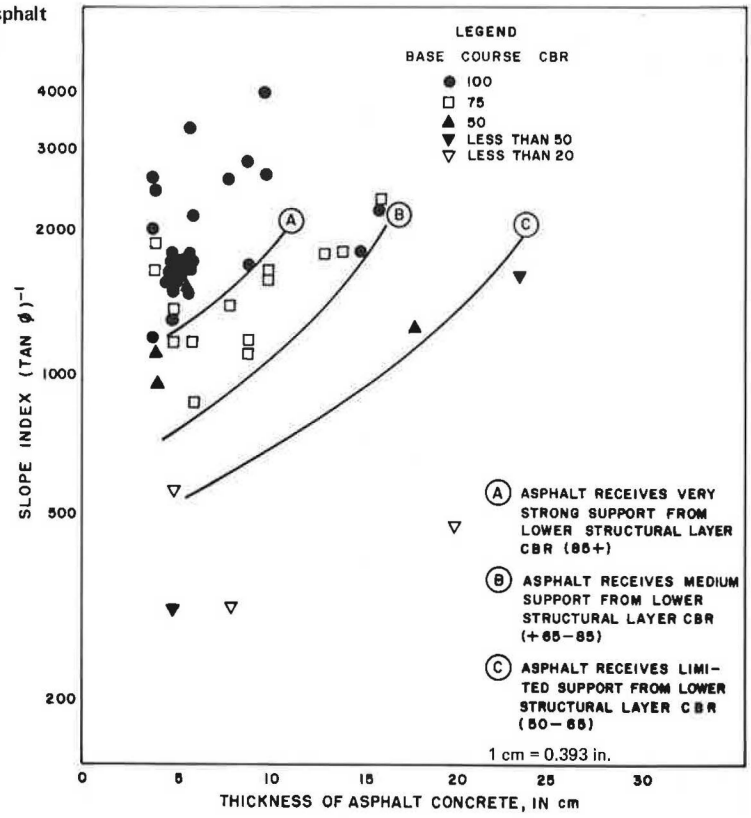

Figure 6. Comparison between measured deflections and calculated deflections.

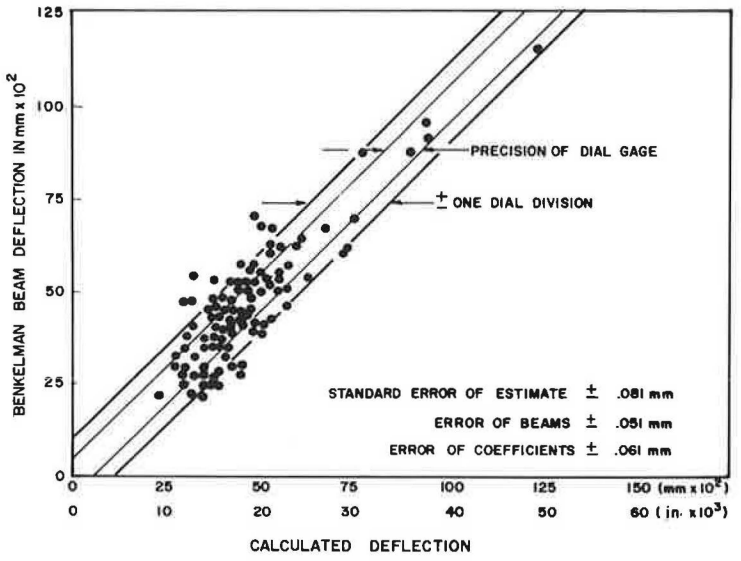

cant strength to the pavement section. However, an asphalt-concrete (AC) surface does provide strength and consequently is considered part of the minimum thickness of cover. In an AC-pavement design, the minimum design thickness of the unbound structural layers equals the minimum thickness of cover less the thickness of AC.

The minimum base-course thickness is determined from Figure 8 and is based on the CBR of the subbase material. The subbase course is the remaining thickness of the cover. Finally, the subgrade thickness for design purposes is the difference between the standard 90-cm (36-in) design and the thickness of the cover.

The adequacy of this first trial design section to carry the design traffic is determined by summing SIs of each pavement layer (Equation 2) and comparing the summed SI to the required SI from the structural design curves shown in Figure 9. SI of each pavement layer is equivalent to the product of its thickness and its structural coefficient (Table 1) to the extent that its thickness or CBR value fall within the strength and design coefficient limits provided in the table. Those portions of the pavement section that do not fall within these limits do not provide strength to the pavement and therefore are excluded from the derivation of SI of the entire pavement section. However, the thickness of those portions is included as part of the standard 90-cm (36-in) section. ST pavement design is the least complex because ST does not impart any strength to the pavement structure.

The benefit of the AC load-spreading characteristic

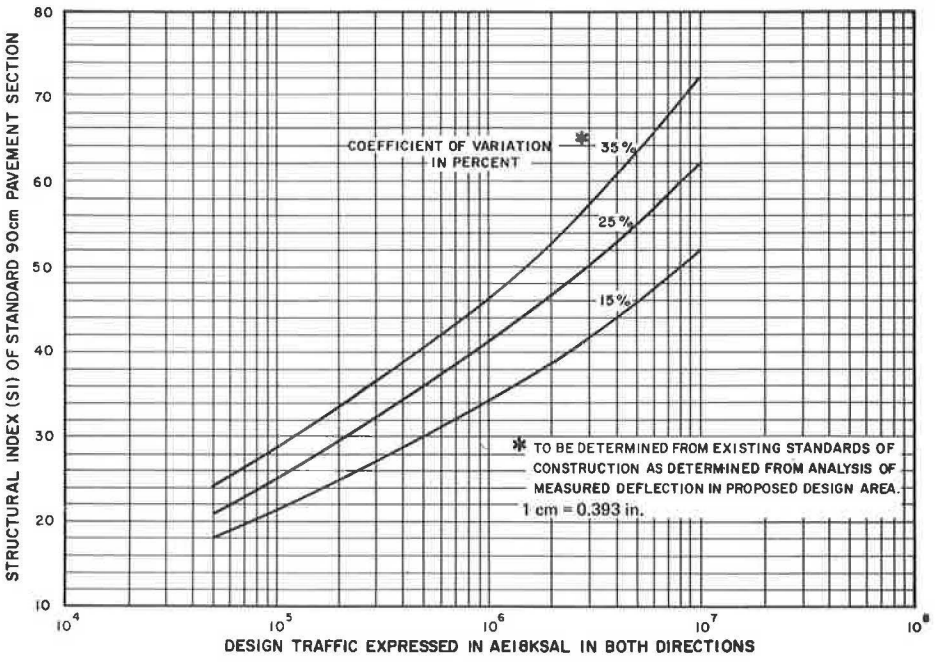

Figure 7. Structural design curves for determining required structural index of the standard pavement section.

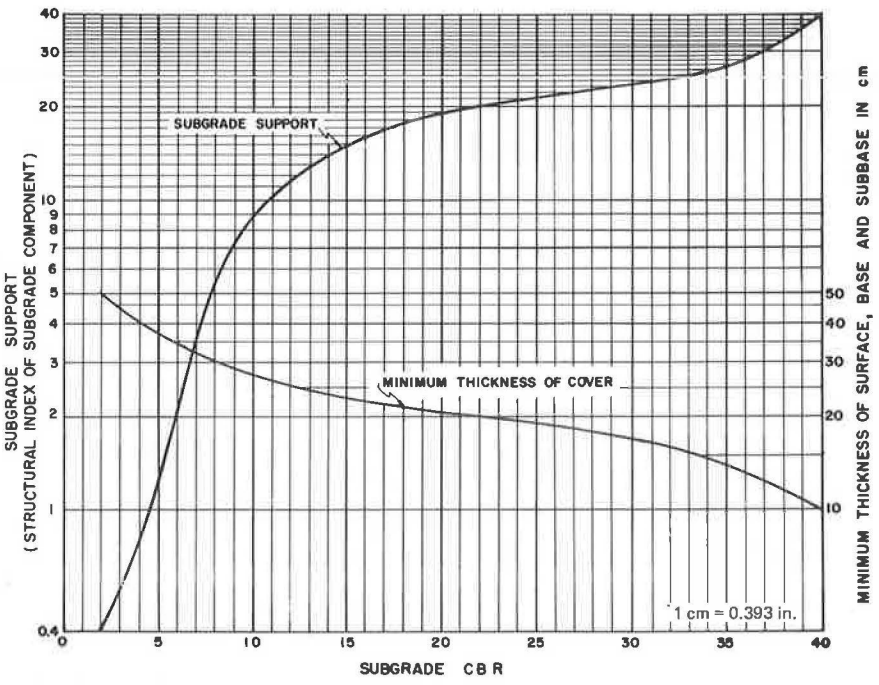

Figure 8. Subgrade support and minimum thickness of cover based on subgrade CBR values.

Table 2. Recommended type and thickness of surface courses.

Total Standard EAL Applications in Both Directions	Strength of Base Course (CBR)							
	+100	90	85	80	75	70	60	50
100 000	ST	ST	ST	ST	ST	ST	ST	ST
200 000	ST	ST	ST	ST	ST	ST	ST	5
300 000	ST	ST	ST	ST	ST	ST	5	5
400 000	ST	ST	ST	ST	ST	5	5	7.5
500 000	ST	ST	ST	ST	5	5	5	10
600 000	ST	ST	ST	5	5	5	5	10
700 000	ST	ST	5	5	5	5	7.5	15
800 000	ST	5	5	5	5	5	7.5	15
900 000	ST	5	5	5	5	5	10	15
1 000 000	ST	5	5	5	5	5	10	15
2 000 000	5	5	5	5	7.5	10	15	20
3 000 000	5	5	5	7.5	10	10	15	20
4 000 000	7.5	7.5	7.5	7.5	10	15	15	21
5 000 000	7.5	7.5	7.5	10	10	15	20	21
6 000 000	7.5	7.5	7.5	15	15	15	21	21
7 000 000	10	10	10	15	15	15	22	22
8 000 000	10	10	10	16	16	16	22	22
9 000 000	10	10	10	17	17	17	22	22
10 000 000	10	10	10	18	18	18	23	23

Notes: ST denotes a double bituminous-surface treatment.

To be used only if higher quality base material is not available and stabilization or modification proves to be too expensive.

Figure 9. Combined strength of pavement section of asphalt and unbound soil layers for 5, 10, 15, 20, and 25 cm of asphalt concrete.

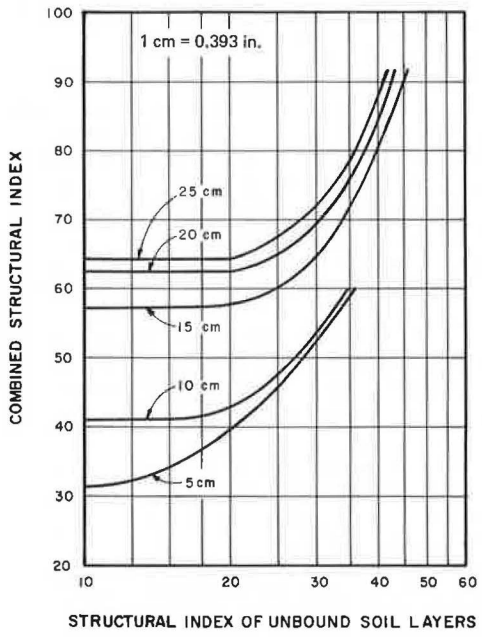

is shown in Figure 9 for 5, 10, 15, 20, and 25 cm (2, 4, 6, 8, and 10 in) of AC surfaces. The load-spreading benefit extends only 50 cm (20 in) below the surface for the 5 and 10-cm (2 and 4-in) AC surfaces whereas the load-spreading benefit extends throughout the entire 90-cm (36-in) design section for the 15, 20, and 25-cm (6, 8, and 10-in) AC surfaces.

If the computed SI is lower than the required SI, shown in Figure 7, then the strength of the pavement may be improved by

1. Increasing the subbase thickness, which increases the minimum thickness of cover but does not affect the surface and base courses;
2. Increasing the base thickness and reducing the subbase by a similar amount, which retains the minimum thickness cover;
3. Using an AC surface instead of ST or increasing the AC thickness and reducing the thickness of the base course; and
4. Any combination of the above.

The engineering decision to undertake one of the above alternatives will be based on economic considerations, local conditions, and the availability of the materials required to increase SI.

DESIGN EXAMPLE

1. Given: Estimated daily traffic in both directions = 1 250 000 SAL; construction variations in nearby highways = 35 percent; and subgrade CBR = 9, base CBR = 80, and subbase CBR = 30.
2. Determine required SI from Figure 8: Enter horizontal axis at the 1 250 000 design traffic and turn to vertical axis after intersection with 35 percent curve. SI = 36.
3. Select surface type from Table 2: An AC surface, 10 cm (4 in) thick, is recommended for a base CBR of 80 and SAL of 1 250 000.
4. Determine pavement design thickness from Figure 9: Minimum cover over subgrade (surface, base, and subbase) = 30 cm (12 in) for subgrade CBR of 9; minimum cover over subbase = 17 cm (7 in) for subbase CBR of 30; and minimum cover over base = 0 for base CBR of 80. Therefore, for the first trial the thicknesses are 10 cm (4 in) of AC, 10-cm (4-in) base, 10-cm (4-in) subbase, and 60-cm (24-in) subgrade.
5. Determine a subgrade support index (SSI) from Figure 8 with a subgrade CBR of 9. SSI = 7.
6. Determine SI of unbound soil layers: SI = the summation of the products of the structural coefficients (Table 1) and the layer thicknesses. Base-course coefficients are applicable only between 0 and 25 cm (0 and 10 in) from the surface. Subbase coefficients are applicable only between 25 and 50 cm (10 and 20 in) below the surface. The base and subbase-course thicknesses used in determining the SI are referred to as standard base and subbase courses and are not to be confused with the actual base and subbase design thicknesses. Determine SI of unbound soil layers as follows (1 cm = 0.393 in):

$$\begin{aligned}\text{SI for unbound soil layer} &= \text{subbase-course SI (50-25 cm)} \\ &\quad + \text{base-course SI (25-10 cm)} \\ \text{SI} &= [(\text{Coeff. of CBR 9} \times 20\text{ cm}) \\ &\quad + (\text{Coeff. of CBR 30} \times 5\text{ cm})] \\ &\quad + [(\text{Coeff. of CBR 30} \times 5\text{ cm}) \\ &\quad + (\text{Coeff. of CBR 80} \times 10\text{ cm})] \\ \text{SI} &= [(0 \times 20) + (0.205 \times 5)] \\ &\quad + [(0 \times 5) + (1.10 \times 10)] \\ &= [(1.02) + (11.02)] \\ \text{SI} &= 12.04 \qquad (5)\end{aligned}$$

7. Determine combined SI of all structural layers: AC increases the strength of the pavement and reduces the stress on the unbound structural layer. The combined SI that accounts for this relation in a 10-cm AC is shown in Figure 9. Enter the SI compacted in step 6 (12.04) in the horizontal axis and turn to vertical axis upon intercepting the AC = 10 curve. The combined SI = 41.
8. Determine adequacy of first trial design:

$$\begin{aligned}&\text{Required SI} = 48 \text{ (step 2), and} \\ &\text{Calculated SI} = 9 \text{ (step 5)} + 41 \text{ (step 7)} = 48 \qquad (6)\end{aligned}$$

Therefore, the adequate design is 10-cm AC, 10-cm base, 10-cm subbase.

CONCLUSIONS

A new design procedure called the tropical design procedure for flexible pavements was developed for tropical regions through the analysis of over 200 test sections in Brazil and augmented by earlier studies in Africa. Relations were established between performance and deflection and between deflection and the structural strength of component layers in the pavement structure.

Deflection tests were conducted at six stations within each test section. Rebound deflection and the slope of the deflection basin were determined as well as the coefficient of variation within the test sections. Traffic data, compiled by the Brazilian State and National Highway Department, were classified and traffic equivalent factors and equivalent standard axle-load applications were calculated. A subjective pavement rating was applied to each test section, and pavement performance, which was determined by the rating, was related to representative deflections (mean deflection plus two standard deviations) to establish a deflection criterion for tropical conditions.

A design deflection was devised that incorporates an allowable degree of variation, recommended as 35 percent, to the deflection criterion. Maximum values of the slope of the deflection basin are also proposed that reduce pavement cracking to acceptable limits.

Structural coefficients were established and were based on the relations between deflection and strength of the pavement component layers. The structural coefficients were based on CBR of the unbound structural layers as well as the position of the layers in the pavement structure. A strength factor for asphalt layers was established and was based on the thickness of the asphalt layer and the strength of the underlying soil layers. A relation between the slope of the deflection basin, asphalt thickness, and base-course CBR was established. This relation defines the minimum thickness of asphalt required to prevent excessive pavement cracking within a given traffic period.

A flexible pavement design procedure is described. Structural design curves are provided for design traffic and various degrees of construction uniformities. A design equation is used in the basic design procedure to compute SI of trial sections. Structural coefficients are selected for unbound soil layers and are a function of CBR value of the layer and the position of the layer within the pavement structure. AC surfacing increases the strength of the pavement sections when it is used in the design. Asphalt-strength curves are given for five standard AC thicknesses of 5, 10, 15, 20, and 25 cm (2, 4, 6, 8, and 10 in). Suggested asphalt thicknesses are given for various ranges of traffic and base-course CBR values.

ACKNOWLEDGMENTS

This study was part of a worldwide engineering study of tropical soils sponsored by the U.S. Agency for International Development. Phase 1 covered Southeast Asia, phase 2 covered Africa, and phase 3 synthesized the findings of the first two and also covered South America and Central America. The pavement evaluation studies were conducted in South America and Africa by Lyon Associates, Inc., and by the cooperating host country organizations, the Departamento Nacional de Estradas de Rodagem (DNER) in Brazil and Building and Road Research Institute (BRRI) in Ghana.

REFERENCES

1. W. J. Morin and P. C. Todor. Laterite and Lateritic Soil and Other Problem Soils of the Tropics. Lyon Associates, Inc., Rept., Vols. 1 and 2, 1975, 369 and 92 pp.; U.S. Agency for International Development.
2. Laterite and Lateritic Soils and Other Problem Soils in Africa. Lyon Associates, Inc., and Building and Research Institute in Ghana, Africa, Rept., 1971, 290pp.; U.S. Agency for International Development.
3. K. Y. Kung. A New Method in Correlation Study of Pavement Deflection and Cracking. Proc., Univ. of Mich., 2nd International Conference of Structural Design of Asphalt Pavements, 1967, pp. 1037-1046.
4. P. C. Todor and S. L. Yeboa. Pavement Deflection and Performance in Ghana. Proc., 5th African Conference on Soil Mechanics and Foundations Engineering, Angola, Africa, Vol. 1, 1971, Section 5, pp. 44-54.
5. Y. A. Huang. Strain and Curvature as Factors for Predicting Pavement Fatigue. Proc., 3rd International Conference on Structural Design of Asphalt Pavements, London, Vol. 1, 1972, pp. 622-628.
6. Y. Miura. A Study of Stress and Strain in the Asphalt Pavement of Tomei-Highway. Proc., 3rd International Conference on Structural Design of Asphalt Pavements, London, Vol. 1, 1972, pp. 476-489.
7. Estatisticas do Servico de Transito do 6º Distrito Rodoviario Federal do DNER, Departamento Nacional de Estradas de Rodagem, 1970, 62 pp.
8. Interim Guide for Design of Pavement Structure, AASHO, 1972, 125 pp.
9. R. I. Kingham. Development of the Asphalt Institute's Deflection Method for Designing Asphalt Concrete Overlays for Asphalt Pavements. Asphalt Institute, Res. Rept. 69-3, 1969, 23 pp.
10. W. S. Housel and S. A. Ito. The Structural Analysis of Asphalt Pavements From Field Loading Tests. Proc., 3rd International Conference on Structural Design of Asphalt Pavements, London, Vol. 1, 1972, pp. 823-843.

Publication of this paper sponsored by Committee on Flexible Pavement Design.

Road Test to Determine Implications of Preventing Thermal Reflection Cracking in Asphalt Overlays

Ramesh Kher, Research and Development Division, Ontario Ministry of Transportation and Communications

In predominantly cold climatic regions, thermal cracking of asphalt pavements and its reflection through bituminous resurfacings is a problem of great concern to the pavement engineers. Reflection cracking causes poor riding quality prematurely, reduces the useful life of a resurfacing, requires accelerated maintenance, and results in an uneconomic use of physical and fiscal resources. Over the years, many treatments have been tried to minimize the reflection cracking in bituminous resurfacing. These treatments have exhibited varying degrees of success; however, none has been consistently successful under all conditions. In Ontario, Canada, eight test sections were constructed in 1971 to determine a viable alternative to the predominantly used conventional resurfacing. A special feature of this experimental road is the two test sections in which the existing asphalt surface was pulverized and used with or without additional asphalt binder as a base for the resurfacing. In this paper, the phenomenom of thermal cracking and its mechanisms and manifestations are discussed. The experimental road is described and the performance of its various test sections over the past 5 years is documented. An economic analysis is conducted in which the trade-offs between the initial construction and the future maintenance costs of various treatments are compared to the costs of a conventional resurfacing. This analysis concludes that pulverization of the existing pavement surface and use of that surface as a base for resurfacing is the most viable alternative to a conventional resurfacing. The paper also describes three full-scale contracts, totaling about 50 km (31 miles), in which treatment was recently used in Ontario.

In most Canadian provinces and in the northern United States, non-load-associated transverse cracking caused by severe climatic conditions is a predominant form of distress on bituminous pavements. This form of cracking occurs mainly in the bituminous-surface layers when tensile stresses caused by rapid drops in temperatures during the winter exceed the tensile strength of the bituminous material.

Effective rehabilitation of hundreds of kilometers of these cracked pavements is a task that challenges pavement engineers. Bituminous resurfacing has been predominantly used in the past to rehabilitate these pavements; however, this kind of resurfacing has not been a satisfactory form of rehabilitation because the cracks existing in the original pavement reflect through the resurfacing. This cracking is called reflection cracking and is caused when the cracked underlying pavement contracts over subsequent winters and restraint stresses along the underside of the resurfacing are set up. These restraint stresses create high tensile stresses immediately above the existing cracks and therefore lead to a fracture of the resurfacing generally above the crack.

Thermally induced cracks begin as hairline cracks in the first winter and slowly widen with time. As shown in Figure 1, these cracks are partial transverse cracks at first but slowly, during the subsequent winters, extend over the full width of the pavement. These cracks are generally at right angles to the pavement centerline, but sometimes take a different form when two partial cracks are joined by a small longitudinal crack, or when a main crack manifests into multiple or alligator-type cracking.

Figure 2 shows two extreme cases of thermal cracking in Ontario. As shown by the solid lines in this figure, the thermal cracks in new pavements are widely spaced for the first 3 or 4 years, after which one of the following two conditions occurs.

1. Cracks per kilometer progressively increase every winter in proportion to the severity of the winter. In extreme cases, these cracks reach a spacing of 1.5 m (5 ft) or less in 12 to 15 years.
2. Cracks per kilometer increase sharply in the fourth or fifth winter to a spacing of approximately 30 m (100 ft), after which the spacing remains practically constant.

The thermal cracks are hairline for the first 4 to 5 years, after which they progressively widen and eventually become 10 to 20 mm (½ to ¾ in) wide. The cracks are partial or full-width singular for the first 4 or 5 years, after which secondary cracks may form, and, during the twelfth to fifteenth year, severe spalling and alligatoring may be observed.

As shown by the dotted lines in Figure 1, the two crack patterns described above progress at a much faster rate in the case of a resurfaced pavement. In the first case, complete reflection of the cracks in the underlying pavement may occur in 5 to 6 years, with most of the reflection occurring in the initial winters. As in new pavements, cracking is proportional to the severity of winter: The severer the winter, the greater the number of new cracks that develop during that year. In the second case, complete reflection may take place in the first winter after the resurfacing.

In new as well as in resurfaced pavements, the primary distress mode of cracking is generally manifested by many types of secondary distresses. Water and deicing salts infiltrate through the cracks and soften the base material underneath. This infiltration results in partial loss of support that often leads to multiple or even alligator-type cracking around the main crack.

The softened base around the crack, especially during the winter months when deicing solutions cause localized thawing of the base, also results in a depression around the crack called dipping of the crack. At other times, water entering the cracks may freeze and form an ice lens below the crack, thus elevating the crack edges. This elevation is called lipping or tenting of the crack. The lipping and dipping of the crack may occur any time after five to seven winters on new as well as resurfaced pavements.

CONSEQUENCES OF REFLECTION CRACKING

The secondary distress manifestations described above result in the following:

1. Poor riding quality at an earlier date, especially during the winter;
2. Accelerated deterioration of the resurfaced pavement;
3. Increased maintenance demand;
4. Inconvenience to the motoring public;
5. Unsafe driving; and
6. Uneconomical use of physical and fiscal rehabilitation resources.

Therefore, it is important that new techniques be explored to reduce reflection cracking so that existing thermally cracked highway pavements can be economically rehabilitated.

Figure 1. Typical partial and full transverse cracking.

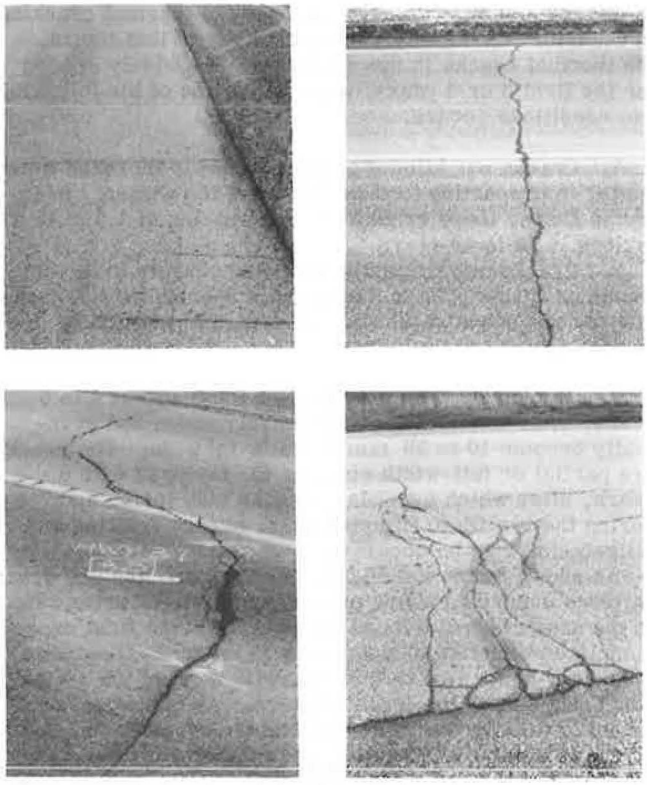

CONVENTIONAL SOLUTIONS

Over the years, many different construction techniques and materials have been tried to minimize or eliminate the reflection cracking of bituminous resurfacings. These treatments have shown varying degrees of success: Some have been successful on specific projects; however, none has completely eliminated reflection cracking or has been consistently successful in minimizing reflection cracking. These treatments generally fall in the following three categories:

1. Use of improved mixes for resurfacing such as the use of high binder content, softer asphalts, mastic-like mixes such as Gussasphalt, and the use of rubber and polymer-asphalt additives;
2. Use of intervening layers such as granular materials and open-graded asphalt mixes; and
3. Stress-relieving interfaces such as rubber-tire aggregate slurry and thermoplastic rubber that is mixed with asphalt cement and filler.

TROUT CREEK EXPERIMENTAL ROAD

In view of the wide variety of treatments that have been tried but have not been consistently successful for all environmental conditions and the fact that severe winter conditions such as those existing in northern Ontario may have unique influences toward the propagation of reflection cracking, an experimental road consisting of eight treatment sections was constructed in 1971 to study the treatments that may minimize or eliminate reflection cracking in Ontario.

The experimental road site is located about 29 km (18 miles) south of North Bay in Ontario. In the original pavement, the transverse cracks were spaced 1.5 to 3 m (5 to 10 ft) apart, were generally 6 to 12 mm (¼ to ½ in) wide, and were depressed 2.5 to 5.0 cm (1 to 2 in) below

Figure 2. Schematic representation of transverse cracking in new and resurfaced pavements.

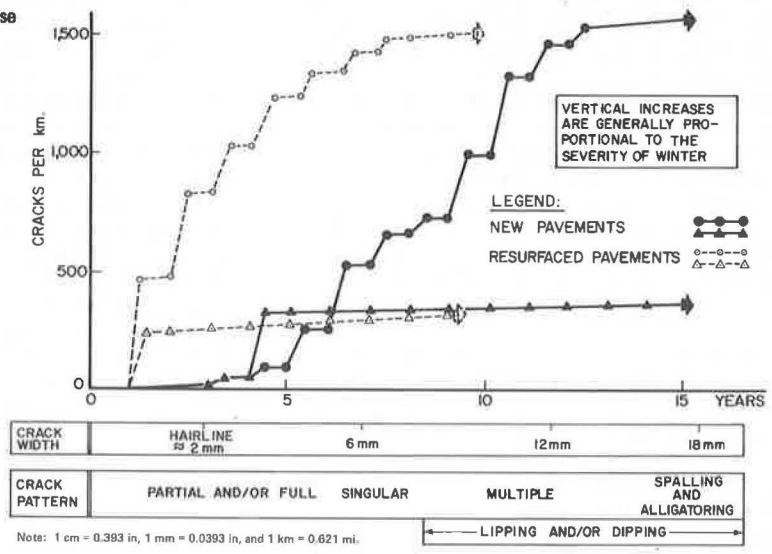

the pavement surface. This situation resulted in a rough ride during the winter months. The experimental construction was carried out between August and October 1971.

Cross Sections and Construction Details

Eight treatments were used in the experiment: Four treatments consisted of interlayers between the resurfacing and the old pavement (sections 1 to 4), two treatments consisted of resurfacings over reworked old pavements (sections 6 and 7), one treatment consisted of removing the old pavement surface and replacing it with a new surfacing (section 5), and the last treatment was a control section that consisted of conventional resurfacing over the old pavement (section 8). The cross sections of the various treatments are shown in Figure 3. A standard well-graded mix with a 150 to 200-penetration asphalt was used as a resurfacing for each treatment.

1. Screenings interlayer—Section 1, 152 m (500 ft) long, consisted of a 2.54-cm (1-in) thick layer of crushed-stone screenings, 9.5-mm (3/8-in) maximum size, that was spread over the old pavement before resurfacing.
2. Granular interlayer—Section 2, 1.07 km (0.67 mile) long, consisted of a 7.6-cm (3-in) thick layer of granular, 22.2-mm (7/8-in) maximum size, that was spread over the old pavement before resurfacing.
3. Granular interlayer—Section 3, 1.07 km (0.67 mile) long, consisted of a 15.2-cm (6-in) thick layer of granular, the same as in section 2, that was spread over the old pavement before resurfacing.
4. Open-graded binder interlayer—Section 4, 1.96 km (1.22 miles) long, was resurfaced with the first resurfacing (binder) layer that was made of an open-graded mix with 100 percent crushed aggregate.
5. Existing surface replaced—For section 5, 2.9 km (1.8 miles) long, the existing pavement surface was removed and replaced with a new surface.
6. Existing surface pulverized—For section 6, 1.61 km (1.0 mile) long, the old pavement surface was pulverized, relaid on the old granular base, compacted, and used as a base for the resurfacing.
7. Existing surface pulverized and enriched—Section 7, 1.4 km (0.9 mile) long, was similar to section 6 except that the pulverized material was enriched with approximately 3 percent of medium curing-250 (MC-250) cutback.
8. Conventional resurfacing—Section 8, 1.8 km (1.1 miles) long, was a control section because the treatment used in this section has been conventionally used in Ontario for pavement rehabilitation purposes.

The effects of grooves on the performance of the resurfacings were studied by cutting approximately 20 lateral grooves in each of sections 2 through 8. These grooves, 12.7 mm (1/2 in) thick and 12.7 mm (1/2 in) deep, were cut across the full width of the finished resurfacing and were filled with hot-poured rubberized joint sealant. At the beginning of each treatment, four grooves were cut at interval spacings of 7.6 m (25 ft), 15.2 m (50 ft), and 22.8 m (75 ft), and seven or eight grooves were cut at random locations where cracks existed in the original pavement.

Observations From Experimental Road Construction

The problems that were encountered during the construction of the various sections are summarized as follows:

1. In section 1, control problems were experienced in maintaining the 2.54 cm (1 in) of crushed stone screenings over the distortions in the existing pavement. One problem was to avoid disturbing this material by the tires of the asphalt paver when the first resurfacing (binder) layer was placed. An increase in the thickness of the binder layer to 5.08 cm (2 in) and a slower paving operation partially reduced this problem.
2. In section 2, control problems were also experienced with the 7.62-cm (3-in) granular layer because this thickness does not uniformly cover the distortions or provide a tight surface that is resistant against traffic. This problem did not exist in section 3, which had a 15.24-cm (6-in) granular thickness.
3. In sections 4, 5, and 8, there were no construction difficulties encountered.
4. In sections 6 and 7, where the existing pavement surface was pulverized and reused, many construction difficulties were encountered but were resolved. In section 6, the old pavement surface was first ripped and windrowed to the side. A small Hammermill pulverizer was initially used to pulverize this material on site. This pulverizer had frequent breakdowns and its teeth wore down considerably each day. This operation was discontinued, and, subsequently, the material was hauled, stockpiled, and pulverized by using a crusher. In section 7, the enriched mix with 4 percent cutback (initially used) would not set up fast enough after placing and was severely distorted when opened to traffic. The material was windrowed to the shoulder and cured with the help of a grader. The amount of MC-250 was reduced to 3 percent so that the residual asphalt content in the mix and the curing time could be reduced.

Performance

Since the construction of the experimental road, each of the eight test sections has been assessed twice a year by the staff of the Ontario Ministry of Transportation and Communications. The results of the crack surveys are shown in Figure 3. As per the last survey in July 1976, section 8 (control), which used the conventional resurfacing, had the maximum cracking [183 cracks/km (294 cracks/mile)]. The cracking in other sections, in terms of percentage of cracking in control section, is as follows:

Section	Percentage of Control Cracking
1 and 4	70 to 80
2 and 3	25 to 35
5, 6, and 7	3 to 10

All surveys conducted to date show that sawn grooves are of no benefit in controlling the reflection cracking. The cracks have appeared within very short distances of these grooves, sometimes even within a few centimeters.

Cost

Based on 1971 bid prices for the experimental project, the construction costs in U.S. dollars of various test sections were computed. Costs varied from a minimum of $19 453/km ($31 300/mile) for section 8 (control) to a maximum of $36 234/km ($58 300/mile) for section 7, which was 186 percent increase over the control. The costs of other sections, in terms of percentage of control, are given in Table 1.

Conclusions

Based on cracking history, construction difficulties, and construction cost comparison as given in Table 1, it is

Figure 3. Cross sections and cracking history of Trout Creek experimental road.

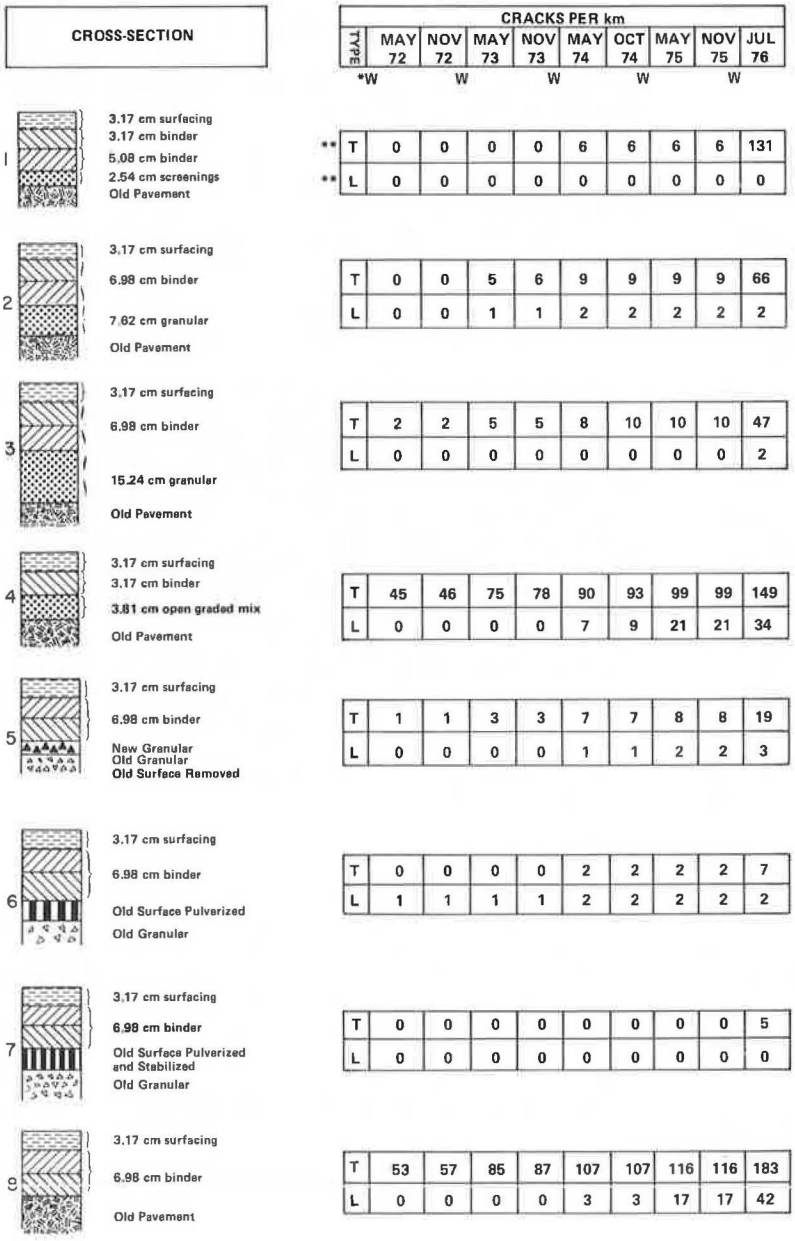

Note: 1 cm = 0.393 in and 1 km = 0.621 mile.

* W Winter
** T Transverse cracks
** L Longitudinal cracks

Table 1. Summary inferences from Trout Creek test road.

Section	Treatment	1976 Cracking (percentage of control)	Construction Difficulties	Extra Cost[a] (percentage of control)	Further Consideration
1	Screenings interlayer	72	Considerable	27	No
2	7.6-cm granular interlayer	36	Moderate	32	Yes
3	15.2-cm granular interlayer	26	None	67	Yes
4	Open-graded binder interlayer	81	None	0	No
5	Surface replaced	10	None	23	Yes
6	Surface pulverized	4	Moderate	31	Yes
7	Surface pulverized and enriched	3	Moderate	86	Yes
8	Conventional resurfacing	100	None	0	Control

Note: 1 cm = 0.39 in.

[a]Based on 1971 bid prices for the test road sections.

Figure 4. Schematic representation of agency cost components.

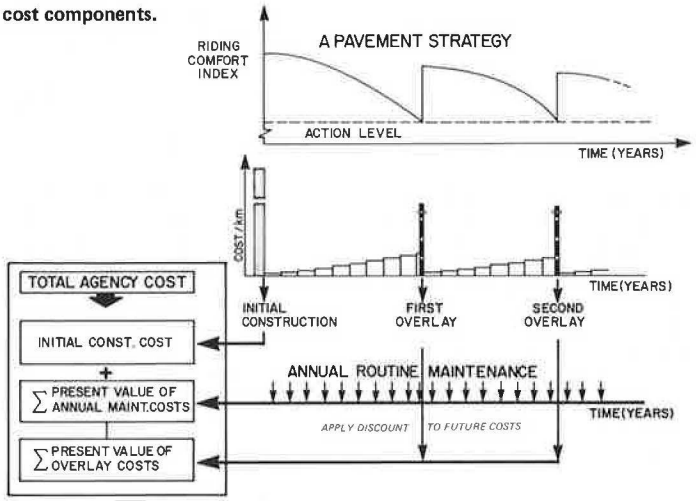

Table 2. Maximum prices for extra life with distortion correction.

Extra Life[a] (years)	Distortion Correction (U.S. $/m²)		
	Severe	Normal	None
AADT >2000			
0	0.60	0.30	0.00
1	0.80	0.50	0.20
2	1.02	0.72	0.42
3	1.21	0.91	0.61
4	1.40	1.10	0.80
5	1.60	1.29	0.99
6	1.75	1.45	1.15
9	2.26	1.96	1.66
12	2.58	2.28	1.99
15	2.93	2.63	2.33
AADT <2000			
0	0.60	0.30	0.00
1	0.78	0.48	0.18
2	0.94	0.65	0.35
3	1.10	0.80	0.50
4	1.26	0.96	0.66
5	1.46	1.16	0.86
6	1.53	1.23	0.93
9	1.88	1.58	1.28
12	2.16	1.87	1.57
15	2.43	2.13	1.83

Notes: 1 m² = 10.8 ft².
This table is based on 1976 U.S. material prices.
[a]In excess of 10 years, which is considered the average life of a conventional resurfacing.

concluded that treatments in sections 1 and 4 are not viable alternatives to conventional resurfacing and should therefore be eliminated from further consideration and analysis.

ECONOMIC ANALYSIS

An economic analysis is conducted to further establish which of the remaining five treatments is the most viable alternative to a conventional resurfacing for field trials through full-scale contracts. Although performance data are being gathered every year at the experimental road site, the interim recommendations already show the benefits from the 5-year experience to date.

Analysis Rationale

The economic consequences of a highway improvement are twofold: the agency costs of initial improvement and subsequent maintenance, and user benefits of operating on such an improved facility. The trade-offs between the cost of initial construction and that of subsequent future maintenance are important to a highway agency. When compared to a conventional resurfacing, if the extra initial cost (Δ_c) of a treatment is completely offset by the future maintenance cost savings (Δ_r), the treatment may be considered a viable alternative. The ratio of Δ_r to Δ_c, as in any benefit/cost analysis, determines the degree of viability for such a treatment.

The user-associated costs and savings, those of motorists' discomfort and delay, also impinge on the determinations of such viability. For this analysis, user delay costs in U.S. dollars have been calculated; however, they have not been included in this paper because they are subject to varying interpretations. A reader may still superimpose the motorists' considerations exogenously on the results of this economic analysis.

As shown in Figure 4, the future maintenance cost in U.S. dollars of a pavement facility has two components: the annual routine maintenance cost and resurfacing or overlay cost. For economic analysis, these costs are calculated as they incur over a certain analysis period, e.g., 30 years, and are then discounted to their current values so that the trade-offs can be analyzed in terms of current dollars.

A prerequisite for calculating future maintenance costs is that the times must be known when such costs are incurred, i.e., the life of initial improvement as well as those of future rehabilitative actions must be predictable. The exact life of these treatments cannot be estimated because the experiment is only 5 years old; therefore, a general analysis was conducted in which the future savings were calculated. It was assumed that a treatment may last any number of years, and this assumption was compared to a conventional resurfacing. The extra initial cost of a treatment can then determine the number of additional years that such a treatment may last so that this extra cost is offset by the future savings. The following example illustrates this concept.

1. Assume an initial life of T_1 years for a conventional resurfacing and t_1, t_2, ... t_i years for a treatment. Calculate for the conventional resurfacing by using initial cost (R_s) and future cost (R_f). Calculate for the treatment by using initial cost (C_s) and future costs (C_1, C_2, ... C_i). The extra initial cost ($\Delta_c = C_s - R_s$) and the future cost savings (Δ_r) respectively are as follows:

$$\Delta_{F1} = R_f - C_1$$
$$\Delta_{F2} = R_f - C_2$$
$$\vdots$$
$$\Delta_{Fi} = R_f - C_i \quad (1)$$

Plot Δ_{Fi} versus t_i and compare it with Δ_c to determine t_i at which $\Delta_{Fi} = \Delta_c$. The analysis will thus give the additional life $[(t_i - T_1)]$ that a treatment should last to justify its extra initial expenditure.

2. Repeat step 1 to study a range in price at which a treatment can be constructed by using different values for C_s, which would also require using different additional lives.

3. Repeat steps 1 and 2 for a range of initial life values (T_1, T_2, ... T_i) for the conventional resurfacing.

Analysis Details

As per the rationale given, Table 2 gives the maximum treatment prices that can be allowed if the corresponding extra lives are obtained. The prices are for two types of facilities: low-volume roads with annual average daily traffic (AADT) less than 2000, and roads with AADT greater than 2000. The major differences in the two cases are the routine maintenance and the resurfacing thicknesses used for future maintenance.

Because pavement distortions have to be corrected to restore a proper crossfall when a conventional resurfacing is applied, the cost of correcting such a distortion has been added to the allowable treatment price for which no distortion correction is generally warranted. Table 2 gives the allowable treatment prices for the following conditions.

1. No distortion correction;
2. Normal distortion correction, i.e., an average of 6.35-mm (¼-in) correction over the entire project; and
3. Severe distortion correction, i.e., an average of 12.7-mm (½-in) correction over the entire project.

The analysis given in Table 2 is for a case in which the same resurfacing thickness will be provided on the treated pavement as well as on the conventionally resurfaced pavement. However, if the resurfacing thickness on the treated pavement can be reduced by a certain amount, the corresponding saving can be added to the allowable treatment price. For this purpose, the cost in U.S. dollars of 1 cm (0.393 in) of hot mix and shoulder upgrading shall be approximately $\$0.47/m^2$ ($\$0.39/yd^2$).

The details of the entire economic analysis leading to Table 2 cannot be described in this paper. However, the unit material prices used in the analysis are given as follows in U.S. dollars: $\$37.93/m^3$ ($\$29.00/yd^3$) for hot mix for resurfacing and $\$9.81/m^3$ ($\$7.50/yd^3$) for granular material for shoulder upgrading.

The use of Table 2 is demonstrated by the following example. Assume that a thermally cracked low-volume facility is to be rehabilitated and the alternatives being considered are

1. A pavement resurfaced with 7.62 cm (3 in) of hot mix and no distortion correction is needed, and
2. A pavement treated (pulverized) and resurfaced with 6.35 cm (2.5 in) of hot mix.

Assume further that the treated pavement may last 3 years longer than the pavement with the conventional resurfacing. By using Table 2, it can be seen that treating the pavement will be a viable solution if pulverization can be achieved at less than $0.50 + (7.62 - 6.35) \times 0.47 = \$1.10/m^2$.

Observations From Economic Analysis

The average 1976 prices in U.S. dollars of various treatments are given in Table 3. Also given are the extra lives required, in excess of conventional resurfacing, that will justify the average treatment prices. By comparing these extra lives with the cracking experience to 1976 at the Trout Creek experimental road, the following general observations were made.

1. The treatment for section 3, 15.2-cm (6-in) granular interlayer, is not a viable alternative because it requires 15 years of extra life (total life is 25 years if a conventional resurfacing lasts 10 years) to be cost-effective.
2. The treatment for section 2, 7.6-cm (3-in) granular interlayer, may be a viable alternative when a pavement is severely distorted; however, in such cases, the construction difficulties of control may prohibit the use of this treatment. Intermediate granular thicknesses such as 10.2 cm (4 in) are also not justified because of the extra life requirement. There is a small difference in cracking performance between treatments 3 and 2.
3. The treatment for section 7, pulverization and enriching, is also not a viable alternative because its extra life requirement is high. A reduction of at least 2.54 cm (1 in) in resurfacing thickness may, however, justify this treatment for a pavement that needs severe distortion correction.
4. The treatment for section 5, pavement surface removal and replacement, is a viable alternative if stockpiling of the old pavement is environmentally acceptable. Another disadvantage in this case is that the total thickness of the pavement structure remains unchanged.
5. The treatment for section 6, pulverization, is a viable alternative to conventional resurfacing. It reuses the existing materials and contrary to the treatment for section 5, the total structure thickness in this case increases. This treatment is the most cost-effective if the resurfacing thickness can also be reduced by 1.27 cm (½ in) or more. It should be noted, however, that such a reduction is only possible if the pulverization operation does not pick up large quantities of the underlying granular material that minimize the effectiveness of the residual asphalt expected from the pulverized pavement surface.

FIELD TESTS

As a result of the above analysis, the Ontario Ministry of Transportation and Communications initiated three full-scale contracts for pulverization totaling about 50 km (31 miles), as shown in Figure 5. These contracts were intended mainly to further investigate various construction difficulties posed by pulverization and explore possible solutions, and to obtain further data on performance of this treatment. The following is a brief description of the three contracts.

Highway 68

Highway 68, near Sudbury, Ontario, is 15.3 km (9.5 miles) long. This pavement, about 15 years old, showed the following pavement conditions prior to pulverization: (a) fair to poor rideability, (b) transverse cracking with 4.5 to 6.0-m (15 to 20-ft) spacing, and (c) moderate lipping. The pavement, 7.6 cm (3 in) thick and 6.7 m (22 ft) wide, was ripped and windrowed to the middle of the driving lane. The broken pavement was hauled to a

Table 3. 1976 treatment prices for extra life with distortion correction.

Section	Treatment	Price Range (U.S. $/m²)	Average Price (U.S. $/m²)	Distortion Correction (years)		
				Severe	Normal	None
2	7.6-cm granular interlayer	1.34 to 1.53	1.44	4	6	8
3	15.2-cm granular interlayer	2.68 to 3.06	2.87	14	>15	>15
5	Surface replaced	0.24 to 0.36	0.30	-1	0	1.5
6	Surface pulverized	0.97 to 1.20	1.08	2	4	5.5
7	Surface pulverized and enriched	2.69 to 3.17	2.93	15	>15	>15

Note: 1 cm = 0.39 in and 1 m² = 10.8 ft².

Figure 5. Three pulverization contracts in Ontario.

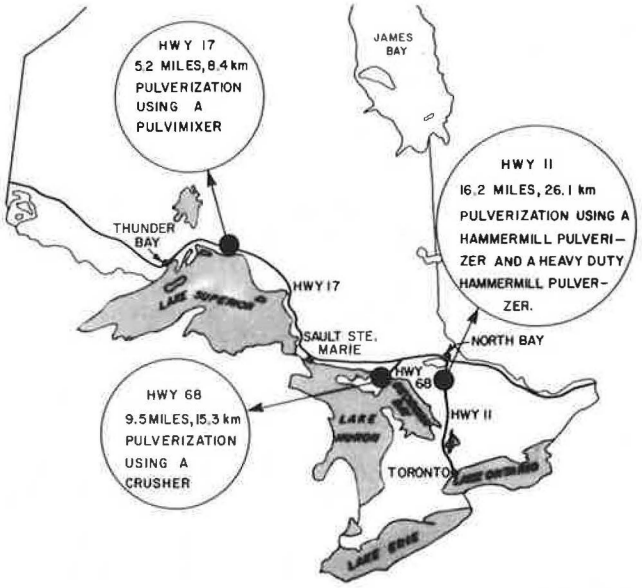

Figure 6. Pulverization by using a crusher.

Figure 7. Pulverization by using a Hammermill pulverizer.

crusher, crushed to a minus 2.54-cm (1-in) size, then hauled back to the road and relaid. The production rate obtained was about 457 m (1500 ft) of two lanes/d. Figure 6 shows the hauling and the crushing operations.

Highway 11

Highway 11, near North Bay, Ontario, is 26.1 km (16.2 miles) long. This pavement, also about 15 years old, showed the following conditions prior to pulverization: (a) fair to poor rideability that became very poor during the spring, (b) transverse cracking with an average 1.5-m (5-ft) spacing, and (c) severe lipping. Approximately 19.3 km (12 miles) of this project were pulverized by using a Hammermill pulverizer. The old pavement with a minimum thickness of 11.4 cm (4.5 in) was ripped one lane at a time and windrowed to the shoulder. This material was then brought inside the lane in small windrows and pulverized. Two or three passes of the pulverizer were generally required to pulverize the material to required size. A production rate of about 213 m (700 ft) of two lanes/d was obtained. Figure 7 shows pavement ripping and pulverization of the pavement.

Approximately 6.4 km (4 miles) of this project were pulverized by using a heavy-duty Hammermill pulverizer. This pulverization was often followed by one pass in the smaller pulverizer, mentioned above, to obtain the required maximum size. Ripping of the pavement was not

Figure 8. Pulverization by using a heavy duty Hammermill pulverizer.

Figure 9. Pulverization by using a pulvimixer.

needed with this equipment. A production rate of about 610 m (2000 ft) of two lanes/d was obtained. Figure 8 shows this equipment in operation.

Highway 17

Highway 17, near Thunder Bay, Ontario, is 8.4 km (5.2 miles) long. This pavement, about 18 years old, showed the following pavement conditions prior to pulverization: (a) fair rideability that became very rough and uncomfortable during the spring, (b) transverse cracking with 0.6 to 3.0-m (2 to 10-ft) random spacing, and (c) severe lipping.

The pavement, 7.3 m (24 ft) wide and 7.6 cm (3 in) thick, was pulverized by a pulvimixer. It was not necessary to rip the pavement because this equipment was used. One to two passes of the pulvimixer were required to pulverize the material to a minus 2.54-cm (1-in) size. A production rate of about 366 m (1200 ft) of 2 lanes/d was obtained. Figure 9 shows this equipment in operation.

CONCLUSIONS

The Trout Creek experimental road has provided valuable information on the performance of various alternatives to conventional resurfacing for rehabilitating thermally cracked asphalt pavements. Of the seven alternatives tried, the economic analysis and other implications indicate that

1. Pulverizing the existing pavement surface and using it as a base for resurfacing is the most viable alternative;
2. Removing and replacing the existing pavement surface is also a viable alternative, if it is environmentally acceptable;
3. Placing interlayers between the old pavement and the resurfacing such as crushed stone screenings, different thicknesses of granular material, and open-graded binder course is not cost-effective; and
4. Enriching the pulverized material and using it as a base for resurfacing is not a cost-effective alternative.

The three full-scale contracts undertaken to date have demonstrated that construction difficulties associated with the pulverization operation can be resolved.

Publication of this paper sponsored by Committee on Design of Composite Pavements and Structural Overlays.

Analytical Modeling and Field Verification of Thermal Stresses in Overlay

K. Majidzadeh and G. G. Suckarieh, Department of Civil Engineering, Ohio State University, Columbus

This paper describes analytical and graphical procedures for computing thermal stresses at joint locations in pavement overlays. Equations and nomographs are used to calculate stresses caused by horizontal and vertical movements of slabs. Both average temperature drop and maximum temperature differential expected in pavement slabs are determined from temperature distribution noted at time of overlay construction. Stresses caused by slab movement are calculated for different overlays. The results confirm that these stresses often exceed the maximum stresses in asphalt-concrete overlays; therefore, reflective cracking occurs when asphalt concrete is laid over jointed pavements.

The movement of pavement slabs under flexible overlays has been well known for its damaging effect on overlays. This effect is usually manifested by the phenomenon of reflective cracking. The slab movements induced by temperature are usually considered from two points of view: One arises from slow changes in average temperature of pavement, and the second arises from quick changes in average temperature of pavement, i.e., a cool night to a hot day and vice versa. In the first case, pavement slabs contract and expand because of a change in the average temperature of pavement. In the second case,

pavement slabs curl and warp because of a definite temperature gradient in pavement.

In relation with a current research project at the Ohio State University, actual field data on movements at joint locations in joint-reinforced concrete pavement (JRCP) were collected under different temperature distributions. The data were fitted to theoretical models to study the induced thermal stresses in the overlay at the joint locations.

FIELD INSTRUMENTATION

Instruments for measuring temperature distribution and vertical and horizontal movement of the slabs were placed at joint locations and in the middle of pavement slabs. Temperature sensors measured temperature distribution, and special strain gauges detected and measured slab movement. Figure 1 shows a schematic view of the field instrumentation. The field study was conducted on slabs of various lengths and thicknesses and at different times and locations. Some of the slabs were newly constructed and others were overlaid with asphalt-concrete layers. The overlaid slab data were taken before and after the occurrence of reflective cracking.

HORIZONTAL MOVEMENT OF SLABS

The previously mentioned field set-up was used to study the horizontal movement of the slabs. The average slab temperature, measured by the temperature sensors, was plotted against the distance between the strain gauges embedded at both sides of the joints, and a regression analysis was made. A typical curve of temperature-joint horizontal movement is shown in Figure 2. Comparisons were made between different slab curves similar to the one shown in Figure 2. The following results were concluded.

1. The diagram of the friction forces between the concrete slabs and the subgrade is triangular. (This assumption is also made for calculating the minimum steel required in the pavement.)
2. When the slabs were subjected to the same temperature changes, the use of relatively thin overlays [between 0 and 9 cm (0 and 4 in)] showed no significant effect on the movement of the underlying slabs.
3. When reflective cracking occurred, the horizontal movements of the underlying slabs followed the same temperature-movement curve as the before cracking curve.

It was concluded that the horizontal movement of the overlaid slabs at the joint location could be predicted by using the following formula:

$$\Delta_h = (\alpha \Delta T_h L) - (\gamma_c h_c + \gamma_{ac} h_{ac}) f (L^2/2)(1/A_c E_c) \quad (1)$$

where

Δ_h = horizontal movement at joint location,
α = temperature coefficient,
ΔT_h = average temperature drops,
L = length of slabs,
γ_c, γ_{ac} = unit weight of concrete and asphalt concrete,
f = coefficient of friction between subgrade and slab,
A_c = unit cross section of slab, and
E_c = modulus of elasticity of concrete.

EFFECT OF HORIZONTAL MOVEMENT AT JOINT LOCATION ON FLEXIBLE OVERLAYS

The effects of the horizontal movement at joint location on overlays was studied by using the finite element method for a two-dimensional structural analysis. Figure 3 shows a sample of the mesh used for this analysis. The model consists of two concrete slabs with an asphalt overlay on the top and a thin asphalt-tack coat between the slabs and the overlay. The thicknesses and moduli of elasticity for both the asphalt-concrete overlays and concrete slabs in addition to the joint width were made variable. A horizontal movement was induced into the slab at the joint location and the resulting overlay stresses were studied. From this study it was concluded that

1. For a given movement at the joint the overlay stresses are not affected by either the modulus of elasticity of the concrete or by the slab thickness;
2. There is a one-to-one relation between the induced movement at the joint and the stresses in the overlay; and
3. When the induced movement at the joint exceeds 0.000 50 cm (0.000 20 in), the shearing stresses between the slabs and the overlay would exceed the allowable bond strength between the pavement and overlay, and this condition could result in the sliding of the overlay on the top of the slab.

The results of field observations and analytical simulation of finite element were used to construct the nomographs shown in Figures 4 and 5, which facilitated the computation of stresses in the overlay.

VERTICAL MOVEMENT OF SLABS

The model of slabs on elastic foundation was used to fit the vertical movement of slabs to field data. A computer program was developed at the Ohio State University, Columbus, to calculate the curling and warping shape of slabs under temperature differential (ΔT_v) conditions. The interrelation between deflected shape of pavement and temperature differential is written as follows:

$$[(d^4w/dx^4) + (2d^4w/dx^2dy^2) + (d^4w/dy^4)] = \{(q/D) - [K(w - c)/D]\} \quad (2)$$

where

w = plate deflection in x, y plane,
q = load,
$D = [E_c h_c^3/12(1 - \nu^2)]$ = plate stiffness,
E_c = concrete modulus of elasticity,
h_c = concrete slab thickness,
ν = concrete Poisson ratio,
$c = (\alpha \Delta t d^2/2h_c)$ = curling,
α = temperature coefficient of concrete,
Δt = temperature differential in slabs, and
d = distance from center of the slab.

The program is generalized to consider any pavement geometry, and, at the same time, it takes the partial subgrade contact condition into consideration by assuming zero subgrade reaction at the points where temperature curling is greater than slab deflections.

The program results were checked against the vertical movement of the slab edges obtained from the field data. The case of partial contact gave a better confirmation with the field data than the case that used an assumption of full contact (Figure 6). Comparison of different field results on different slabs showed that the asphalt-concrete

overlay does not significantly affect the vertical movement of the slab.

EFFECT OF VERTICAL MOVEMENT AT JOINT LOCATIONS ON FLEXIBLE OVERLAYS

The vertical curling and warping in concrete slabs causes bending-type stresses in the overlay at the joint location (Figure 7). If the curling or warping slope in the pavement is known, the radius of curvature of the overlay at the joint location can be calculated as follows:

$$R = (j/2\theta) \quad (3)$$

from which the maximum stress on the overlay could be found as follows:

$$\sigma = (E_{ov}H_{ov}/j)\theta \quad (4)$$

where

R = radius of curvature of the overlay,
j = joint width,
θ = edge slope of the slab,

Figure 1. Schematic view of pavement instrumentation.

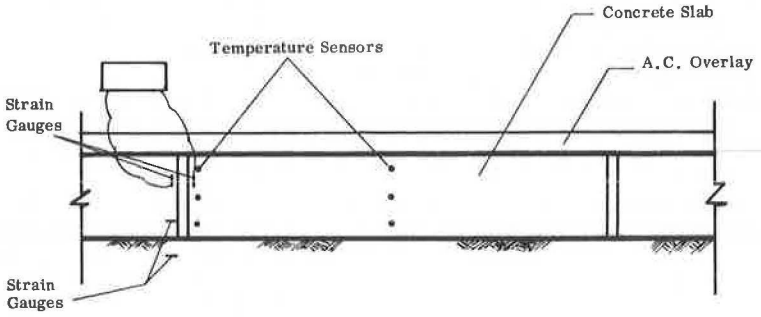

Figure 2. Horizontal movement because of temperature change.

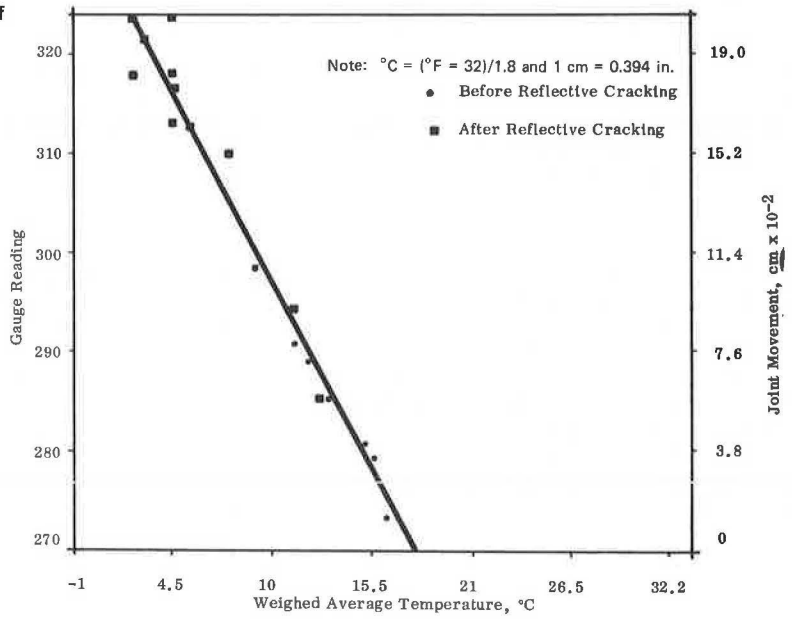

Figure 3. Finite element mesh to study stress in overlay.

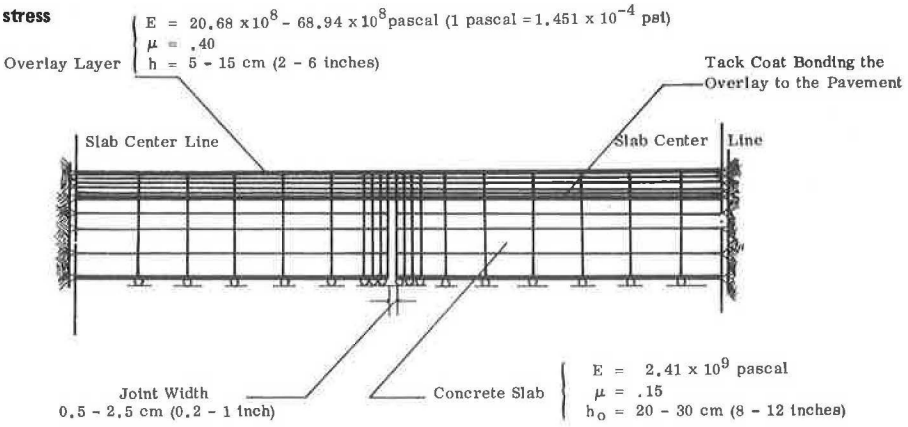

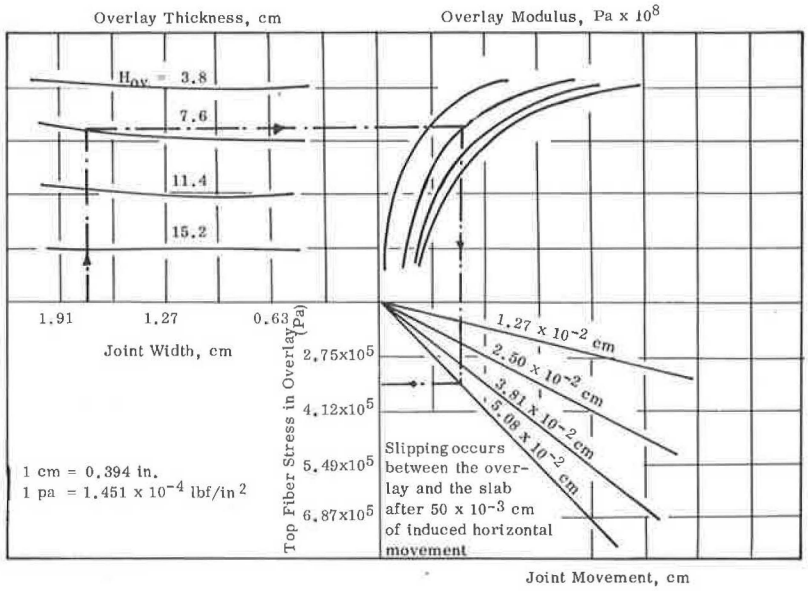

Figure 4. Top fiber stress in overlay because of joint movement in a joint-reinforced concrete pavement.

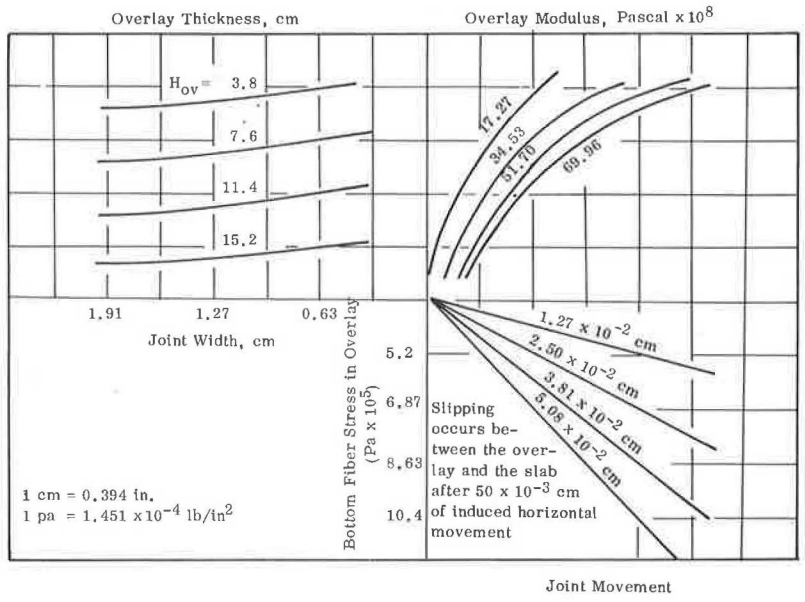

Figure 5. Bottom fiber stress in overlay because of joint movement in a joint-reinforced concrete pavement.

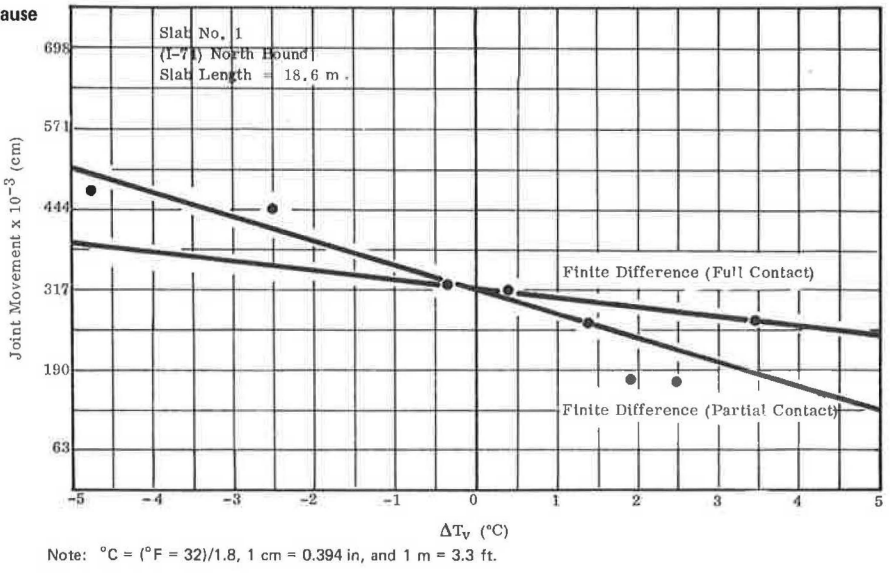

Figure 6. Vertical movement of joint because of temperature differential.

Note: °C = (°F = 32)/1.8, 1 cm = 0.394 in, and 1 m = 3.3 ft.

Figure 7. Bending of overlay by vertical movement of joint.

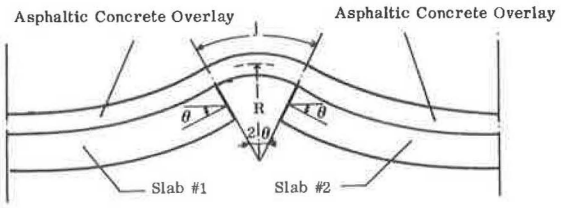

Figure 8. Maximum stress in overlay because of ½°C temperature differential in a rigid pavement.

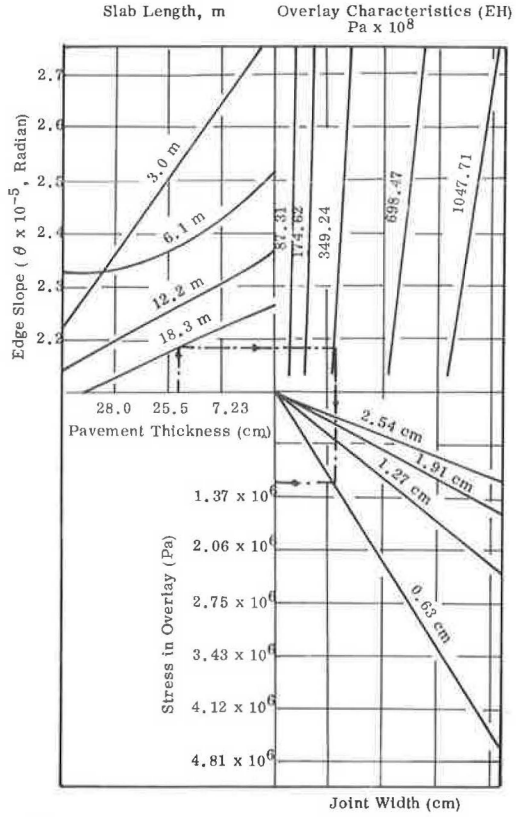

Note: 1 cm = 0.394 in, 1 m = 3.3 ft, 1 Pa = 0.000 145 lbf/in^2.

E_{ov} = modulus of elasticity of the overlay,
H_{ov} = thickness of the overlay, and
σ = maximum stresses in the overlay.

The slope (θ) of different slabs caused by temperature differential can be calculated by using the computer program that had been previously checked against the field data. The following results were concluded.

1. The subgrade reaction modulus does not significantly affect the edge slopes of the slab nor does it significantly affect the partial contact resulting from temperature differential, and
2. The only factors affecting the edge slopes of the slab are the slab thickness and length.

The output of the edge slopes was used in conjunction with the formula for overlay stresses to construct the nomographs shown in Figure 8. These nomographs were used to compute the maximum stresses in the overlay that result from a temperature differential in the pavement slabs. For any other temperature differential values (ΔT_v) the result of the nomographs should be multiplied by ΔT_v. The curling case would give maximum tensile stress in the uppermost fiber of the overlay. The opposite is true in the case of warping.

CONCLUSIONS

The maximum stresses in the overlay at the joint location caused by horizontal slab movement can be calculated by using Equation 1 and nomographs shown in Figures 4 and 5. For stresses caused by vertical movement, the results of the nomograph shown in Figure 7 should be multiplied by the expected temperature differential in the pavement slabs. It is important to know the temperature distribution at the time of overlay construction so that both the average temperature drop and the maximum temperature differential expected in the pavement slabs can be found. Calculation of stresses in different overlays caused by movement at joint location showed that these stresses often exceed the maximum tensile stresses in asphalt-concrete overlays; therefore reflective cracking occurs when asphalt concrete is laid over jointed pavements.

Publication of this paper sponsored by Committee on Design of Composite Pavements and Structural Overlays.